TRANSFORMATION OF POINT RAINFALL TO AREAL RAINFALL BY

ESTIMATING AREAL REDUCTION FACTORS, USING RADAR DATA, FOR

TEXAS

A Thesis

by

TARUN DEEP GILL

Submitted to the Office of Graduate Studies of
Texas A&M University
in partial fulfillment of the requirements for the degree of

MASTER OF SCIENCE

May 2005

Major Subject: Civil Engineering

TRANSFORMATION OF POINT RAINFALL TO AREAL RAINFALL BY

ESTIMATING AREAL REDUCTION FACTORS, USING RADAR DATA, FOR

TEXAS

A Thesis

by

TARUN DEEP GILL

Submitted to the Office of Graduate Studies of
Texas A&M University
in partial fulfillment of the requirements for the degree of

MASTER OF SCIENCE

Approved as to style and content by:

Francisco Olivera	Anthony Cahill
(Chair of Committee)	(Member)
Raghavan Srinivasan	David Rosowsky
(Member)	(Head of Department)

May 2005

Major Subject: Civil Engineering

ABSTRACT

Transformation of Point Rainfall to Areal Rainfall by Estimating Areal Reduction

Factors, Using Radar Data, for Texas. (May 2005)

Tarun Deep Gill, B.E., Thapar Institute of Engineering and Technology,

Patiala, Punjab, India

Chair of Advisory Committee: Dr. Francisco Olivera

Information about extreme precipitation is of great interest for a variety of purposes, which include dam design and its operation, public safety, engineering projects concerned with river management and drainage as well as rainfall-runoff relations. These require knowledge about the spatial and temporal variability of average rainfall over an area. Design rainfall values are generally expressed in the form of point rainfall intensity values which is the rainfall depth at a location. In order to obtain areal average values for an area, hydrologists and engineers require techniques whereby point rainfall amounts can be transformed to average rainfall amounts over a specified area. This problem of point-to-area rainfall conversion can be addressed using depth–area curves which require the use of areal reduction factors. The derivation of areal reduction factors is a focal issue and has been dealt with in diverse manners. Though the methods of derivation of the areal reduction factors vary, results shown by them are comparable. But all these methods have certain shortcomings in the procedures adopted by them. In this application the analysis is based on radar rainfall values obtained from NEXRAD for the study area of Texas as provided by West Gulf River Forecasting Centre (WGRFC). Using NEXRAD

radar rainfall data, geographically fixed depth area relationships will be determined. Here the objectives are to develop areal reduction factors using radar data and to identify the potential obstacles that might hinder the use of such data. The values of the factors developed will be finally compared to other studies which have been carried out. This approach aims to mitigate the difficulties faced in the applications of various procedures and the shortcomings of the various techniques used to determine the values of areal reduction factors.

DEDICATION

To my parents, without whose love and support the completion of this work would not

have been possible.

Papa and Mama, I love you.

ACKNOWLEDGEMENTS

First of all, I would like to thank my parents for supporting me and for providing me with love and encouragement at all times.

I would like to express my deepest appreciation to my committee chair, Dr. Francisco Olivera, for his knowledge, expertise, direction, and supervision all along. Dr. Olivera's recommendations and suggestions have been invaluable for this project. I also thank him for giving me a word of confidence and encouragement every once a while.

Sincere thanks are due to my other committee members, Dr. Raghavan Srinivasan and Dr. Tony Cahill, for their trust, assistance and contributions through my research. Their guidance, persistent help and support are highly appreciated.

I express special thanks to my student colleague and good friend, Jangwong Choi, for always being there for helping me and supporting my ideas.

TABLE OF CONTENTS

LIST OF FIGURES

LIST OF TABLES

1. INTRODUCTION

Information about extreme precipitation is of great interest for a variety of purposes, which include dam design and its operation, public safety, engineering projects concerned with river management and drainage, as well as rainfall-runoff relations. These entail knowledge about the spatial and temporal variability of average rainfall over an area. Design rainfall values are generally expressed in the form of point rainfall intensity values which is the rainfall depth at a location. In order to obtain average values for an area, hydrologists and engineers require techniques whereby point rainfall amounts can be transformed to average rainfall amounts over a specified area. These average values are the mean rainfall depth over the entire catchment. This problem of point-to-area rainfall conversion can be addressed using depth–area curves. Current practices of using these are dominated by the use of areal reduction factors. Catchment intensity-duration-frequency (IDF) curves are obtained by multiplying the rainfall intensity estimates from the point IDF curves by the areal reduction factors corresponding to that area. Therefore, areal reduction factors are applied to point rainfall depths to convert them to equivalent measurements for the whole catchment area. Areal reduction factors are thus key parameters in the design of hydrologic extremes (Veneziano, 2004). They are functions of storm characteristics, such as size, shape, and geographic location (Asquith and Famiglietti, 2000).

_____

This thesis follows the style of *Water Resources Research*.

1.1 OBJECTIVES

In order to obtain areal average values for an area, hydrologists and engineers require techniques whereby point rainfall amounts can be transformed to average rainfall amounts over a specified area. This problem of point-to-area rainfall conversion can be addressed using depth–area curves which require the use of areal reduction factors. The derivation of areal reduction factors is a focal issue and has been dealt with in diverse manners. Though the methods of derivation of the areal reduction factors vary, results shown by them are comparable. But all these methods have certain shortcomings in the procedures adopted by them. In this application the analysis is based on radar rainfall values obtained from NEXRAD for the study area of Texas as provided by West Gulf River Forecasting Centre (WGRFC). Using NEXRAD radar rainfall data, geographically fixed depth area relationships will be determined. Here the objectives are to develop areal reduction factors using radar data and to identify the potential obstacles that might hinder the use of such data. The values of the factors developed will be finally compared to other studies which have been carried out. This approach aims to mitigate the difficulties faced in the applications of various procedures and the shortcomings of the various techniques used to determine the values of areal reduction factors.

1.2 OUTLINE

The thesis consists of 8 sections. The first part provides the introduction, objectives and a brief outline of this research study. The fundamentals of Areal reduction factors and literature review, along with some of the previous used methods,

are described in the second section. The third section comprises of a general description of the NEXRAD Radars, kinds of data available and a description of the West Gulf River Forecasting Centre, the RFC which distributes the data for the present study. Section 4 gives an overview of the various studies carried out using the NEXRAD data. A description of the kinds of data used and the study area is given in section 5. Section 6 throws light on the methodology used for the derivation of the ARFs. The results and discussions are provided in the seventh section of this thesis. Finally, section 8 consists of the conclusions.

2. BACKGROUND

2.1 ARF FUNDAMENTALS

Areal reduction factors, as defined by Natural Environmental Research Council (NERC, 1975), "are factors which when applied to point rainfall values for a specified duration and return period give areal rainfall for the same duration and return period". The concept of areal reduction factors provides a powerful framework for studying the spatial variability of the different hydrological processes. This problem of reduction of extreme rainfall with respect to area covered by storm and its duration is a focal issue and has been dealt with in sundry manners.

2.1.1   Types of Areal Reduction Factors

The two types of areal reduction factors commonly in use are *Geographically Fixed* and *Storm Centered* relationships (U.S. Weather Bureau, 1957, 1958a, 1958b; Miller et al., 1973; Srikanthan, 1995).

2.1.1.1 Geographically Fixed Areal Reduction Factors

Geographically fixed areal reduction factors (also known as *Fixed Area*) relate to rainfall at any arbitrary point. They are estimated from the average of frequency-based quantile estimates using annual maxima rainfall series observed at a fixed location (Osborn et al., 1980). These relate the point depth precipitation (precipitation depth at a point in the watershed) of a given area to the average depth for that particular area. The representative point in this case is an average point having the mean of all

point rainfalls in the area. It is a hypothetical point rather than a point at any particular location. The area under observation is, both, fixed in time and space and hence these kinds of areal reduction factors are referred to as *Fixed Area Areal reduction factors.* In this case, the centre of the storm need not coincide with the centre of the watershed and so the values of the areal reduction factors are based on different parts of different storms instead of the highest point values at the respective storm centers. These areal reduction factors originate from rainfall statistics and not from individual storms and are often referred to as *Statistical Reduction Factors*.

They can be represented by:

$$ARF = R / P \tag{1}$$

where R is the mean of annual maximum rainfall values while P is the mean (generally the weighted mean because of uneven spatial distribution of rain gauges) of annual maximum point rainfall values at gauged points located within the area under consideration (Bell, 1976).

The values of these Areal reduction factors are based on the magnitude of the annual maximum mean precipitation computed for a particular watershed and the frequency analysis of its time series. The frequency of the point precipitation is generally taken to be equivalent to the frequency of the areal precipitation. The annual maxima at individual gauge stations very rarely occur at the same time and for the same storm event. Therefore, they necessitate a very dense network of rain gauges, which have to be closely spaced. These types of Areal reduction factors represent aggregate storm behavior and not discrete individual storm behavior. So these, by and large, have to be used with information from precipitation frequency studies.

2.1.1.2 Storm Centered Areal Reduction Factors

Storm Centered areal reduction factors are associated with the calculation of the effective depth for discrete storms. They represent profiles of individual storms and are supported by data provided by U.S. Army Corps of Engineers' historical storm rainfall atlases. In reality, the area in which the rain falls is not preset but changes with each storm. In this case, the point of maximum rainfall is the centre of the storm and is a representative for calculating the areal reduction factors. The ratio of average storm depth over an area and maximum rainfall depth of the storm is epitomized with the help of these values. Contour lines of depth are divided by the maximum depth of the storm and then they are integrated to obtain the average storm depth. Storm centered areal reduction factors are given by:

$$ARF = R / P \qquad\qquad (2)$$

where R is the areal storm rainfall enclosed by a selected isohyet and within which the rainfall is everywhere equal to or greater than the value for the isohyte. P is the maximum point rainfall at the storm center.

These areal reduction factors are not widely used because this kind of approach is very difficult to implement on multicentered storms. They are only used for individual storms. Also, they are incorrect for estimating areal rainfall of a particular frequency from point rainfalls (Omolayo, 1993). Studies relating to Probable Maximum Flood (PMF) generally require these types of areal reduction factors (Omolayo, 1993; Allen, 2003). Storm centered areal reduction factors refer to a discrete storm.

2.1.1.3 Annual Maxima Centered Areal Reduction Factors

Recently a third approach known as annual maxima centered approach (Asquith and Famiglietti, 2000) has also been adopted. This approach considers the spatial distribution of rainfall occurring concurrently with and surrounding an annual maximum at a point within the watershed. This approach requires the achievement of the following steps. For every annual maximum in the rainfall database the ratio of the annual maxima depth to the concurrent precipitation is calculated and then the separation distance between the rain gauges is calculated. Then from the sample ratios a description of relation between criteria conditioned sample ratio value and separation distance is given. These relations are defined by specific functions fitted to the empirical ratio relation. This produces a best fit line that gives the expected ratio. Then from this the areal reduction functions are computed for a user defined area and design criteria. Empirical depth–distance relations provide the basis of this approach of annual maxima centered areal reduction factors. This approach shows that the areal reduction factors are a function of watershed size, location, shape and the return period.

2.2 PREVIOUS STUDIES

Based on the correlation structure of the extreme storms and the fact that their characteristics are associated with each other, theoretical approaches for the derivation of the areal reduction factors were developed Roche. The earliest studies were based on empirical analysis of single storm events and seldom took into account the return period of the event (U.S.Weather Bureau, 1958a, 1958b). In some countries like Italy, these kinds of studies were some of the pioneering ones (Supino, 1964) and even today they

are very popular in the definition of a design storm for urban drainage systems. The theoretical approach was further extended with the introduction of variance functions and reduction factors (Rodriguez-Iturbe and Mejia, 1974a). A stochastic derivation based on the analysis of the areal reduction factors for rainfall processes aggregated both in space and time was also presented (Waymire et al., 1984; Sivapalan and Blöschl, 1998; Bacchi and Ranzi, 1995). Prototype studies directed towards estimating areal reduction factors using digitized radar-returned data were also conducted (Frederick et al., 1977).

2.3 SOURCES OF AREAL REDUCTION FACTORS

The most common sources of areal reduction factors and depth-area curves for the United States are Technical Paper TP-29 (U.S. Weather Bureau, 1957), TP-40 (Hershfield, 1961a, 1961b), NOAA Atlas 2 (Miller et al., 1973). Areal reduction factors from areas ranging from 0 to 1024 sq. km. and for durations from 30 min. up to 24 hours are presented in TP-29. Data used were from seven dense gauging networks located in the eastern and central United States. The values of areal reduction factors are general values and can be used for any region. They were particularly developed for the regions east of the Mississippi River and represent an areal reduction factor-area curve based on a 2 year recurrence interval. This curve can be employed for all return periods up to 100 years (Allen, 2003). According to TP-29, areal reduction factor is defined as the ratio of mean annual maxima of areal precipitation to the mean annual maxima of point precipitation. Conclusion of this report was that area and storm duration were the parameters that affected depth-area factors. It assumes that the depth-

area relations are not influenced by the recurrence interval of point precipitation. Therefore, the frequency of the areal precipitation is equal to the frequency of the point precipitation. The data used for the estimation of depth-area relations, in TP-29 part 2, was obtained from additional dense gauging networks in the Western United States. Leclerc and Schaake (1972) expressed the results of TP-29 by giving a formula for the areal reduction factors:

$$ARF = Z_E / Z_T = 1 - e^{-1.1t^{0.25}} + e^{(-1.1t^{0.25} - 0.25A)} \tag{3}$$

where Z_E is effective (or average) precipitation over the area in inches, Z_T = point precipitation of the design storm depth for recurrence interval T, in inches, t = duration time, in hours and A=area, in square miles (Allen, 2003).

Depth area reduction curves published in parts 3 to 5 of TP-29, TP-40 and the NOAA atlas 2 were identical to those published earlier in parts 1 and 2. These results were extended in TP-49 with storm duration up to 10 days. Estimates were made for 2, 5, 10, 25, 50 and 100 year depth area reduction factors using annual data series. But the results for different return periods were almost same and so it was concluded that there was no need to publish these results for all these frequencies.

Figure 1 is an illustration of the depth-area curves which were initially published by U.S. Weather Bureau (TP-29) (1958a, 1958b). Theses, along with their recent modifications, are still being used as standard curves all over the U.S. It may be noted here that these curves do not take into account the return period of the storm and hence are independent of frequency of occurrence of the storm.
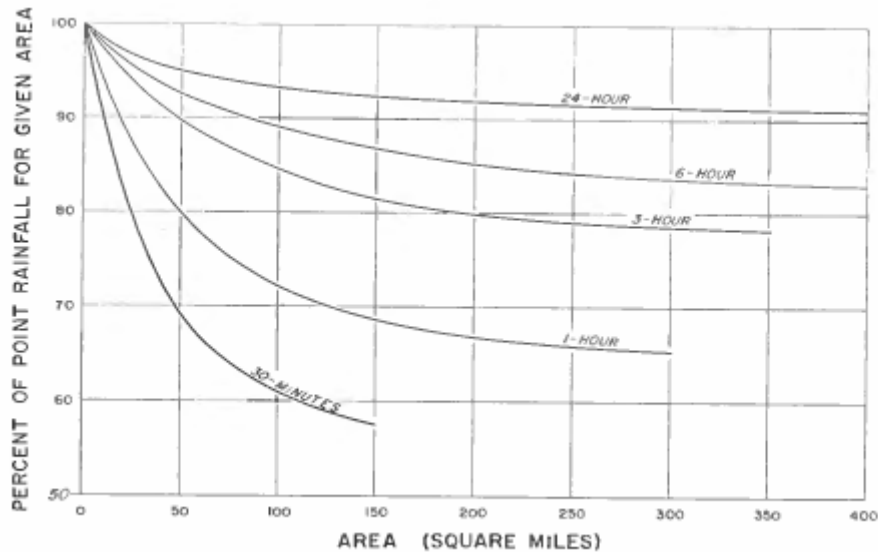
Figure 1. TP-29(1958) Chart Showing Percent Point Rainfall for Different Areas.

2.4 METHODOLOGIES FOR ARF DERIVATION

Areal reduction factors have been mostly developed in U.S., U.K. and New Zealand (Omolayo, 1993). Not much work has been done to estimate these values in other parts of the world because of sparse networks of rainfall stations and short records. For the transposition of these areal reduction factors to different parts of the world there are many methodologies. Some of the major methodologies in practice for the derivation and transposition of areal reduction factors are as follows:

2.4.1   U.S. Weather Bureau Method

As discussed by Omolayo, 1993, in this method the areal rainfall of each event of the chosen duration is calculated using Thiessen weighting factors and the highest of

these in each year of the record is selected. Then the mean of the entire annual series is computed and the highest point measurement at each station in each year is selected. Areal reduction factor is this mean divided by the total mean over all the stations over all the years of record.

$$ARF_{US} = \sum_{j} \sum_{i} w_i U'_{ij} / \sum_{j} \sum_{i} U_{ij} \qquad (4)$$

where Uij is the annual maximum point rainfall at station i in year j, while Uij' is the point rainfall at station i on the day the annual maximum areal rainfall occurs in the year j, w is the Thiessens weighted factor for the station.

2.4.2 U.K. Method

In this method as presented by Omolayo, 1993, the point measurements, Ui's, of the annual maxima are noted. The maximum point recordings Ui, at each station in the same year are identified. The ratio of the two values at each station in the year is calculated and then the grand mean of these ratios over all stations and all years of record is adopted as the areal reduction factor.

$$ARF_{UK} = (1 / IJ) \sum_{j} \sum_{i} U'_{ij} / U_{ij} \qquad (5)$$

where Uij is the annual maximum point rainfall at station i in year j, while Uij' is the point rainfall at station i on the day the annual maximum areal rainfall occurs in the year j, I is the number of stations, J is the length of the data records (years).

2.4.3 Rodriquez-Iturbe and Mejia

Rodriquez-Iturbe and Mejia (1974a) worked with the concept of effective precipitation. A relation for converting the point precipitation to effective precipitation for an area was established. The method developed was a general method and could be used for various areas. This method estimated the effective depths for discrete storms and long term mean effective precipitation including distribution of precipitation for multiple inputs in a rainfall model. A correlation distance, which was the mean distance between two randomly chosen points, was defined. The correlation factor representing this distance was given by:

$$ARF = \sqrt{E\{\rho(d)\}} \qquad (6)$$

where $E\{\rho(d)\}$ represented the expected value of the correlation coefficient for the derived correlation distance.

Although the approach used by Rodriquez-Iturbe and Mejia (1974a) is very simple and provides an extensive framework for transforming point depths to effective precipitation, it does not take into account the estimation of areal distribution for "design storms".

2.4.4 Bell

Bell (1976) developed geographically fixed areal reduction factors based on an empirical approach which was very similar to the approach followed in TP-29, the difference being that it also accounted for return period. Areal rainfall was calculated using Thiessen weights as weighted averages of annual maximum point rainfall values. The values obtained from the annual maximum areal series using Thiessen weights, and

the values of the annual maximum series of point rainfalls for each selected station were ranked. Using Thiessen weights, w_i, point rainfalls of the same rank were weighted and an annual series of weighted maximum point rainfalls was obtained. ARF_r, r representing rank, is the ratio of the areal precipitation of rank r to the Thiessen weighted average point rainfall of the same rank. This indicates the variation in ARF with rank, and therefore the return period. Mathematically, Bell's ARF is represented by:

$$ARF_r = \frac{\sum_{i=1}^{k}\left(w_i \widetilde{R}_{ij}\right)_r}{\sum_{i=1}^{k}\left(w_i R_{ij}\right)_r} \tag{7}$$

where $\widetilde{R}_{ij}$ = point rainfall for station i on the day the annual maximum areal rainfall occurs in year j, R_{ij} = annual maximum point rainfall for station i in year j, k = number of stations in the area

2.4.5   Myer and Zehr

Myers and Zehr (1980) developed depth-area curves based on a new approach which accentuates station pair data. The approach was used in the Chicago region where a dense gauging network covering the entire area was available. It was pointed out that *fixed area* areal reduction factors were the ratio of the expectation of areal average values to the expectation of the point precipitation depths for a given watershed area. Myers and Zehr (1980) underscored the importance of the effect of the return period on the depth-area reduction factors. One of the imperative inferences they came to was that lower depth-area reduction factors were associated with long return period

events than with the short return period events. The values of the factors they came up with are generally not intended to describe the spatial and temporal variability of the "design" storms. Also, by using these expectation values, the multifaceted and complete structure of the storm can not be described. Stochastic simulations (as discussed later) can also not be based on these values. Though the approach followed by Myers and Zehr (1980) is a useful one, it is a computationally complex one and is very difficult to implement in design practice.

2.4.6   Bacchi and Ranzi

Bacchi and Ranzi (1995) proposed a stochastic derivation of the geographically fixed areal reduction factors of the rainfall processes aggregated in space and time. A Poisson distribution of the number of high rainfall intensity processes was assumed, and a hyperbolic tail of probability of exceedence of rainfall intensity was adopted. The work was carried out in parts of northern Italy and the theory was supported by data collected from the analysis of radar maps. These set of radar maps were representative of the rainfall events taking place in that part of the country during the passage of the frontal systems. This theory was based on a stochastic approach and substantial modifications were introduced. The reduction factor was taken to be the ratio of areal and point precipitation intensity values, with the same duration and frequency of occurrence. The analysis was focused on the inference and the calibration of the distribution function aggregated process. The factors derived from the formulation of the statistical analysis were analytically complex and represented power law decay with respect to area and duration of the storm. From the research, Bacchi and Ranzi (1995)

were able to prove that the areal reduction factors depended upon the return period and the size, in space and time, of the domain (area) where the process was considered stationary and homogenous. The probability functions and the expected values of the directional derivatives of the processes were calibrated by analyzing radar data. The data of the cell value was checked with the corresponding rain gauge data collected for that particular place. The analysis of the maps showed that power law functions fitted well in the plots of the expectation of the absolute value of the derivative vs. the spatial and temporal scales of integration. A censored Pareto distribution was chosen for the inference of high intensity levels of rainfall due to its hyperbolic tail and because it could be expressed using a simple analytical expression. The parameters of the distribution were calibrated using the methods of moments. A further testing of methodology is required which should be based on the analysis of the different meteorological events of the convective type before these results can be used for further applications.

2.4.7   Sivpalan and Blöschl

Sivpalan and Blöschl (1998) presented a methodology for the estimation of the catchment IDF curves utilizing the spatial correlation structure of rainfall. This methodology had certain advantages over others as it overcomes the short comings of some of the works carried out by Rodriguez-Iturbe and Mejia, (1974b) by distinguishing between the scaling behavior of parent and extreme value distribution of the rainfall process. Additionally, this methodology takes into account a lesser amount of assumptions. It attempts to correlate different empirically based approaches with

approaches based on current scientific theories of space-time rainfall fields. This approach differentiates between the variance of the point precipitation and that of the areal processes and concludes that the variance of point precipitation is higher than the others. As recommended by Sivpalan and Blöschl (1998), the main control of the IDF curves is the rainfall spatial correlation length, which characterizes the storm type. The methodology adopted was carried out as follows. The foremost step was to specify the parent distribution of the point rainfall process. The exponential probability distribution of point rainfall intensities has been examined in many previous studies and, because of the success of this kind of distribution, it was stipulated in this approach (Sivpalan and Blöschl, 1998). Although they adopted an isotropic, exponential correlogram, the proposed methodology can be generalized for any other type of correlation structure and even for anisotropic situations. In the second step the point rainfall process was averaged over a catchment area. The next step involved the transformation of the parent distribution of the areally averaged rainfall process to the corresponding extreme value distribution. This was done by using the asymptotic extreme value theory as proposed by Gumbel in 1958. While carrying out this study it was assumed that the spatial random field of point rainfall intensities was stationary. This areal averaging produced certain effects such as decrease in the variance of the averaged process and variance reduction factor with increasing area. In other words, when the area becomes zero, the

reduction factor is equal to one and as the area approaches infinity, the variance reduction factor approaches zero. The value of this reduction factor depends upon the size and shape of the catchment and the correlation structure of the rainfall. It was assumed that the catchment was square shaped but this methodology can be generalized for different shapes also. Finally, in the last step the extreme value distribution were matched with observed extreme value distribution of point rainfall. Using this methodology the properties of the Gumbel distribution can be used to estimate the mean, standard deviation and coefficient of variation of extreme rainfall at the catchment scale. Areal reduction factors produced by this method were shown to decrease both with increasing catchment size and increasing return periods. It was also found out that areal reduction factors produced for very large return periods became a function of catchment area and the rainfall correlation structure. Therefore they became independent of particular rainfall regime i.e. point IDF curves.

The next figure (Figure 2) shows the plot of ARFs calculated by Sivapalan and Blöschl.
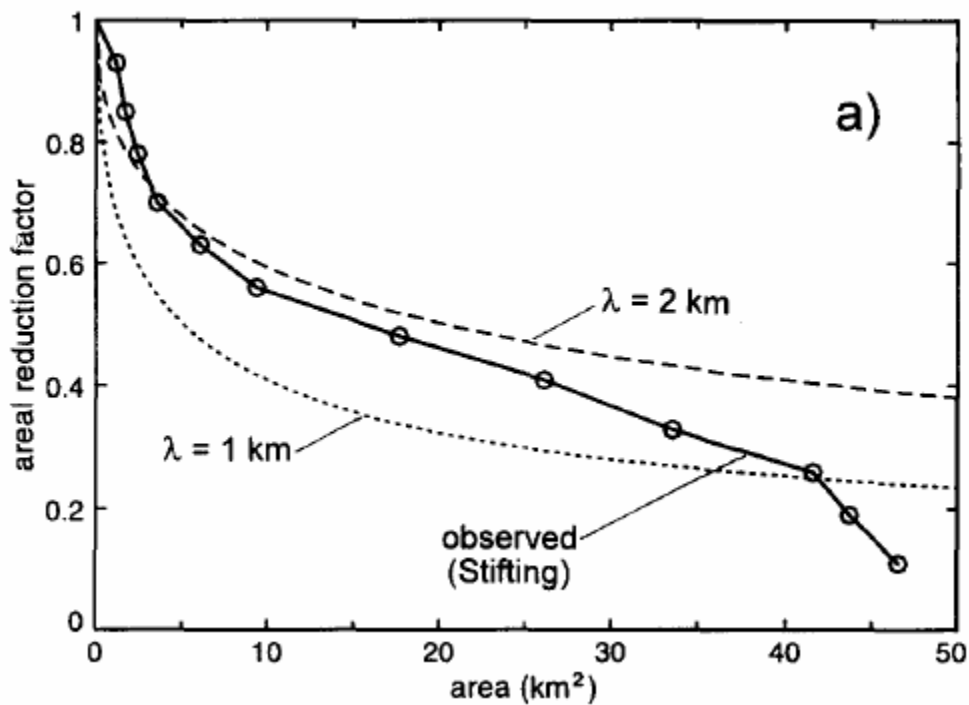
Figure 2. ARFs Calculated by Sivapalan and Blöschl (1998).

Though the methodology proposed by Sivpalan and Blöschl (1998) is an expedient one, but it cannot be used successfully at all times because of the crucial assumption of stationarity in space of the rainfall's random field. Therefore this approach cannot handle finiteness of the storm area and the possible partial coverage of the catchment area. Also it was noted that the mean of the areally averaged extreme rainfall decreased with increasing averaging area, which was not in compliance with the

methodology proposed by Rodriguez-Iturbe and Mejia (1974a). This is probably because the estimates of areal reduction factors derived by Sivpalan and Blöschl (1998) were applied to parent rainfall intensities and not their corresponding extreme rainfall intensities.

2.4.8 Michele, Naathbandu and Rosso

Michele et al. (1999) presented a method for modeling the geographically fixed areal reduction factors for the storm rainfall using the concepts of scaling and multiscaling which provides a dominant framework for studying the temporal and spatial variability of the different hydrological processes. They proposed that the areal reduction factors reflected the scaling properties of rainfall in time and space. The concepts of dynamic scaling and statistical self affinity was used a physical formula for the areal reduction factors was obtained. These concepts were applied first to the rainfall processes and then to the areal reduction factors. Then the relative scaling relation with area and duration were proposed. The study was carried out in Milan, Italy and United Kingdom. It indicated that storms rates in time and space are scalings for extreme events. The rainfall was clumped for area of 0.25 to 300 sq.kms. and for time durations of 20 mins to 6 hours. Annual maxima rainfall values of average rainfall intensities were obtained using the method of kriging. Scaling properties were then applied. It was observed that the dynamic scaling exponent for Milan was equal to one, indicating that there was isotropic behavior of rainfall. A dynamic scaling relation of average rainfall intensity in area and duration was obtained. From this relationship they obtained intensity depth area frequency (IDAF) curves and a particular case of intensity

duration frequency curves (IDF). Then combining both IDAF and IDF curves Michele et al. (1999) obtained the areal reduction factors for that region. The results of the study significantly support the conjecture which scaling holds for the storm rates, in time and space, taking into consideration the extreme events. Further data analysis is needed to assess the variability of scaling exponents with geography and climate.

2.4.9 Asquith and Famiglietti

Asquith and Famiglietti, 2000 proposed that effective depths for a watershed area were computed by multiplying areal reduction factors developed for that particular area by the point rainfall depths. The areal reduction factors calculated were dependent upon watershed characteristics such as the area, shape of the watershed and the recurrence interval which represent the storm characteristics. They put forward a new approach termed as the *Annual Maxima Centered* approach which considers the distribution of concurrent precipitation surrounding the annual-precipitation maxima. This approach requires the achievement of the following steps. For every annual maxima in the rainfall database the ratio of the annual maxima depth to the concurrent precipitation is calculated and then the separation distance between the rain gauges is calculated. Then from the sample ratios a description of relation between criteria conditioned sample ratio value and separation distance is given. These relations are defined by specific functions fitted to the empirical ratio relation. This produces a best fit line that gives the expected ratio. Then from this the areal reduction functions are computed for a user defined area and design criteria. Empirical depth–distance relations provided the basis of this approach of annual maxima centered areal reduction factors.

This kind of approach was adopted for the calculation of areal reduction factors for the cities of Austin, Houston and Dallas in Texas. There was a large database of precipitation data available for Texas and so this approach could be applied there. It did not require spatial averaging of precipitation.

2.4.10 Durrans, Julian and Yekta

Durrans et al. (2003) carried out a research which was believed to be the first one for the evaluation of the potential of NEXRAD radar-rainfall data for the development of geographically fixed depth-area relations. The use of radar-rainfall data for the development of depth-area relationships was evaluated and the potential problems that might hinder the use of such kind of data were identified. They explained that radar data like rainguage data have certain limitations but along with representing a rich source of information on the spatial coverage of rainfall, they can also be expected to become more reliable with the passage of time. Multisensor (radar + rainguage data) Data was provided for their study by the NWS Hydrologic Research Laboratory for a period of 7.5 years. These were recorded for the Arkansas-Red Basin River Forecast Centre. Extension of this study has been carried out in this research.

2.4.11 Omolayo

In a study conducted by Omolayo, 1993 the meaning and the significance of the areal reduction factors for flood frequency studies was estimated. The reduction factors were differentiated and categorized into various types. Areal reduction factors calculated for one region can be transposed to different regions assuming the fact that

the regions being taken into account are climatically similar. Omolayo (1993) transposed the 1 day Areal reduction factors for U.S. to Australia, since the two have similar mean annual rainfall, mean annual temperature, etc which make them climatically similar. One day raingauge data was obtained for duration of nearly 30 years from Commonwealth Bureau of Meteorology in Melbourne and Sydney. Different methodologies like U.S. Weather Bureau method, UK method, Bell's method and Iturbe and Mejia's method were used for the transposition of the areal reduction factors. The results obtained were then compared for eight major cities in Australia. The shortcomings of this study were that variation of Areal reduction factors with return periods were not been taken into account and also Areal reduction factors for areas smaller that 100 sq. kms. could not be calculated due to the wide scatter of stations.
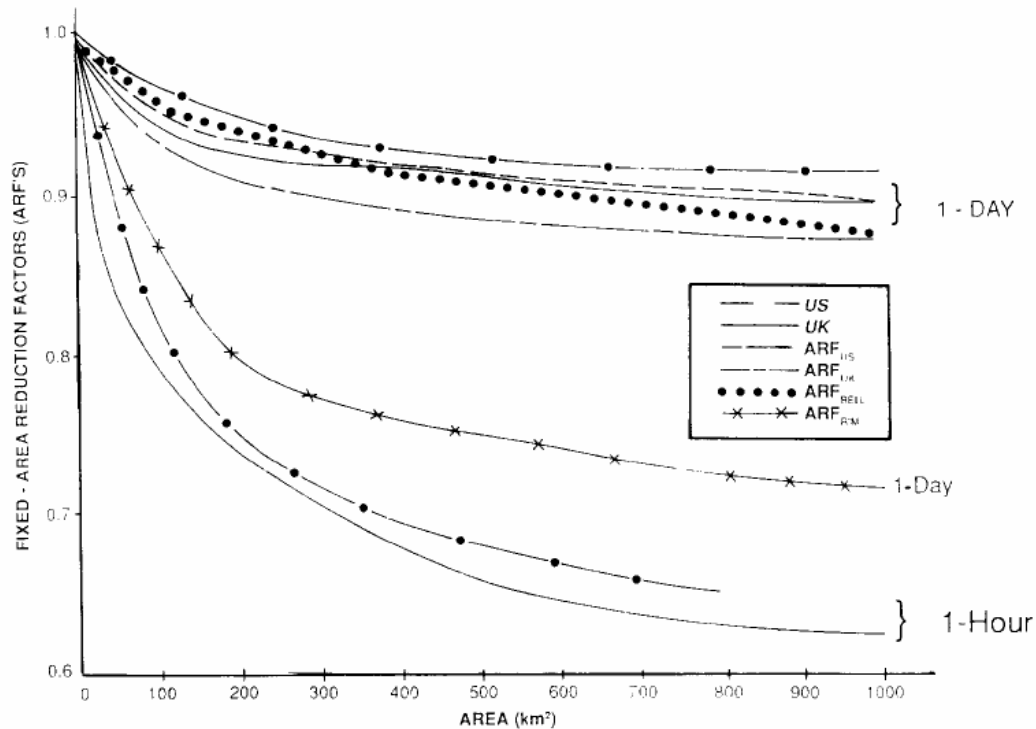
Figure 3. ARFs (Calculated by Omalayo,, 1993).

The above figure (Figure 3) shows the ARF values calculated by Omalayo.

2.4.12 Rakhecha and Clark

Rakhecha and Clark, 2002 provided distribution of areal rainfall for the first time for India. They developed areal reduction factors which were based on envelope curves of major storms to give areal reduction factors for areas of 10-20000 sq. km. The factors calculated varied between 1 and 0.41 but there was no real difference between different durations of rainfall. These values were then multiplied by one to three day Probable Maximum Precipitations (PMP) and corresponding maps describing the spatial distribution of areal PMPs was provided.

2.4.13 Einfalt, Johann and Pfister

Einfalt et al., 1998 pointed out that the validity of point rainfall data of hydrological simulations had been approached by the use of areal reduction which depended upon recurrence interval, area of the catchment and block interval. But in reality actual events did not obey the block interval classification. The spatial distribution of rainfall is highly dependent upon weather type and local climatic variations may cause a spatially varying relationship to point rainfall measurement station. Hence it was suggested that there was a need to classify the events as a function of rainfall volume, general weather type, subcatchment and the season. The main objective of their study was to establish a relationship between the different parameters like spatial variability of rainfall volumes and weather type, season, geographic location, etc. and the deviation of areal rainfall from the station data of the long term rainguage used for design studies. The rainfall data employed was continuously used measured data series and not design storms as used in traditional approaches for determining ARF.

2.5 RAINFALL MODELS

The practical need for studying the spatial and temporal variability of rainfall over an area has compelled many researchers to come up with new space-time rainfall models. The use of space-time rainfall models leads to a more realistic estimation of design storm (and floods) and areal reduction factors for rainfall. They have gained importance because of the limitations of measuring rainfall both in time and space using other techniques. Different models have been proposed as an appendage to the

measurements. Different statistical models can be defined for the rainfall processes. They can be distinguished from one another by their representation of rainfall in time and space. There are three general classes of rainfall models. They are:

2.5.1 Spatial Models

These are used to represent the spatial distribution of storm's total rainfall over a specified duration. There are two general types of spatial models in used at present. They are 1) Gaussian random field models and 2) Cluster models. Model applications for these types of models include designing of precipitation sensor sampling strategies and precipitation frequency analysis.

2.5.2 Temporal Models

These are used to represent the rainfall accumulations at a fixed point over time. There are two general types of temporal rainfall models. They are 1) Discrete Models and 2) Continuous Models. For discreet models, fixed length time intervals (often daily or hourly) are used to divide the time scale. Markov chains and their generalizations are used to describe the rainfall occurrences in these types of models. For continuous models the time interval is not constrained to fall into discrete intervals. For these kinds of models Poisson processes and their generalizations are used for defining rainfall occurrences.

2.5.3   Space Time Models

These kinds of models have come into being from the cluster models framework introduced by LeCam. According to this kind of framework, model rainfall is developed from raincells organized into larger rain bands having individual life cycles and trajectories. These have been used for assessing sensor design and assessment of the role of spatial variability of rainfall in determining spatial characteristics of infiltration.

2.6   RAINFALL MODEL STUDIES

Work on Gaussian models has been done by Bras and Rodriquez-Iturbe, 1985. Cluster models are more in use these days and a combination of recent developments in meteorology with LeCam modeling has produced many sophisticated space-time rainfall models (Gupta and Waymire, 1993 and Waymire et al., 1984; Waymire and Gupta, 1981a, 1981b). Statistical and scaling properties of precipitation time series have been extensively addressed (Waymire and Gupta, 1981a; Zawadzki, 1973). Different point rainfall models have been proposed based on these properties (Rodriguez-Iturbe and Mejia, 1987). Spatial and temporal rainfall models are somewhat different from one another and their stochastic modeling has been developed based on at least three different methods (Austin and Houze, 1972; Zawadzki, 1973; Lovejoy and Schertzer, 1985; 1990; Gupta and Waymire, 1993). Over and Gupta, 1996, follow the approach that exploits self-affinity relationships to produce rain-rate through an iterative random cascade process. Another approach uses the generation of random space-time functions to generate fields with specified spatial-temporal covariance

structures (Rodriguez-Iturbe and Mejia, 1974a; Bell, 1987; Bellin and Rubin, 1996). Still another approach is based on stochastic modeling of the physical processes occurring during a rainfall event (Bras and Rodriguez–Iturbe, 1985; Waymire et al., 1984)

Smith and Krajewski (1987) developed a statistical framework for modeling space-time rainfall using radar and rain gauge data. The cluster model developed was applied to daily rainfall fields in the tropical Atlantic region covered by the GATE experiment (Hudlow and Patterson, 1979). This form of the model dictated three tasks which had to be followed. The first step was referred to as sampling and it determined the relationship between measurement of rainfall fields and the actual values of rainfall. The next step was to determine a rainfall model which fitted the data. The temporal evolution of the model was governed by a Markov chain. It assumed a method in which circular raindrops were organized in ellipsoidal rainbands which were randomly distributed in a plane. Geometry of the rainband was specified using radius of the major axis, radius of the minor axis and the orientation of the major axis from north to south. A method for estimating parameter values for the probability model was also determined in the study. Finally the statistical model developed was applied to the Atlantic tropical region. The sampling model in their study was based on the assumption that the advantage of rain gauge data is accuracy of time integrated observations while the strength of radar is the ability to see the areal extent of rainfall fields.

Due to widespread use of rainfall models, the Australian Bureau of Meteorology operates a suite of Numerical Weather Prediction models (NWP). The latest project

developed a model for characterizing the spatial and temporal properties of rainstorms for various climate regions of Australia. The aim of the project was to develop a nowcasting model for forecasting spatial rainfall and developing a statistical method for seasonal rainfall. This model can be used by researchers requiring spatial temporal storm characteristics for design purposes. Thomas and Gupta introduced a class of space time causal multifractal models based on discrete random cascades describing the properties of the model and comparing these with Poisson point process-based models. Substantial progress has also been made by WRSRL in the development and application of stochastic point process and rainfall field models. The two important modeling systems evolved from these are a) RAINSIM-a rainfall time series analysis and simulation package suitable for hydrologic studies requiring long generated time series at one or more sites and b) MTB-a stochastic space-time rainfall field modeling system which can be used for the simulation and forecasting of frontal rainstorms.

3. WEATHER RADAR DATA

3.1 USE OF RADAR PRECIPITATION DATA

For successfully modeling hydrologic processes, precise estimation of the spatial distribution of rainfall is crucial. Historically, rainfall distributions were estimated by assuming spatial geometry related to point rain gauge observations by using techniques like Thiessen polygons, inverse distance square weighting, kriging techniques etc. (Allen, 2003). Improvements in technology have made radar a viable tool to improve the estimation of rainfall distribution and hence calculation of areal reduction factors. Nowadays radar–derived rainfall data are used which provide a high resolution view of the distribution of rainfall. In USA, one of the most commonly used radar-data set is one which has been collected by S-Band weather surveillance radar 1988 Doppler (WSR 88D). In the 1980's, the National Weather Service deployed the WSR-88D radars for reliable data estimations (Hudlow et al., 1979, 1991). These kinds of radar have been deployed all over the U.S. at about 160 sites. Computer algorithms are used to convert the radar data into hydrometeorological data.

Beginning from the early 1940's, RAdio Detection And Ranging (RADAR), has been in use to remotely judge the environment (Allen, 2003). Radio waves, also called microwaves, were used to detect the existence and the positions of the various objects. Due to this special characteristic of the radar, it is used in many diverse fields which include geology, engineering, meteorology, astronomy etc. Weather radars have been in use for almost 50 years now (Allen, 2003). But the implementation of these radars has been a slow process. In 1953, the U.S. Weather Bureau introduced the WSR-57s

(Weather Surveillance Radar-1957) (Kessler, 1990). By the 1960s, the U.S. had a widespread network of 56 WSR-57s (Kessler, 1990). These were primarily used by the researchers for severe weather studies like tornadoes, thunderstorms etc. During the early times there were only 37 radar systems across the U.S. and all images contained three VIP (Video Image Processing) levels (WSI, 2004).

3.2 NEXRAD DATA

The National Weather Service's Next Generation Weather Radar (NEXRAD) Program was established in 1980 and its aim was to deploy and bring online 137 new NEXRAD radars (called WSR-88D) throughout the country (WSI, 2004). These were based on Doppler effect and have significant improvements over conventional (WSR-57/74) radars. NEXRAD program is a federal government program supported by the National Weather Service (NWS), Federal Aviation Administration, and Air Force Air-Weather Service and Naval Oceanography Command. This collaborative between these three agencies have resulted in the delivery of over 160 S-band Weather Surveillance Radar-1988 Doppler (WSR-88D) radars across the U.S. Initially, these radars were deployed in 1991 and some of the last ones in 1997 (WSI, 2004). The NEXRAD program has been a focal component of the ongoing technology modernization of the NWS and has revolutionized weather forecasting in the U.S. (Fulton et al., 1998).
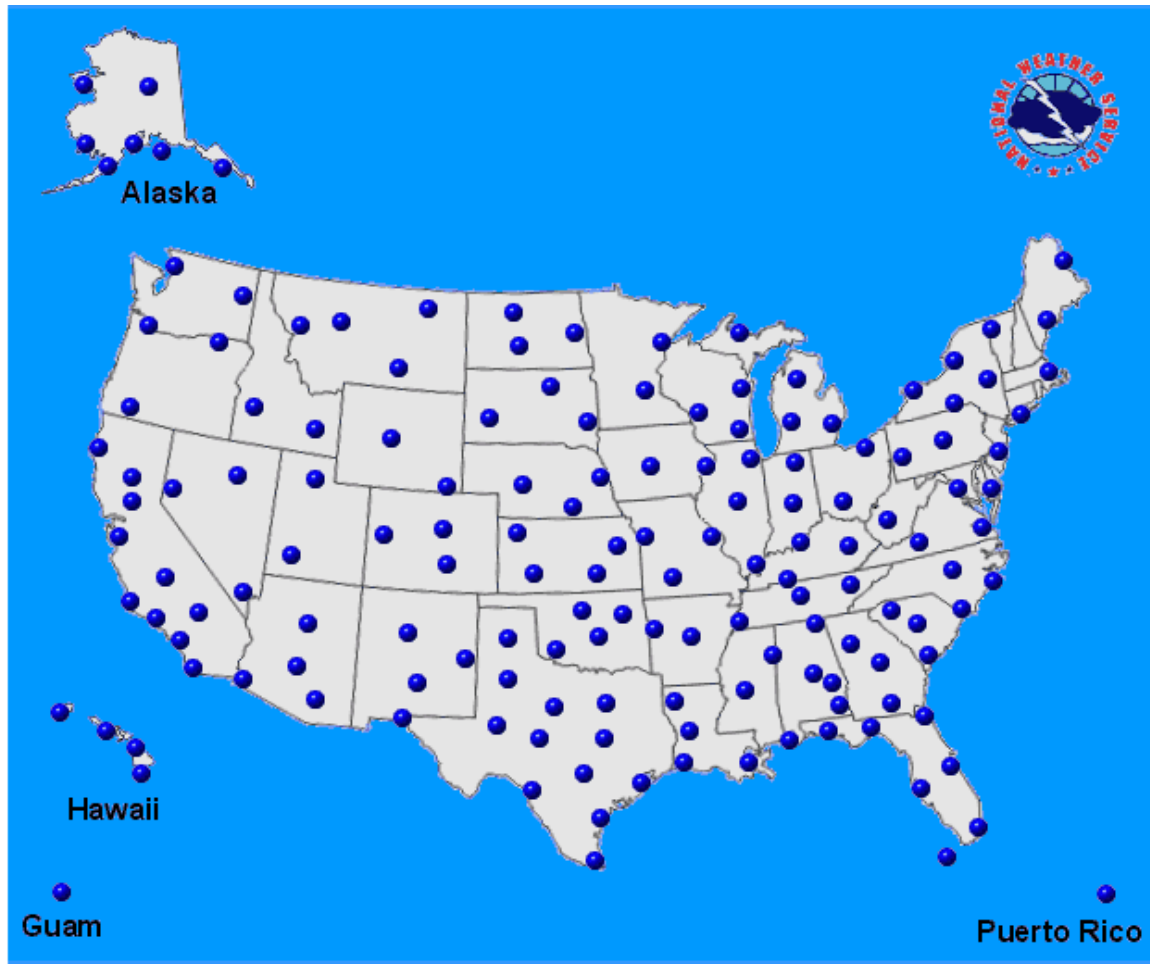
Figure 4. NEXRAD Weather Radar Sites All Over the U.S. (NWS, NOAA, 2005).

Figure 4 illustrates the various NEXRAD sites located over the whole of United States.

3.3 TYPES OF NEXRAD DATA AVAILABLE

NEXRAD precipitation is in the Hydrologic Rainfall Analysis Project (HRAP) grid of 4,762.5 sq. m (approximately a 4x4 sq. km. grid). The projection of this HRAP grid is spherical polar stereographic projection, with an earth-centered datum of radius 6371.2 km. The secant polar Stereographic projection has a standard (true) latitude of

60° North and a standard longitude (longitude of the projection center) of 105° West. One of the main products produced is the Hourly Digital Precipitation Array (DPA). The DPAs contain 1-hour estimates of rainfall on HRAP grid. Figures 5 and 6 show the HRAP grid covering the state of Texas.

Study Area, Texas　　　　　　　　**HRAP grid**
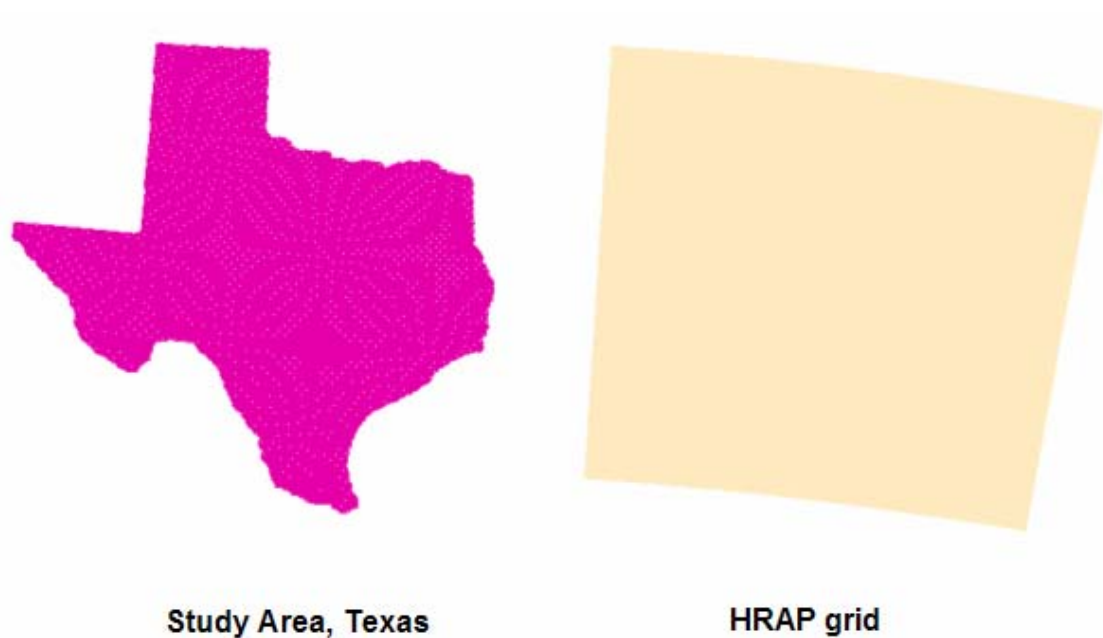
Figure 5. Study Area and HRAP Grid for Texas.

Figure 6. HRAP Grid Covering Texas.

These DPAs are one of two main inputs to the Stage II/III Public Product Service (PPS). There are 4 NEXRAD DPA precipitation products: Stage I, Stage II, Stage III, and Stage IV (also called the MPE data) (NOAA, NWS, 2004a; 2004b; NSLL, 2004).

3.3.1 Stage I

Stage I product is the Hourly Digital Precipitation (HDP) directly derived from Z-R (th-Reflectivity) relationship, with some quality control algorithms applied. The first stage of the PPS is the ingesting of the radar precipitation data. The DPA is a

digital precipitation estimate generated by radar at the top of each hour which has a size resolution of 4 by 4 kilometers and a high data resolution of 256 processing levels. The only quality control which the DPA goes through is the quality control features associated with the WSR-88D precipitation algorithm itself (Allen, 2003).

3.3.2 Stage II

Stage II is the HDP product which is merged with some gauge observations, with mean field bias corrected by using a kalman filter algorithm (Smith and Krajewski, 1991; Seo, 1998). Continental United States (CONUS) stage II precipitation is created by the National Centers Environmental Prediction (NCEP). Recent data can be downloaded from the following site:

http://wwwt.emc.ncep.noaa.gov/mmb/ylin/pcpanl/stage2/. Tape archive from the National Center for Atmospheric Research (NCAR), are available from 1 May 1996.

3.3.3 Stage III

Stage III is the product covering an entire River Forecast Center (RFC) by combining multiple radar stage II products, the combined field is constructed using the average of all stage II estimates available for each HRAP cell (Fulton et al., 1998). Stage III can involve a significant degree of human interaction (Fulton et al., 1998). The archived data from Dec. 1994 can be downloaded from:

http://dipper.nws.noaa.gov/hdsb/data/nexrad/wgrfc_stageiii.html.

3.3.4 Stage IV

Stage IV is mosaicked RFCs stage III product covering the CONUS, created by the NCEP. Recent data can be downloaded from:

http://wwwt.emc.ncep.noaa.gov/mmb/pcpanl/stage4/. Tape archive at the National Center for Atmospheric Research (NCAR), are available from 1 Jan 2001.

Some of these significant improvements of the WSR-88D are the ability to see motion using the Doppler effect, their increased sensitivity which allows one to view atmospheric conditions, such as cold fronts, dry lines, and thunderstorm gust fronts, their improved resolution, and finally their volume scanning function which can give you three dimensional view of the weather.

3.4 COMPONENTS OF NEXRAD

NEXRAD stands for Next generation Radars and they consist of 3 main components as can be seen from Figure 7 (American Met. Society, 1993).
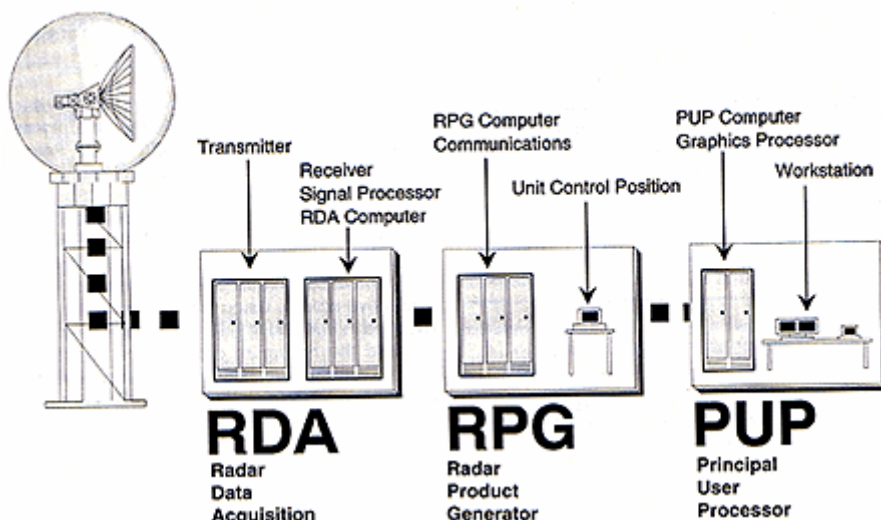
Figure 7. Components of NEXRAD Image (AM, 1993).

3.4.1 Radar Data Acquisition Unit (RDA)

It is a unit which transfers energy and receives the return signals. It consists of a transmitter, receiver, antenna and signal processing circuitry. It is referred to as the data collection point and is used for the conversion of analog signals to digital data. It is in this part that the ground clutter is suppressed, and range ambiguities corrected. It produces a stream of raw digital data and no product is available at this stage.

3.4.2 Radar Product Generator (RPG)

The raw data is sent to this unit and then it is passed to algorithms which create products. There are several (more than 75) base data quantity products which are developed. From these base products a number of derived products are produced like tornadic vortex signature (TVS), vertically integrated liquid (VIL), hail index (HI) and rainfall accumulation estimates (Klazura and Imy, 1993). The three base products are reflectivity, spectrum width and velocity.

3.4.2.1 Reflectivity

It reflects the amount of moisture present in the beam volume and hence the air. It depends upon size, shape, number and state of the particles on which the radar beam falls. Ideally large drops will have more density and hence give larger reflectivity values. It is calculated from the power returned from a series of radar transmitted pulses. To get a fairly good statistical sample for reliable reflectivity measurements, data from about 20 pulses is required.

3.4.2.2 Spectrum Width

It is related to turbulence in the air. It represents the variation in the radial velocities. In order for radar to calculate velocity accurately, numerous pulses of energy must be sent out into the area being sampled. Each of these pulses will return a certain velocity measurement and Spectrum width is the pulse variation of these velocities. The larger the spectrum width the more is the turbulence.

3.4.2.3 Radial Velocity

It represents the wind velocity i.e. the speed of the particles towards or away from the radar antenna. A radial velocity value of zero means that there is no movement of air in the direction of the radar. Radial velocity is calculated from the frequency shift of the returned signal. The signals returned to the radar are not the same as those transmitted from the radar if targets sampled by the radar are moving. The radar calculates the frequency shift and relates it to particle speed.

There are different modes in which the radar can work. In clean air mode, the radar is updated every 10 minutes. In precipitation mode, it is updated every 6 minutes and in the severe weather mode, it is updated every 5 minutes. Weather Services International's (WSI) rainfall estimation procedure uses a dynamic weather condition based algorithm to convert reflectivity values to rainfall estimates. They use a variety of weather parameters to track the weather condition and then choose the most appropriate conversion from reflectivity to rainfall rate.

3.4.3 Principle User Processor (PUP)

This is a workstation where the information obtained can be displayed. The information displayed can be in the form of alphanumeric or graphic formats and can be converted from one type to another. Figure 8 shows a schematic diagram of it.
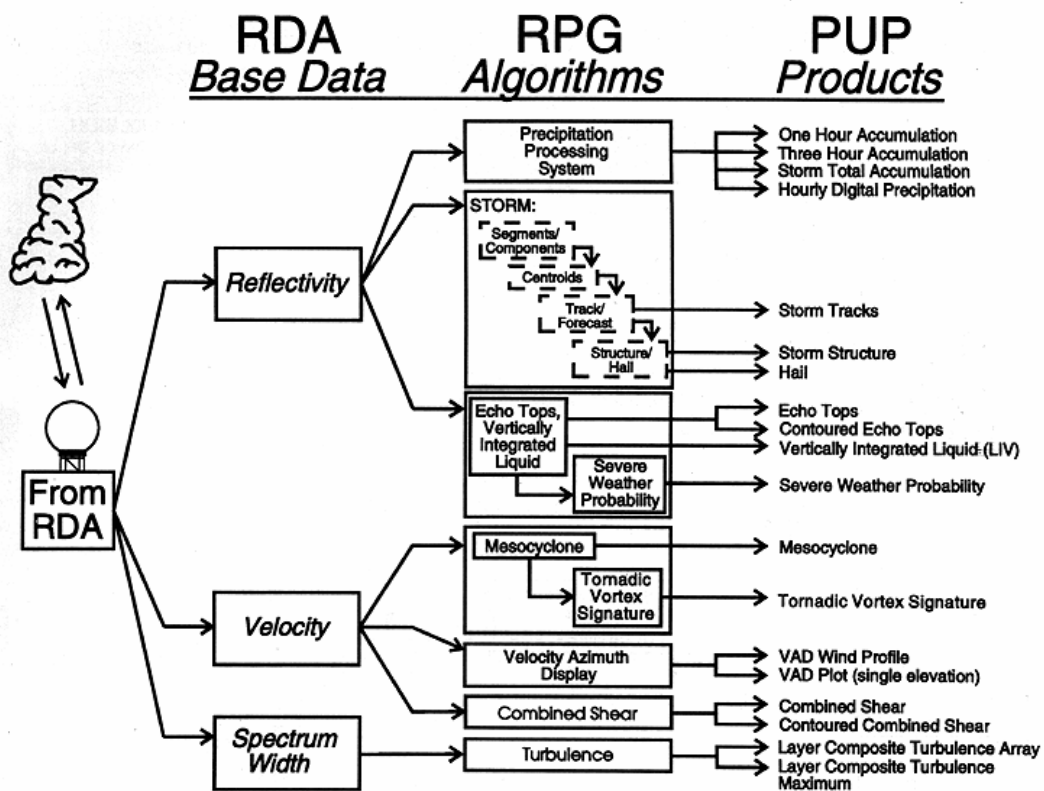
Figure 8. A Schematic Diagram of Different NEXRAD Units and Their Products (AMS, 1993).

3.5 NEXRAD SCANNING STRATEGIES

The WSR-88D radar employs the use of Scanning Strategies in its operation (NOAA, NWS). It has a computer controlled radar antenna and so the operator cannot manipulate the antenna angle or the rotation direction or its rate like in the conventional manual one. One complete revolution of the antenna at a constant angle is called an elevation scan. The radar antenna does "volume scanning" i.e. it automatically rotates through a predetermined number of elevation angles in a preset amount of time. There are currently three strategies used for volume scanning

3.5.1 Strategy 1

Antenna rotation through fourteen angles in five minutes: This strategy also called Volume Coverage Pattern 11 is a precipitation mode, and sometimes called a severe weather mode. This is because more part of the atmosphere is covered in a short duration of time. With the help of this strategy details on storm structure can be determined, especially for storms which are closer to the radar. But this puts a heavy processing load on the system and so it is not used unless necessary.

3.5.2 Strategy 2

Antenna rotation through nine angles in six minutes: Strategy 2 also called Volume Coverage Pattern 21 is also a precipitation mode, with somewhat less information being gathered in a longer period of time. In this way it reduces the load of the product generating processor along with giving quite a bit of details. Every time

precipitation is first detected, this is the standard mode of operation. If the weather turns severe under any circumstances then strategy 1 can be activated.

3.5.3 Strategy 3

Antenna rotation through five angles in ten minutes: Strategy 3, called Volume Coverage Pattern 31 or Volume Coverage Pattern 32, is a clear air mode, in which the antenna is rotated very slowly, and as much information as possible can be gathered from the very small particles in the atmosphere such as insects, cloud droplets and refractive index gradients. The display thresholds are lowered to suggest the fact that only very small amounts of energy are returning to the radar.

The scanning strategy determines the number of angles scanned in a given interval of time and can have more than one Volume Coverage Pattern associated with it. The two terms are often interchangeable but should not be confused with one another. Currently three scanning strategies and four Volume Coverage Patterns have been defined.

3.6 PRECIPITATION ALGORITHM FOR NEXRAD

As already discussed in the RPG raw data is passed through algorithms with the help of which products are created. This precipitation algorithm PPS, is very complex in nature. It contains 46 adaptable parameters which controls the radars performance (Fulton et al., 1998). These are designed to optimally measure and convert the backscattered energy into rainfall accumulations. The algorithms present in the RPG consist of various quality control routines, including partial beam blockage, ground

clutter suppression, and range degradation correction, as well as the hybrid scan look-up table (which gives the optimal radar elevation angle to use for a given distance and direction), reflectivity to rain rate conversion, hail correction and gauge-radar adjustment.

The algorithm consists of five main scientific processing components called "sub-algorithms". The five scientific sub-algorithms are: 1) preprocessing, 2) rainfall rate, 3) rainfall accumulation, 4) rainfall adjustment, and 5) precipitation products. It also contains two external support functions which execute independently of the main algorithm. They are precipitation detection and rain gauge data acquisition. As long as the first support function determines the occurrence of rain the five major processing steps of the precipitation algorithm execute in sequence.

The base reflectivity data goes through a preprocessing stage. It includes quality control step, corrections for beam blockage using a terrain-based hybrid scan, check for anomalous propagation (AP), and bi-scan maximization. In the next step the base reflectivity data is assigned a rainfall rate using a conversion known as a Z/R relationship. Again at this stage quality control is executed and correction is made for range degradation. Then precipitation accumulations are determined. Here along with simultaneously running clock hour accumulations, scan to scan accumulations are interpolated. After the precipitation adjustment algorithm is run precipitation products are generated. These are updated every volume scan.

3.6.1 Limitations of the Precipitation Algorithm

3.6.1.1 Radar Reflectivity Calibration

If the value of reflectivity (returned power) from a rainfall target is very large or very small then precipitation estimates can be subjected to significant error. Chrisman et al., 1999 have done an in depth study on this issue. Using internally generated test signals, the WSR-88D calibrates reflectivity every volume scan. For standard Z/R relationship ($Z=300R^{1.4}$), these calibration check should maintain an accuracy of 17 %, i.e. around 1 dB. Various factors including hardware problems causes reflectivity values to change over time. Since radar reflectivity calibration is such a critical tool in improving precipitation estimates, the WSR-88D Radar Operations Center (ROC) has developed absolute calibration procedures which make certain that reflectivity data is within +/- 1 dBZ (Allen, 2003).

3.6.1.2 Proper Use of Adaptable Parameters

There are several adaptable parameters which have to be optimized in the precipitation algorithm, the most impotant being the Z/R relationship and the "maximum precipitation rate". Default values of these are given by: $Z=300R^{1.4}$ and "maximum precipitation rate" = 53 dBZ. These estimates have been established to eliminate the hail effects on rainfall estimates but higher rainfall rates were observed. In the tropical rainfall regimes, where larger diameter drop sizes exist (Baeck and Smith, 1998), extreme precipitation occurs and to compensate for this a new Z/R relationship, called the Rosenfield tropical Z/R relationship ($Z=250R^{1.2}$) is used. With the use of this

relationship significantly more rainfall is determined for reflectivities higher than 35 dBZ (Vieux and Bedient 1998). Changing the Z/R relationship leads to the radar operator changing the maximum precipitation rate parameter so that higher rainfall rate can be used in the accumulation function of the precipitation algorithm. Therefore changes in Z/R relationships and maximum precipitation rate values can have a great impact on rainfall estimation. Other Z/R relationship in use these days are the Marshall-Palmer relationship ($Z=200R^{1.6}$), and two cool season stratiform relationships (East $Z=200R^{2.0}$ and West $Z=75R^{2.0}$) (Vieux and Bedient 1998).

3.6.1.3 Hail Contamination, Bright Band, Snow, and Sub-Cloud Evaporation

Frozen and wet frozen precipitation causes significantly enhanced reflectivity values (Wilson and Brandes 1979). As hail stones become larger and as ice crystals fall through freezing levels, they reflect high amounts of power back to the radar which can be higher than that returned from the actual precipitation. Due to this high amount of power reflected precipitation estimates are overestimated and also leads to bright band enhancement. Snow flakes can be sampled very easily by the radar but improper Z/R Relationships lead to underestimation of the values (Wilson and Brandes 1979). Sub-cloud evaporation below the radar beam causes overestimation of the values. This occurs when the rain falls into a dry sub-cloud layer. This may give fairly accurate rainfall estimates in the cloud but these estimates become either too high or to high as the rain reaches the ground.

3.6.1.4 Range Degradation

Partial beam filling results in signal degradation which results in rainfall rates being reduced. Currently range correction is not implemented on WSR-88D radars (Wilson and Brandes 1979). Other problems include stratiform rains which show strong vertical reflectivity gradients. This remains positive till the "bright band" and then it decreases sharply. Sharp reflectivity events show reasonably strong range degradation. The reflectivity values show a sharp decrease with height and the radar underestimates more as its beam increases with altitude. Therefore the beam height becomes the single contributor to radar rainfall underestimations (Chrisman and Chrisman, 1999). Also another problem is that in stratiform rains, rainfall underestimation occurs due to radar beam overshooting the precipitation at far ranges which is a problem of lack of detection.

3.6.1.5 Anomalous Propagation (AP) and Clutter Suppression

In a WSR-88D reflectivity returns are displayed at locations where the beam is refracting normal to a standard atmosphere. But during several times, layers with large vertical gradients of temperature and water vapor experience deviations from these standard conditions. This leads to superrefraction of the radar beam which in turn leads to inaccurate calculation of the actual beam height. These changes, which occur in the lower troposphere, lead to persistent and quasistationary returns of high reflectivity. This anomalous propagation can lead to extreme precipitation accumulations from false echoes. The WSR-88D employ default clutter suppression which allows the radar operator to define further clutter suppression regions to eliminate AP (Chrisman and

Chrisman, 1999). But this capability depends upon the radar operator's ability to recognize the AP and react quickly to it. The tilt test algorithm further accounts for AP. This algorithm rejects the lowest tilt (0.5°) if areal echo coverage of the tilt just above it (1.5°) is reduced by an amount greater than that expected from meteorological targets (Fulton et al. 1998). But sometimes improper clutter removal can lead to underestimation of the rainfall rates.

3.6.1.6 Beam Blockage

In many parts of western U.S., which have mountainous regions, one of the major problems is that of beam blockage. Blockages of more than 60% and 2° in azimuth is common and have no corrections applied to them. The WSR-88D employs a terrain-based hybrid scan (Chrisman and Chrisman, 1999), so radials which experience beam blockages of more than 60% and more than 2° in azimuth use the next higher elevation slice for the PPS for that radial (up to a maximum elevation to the 3.4° slice). This leads to range degradation which results in the underestimation of precipitation estimates.

3.6.1.7 Attenuation

In case of precipitation estimates wet radome and intervening precipitation are the principal attenuators of energy to and from the target. Both being small for S-Band wavelength, still attenuation caused by them have a great impact on the rainfall estimates. Because of this effect there is often underestimation of rainfall estimates

during heavy rains. The gaseous attenuation of the microwave signals is corrected by the radar and so that does not cause any problems in rainfall estimation.

3.6.1.8 Polarization

WSR-88Ds are single, horizontal, linear polarized radars. Dual polarization radar measurements of a specific differential phase at two orthogonal polarizations (vertical and horizontal) have shown to give better results than linear polarized radars. With the help of vertical polarization additional hydrometeor microphysical information can be obtained. This can help obtain more precise and improved precipitation estimates.

3.7 DISTRIBUTION OF NEXRAD DATA

NEXRAD data is distributed all over the United States by the National Weather Service River Forecasting Centers (RFCs). There are in total 12 RFCs throughout the country which are responsible for collecting and distributing this data. The data obtained for this study was obtained by the West Gulf River Forecast Centre (WGRFC). This section gives a description about the WGRFC.

3.7.1 About WGRFC

Founded in 1961 at Fort Worth, Texas, the West Gulf RFC was given the responsibility of hydrologic forecasting for the Rio Grande basin and the Texas rivers which drain into the Gulf of Mexico (NOAA, NWS). Before the formation of WGRFC, this area was served by several River District Offices (RDOs) with long, narrow areas

of responsibility, none of which had a full-time hydrology position. Due to the floods of April-May 1957 across the entire southwestern United States, it was decided that there should be one RFC which should serve the entire region. Another reason for its formation was a detailed report on "River Forecasting and Hydrometeorlogical Analysis" to the Select Committee on National Water Resources of the U.S. Senate, dated Novmeber 1959, because it showed New Mexico and most of Texas as an area not covered by an RFC and clearly defined a need to complete RFC coverage for the entire nation.

The WGRFC area of responsibility has fundamentally remained unchanged since the RFC was formed in 1961, except for the transfer of the Calcasieu basin to the Lower Mississippi RFC (in Slidell, LA).

3.7.2 Area of Responsibility

The area covered by WGRFC is defined by the numerous Gulf of Mexico draining river basins of Texas along with the New Mexico, Colorado, and Mexico portions of the Rio Grande basin. The WGRFC area of responsibility covers more than 315,000 square miles (815,000 square kilometers) of land in the United States and over 87,000 square miles (225,000 square kilometers) in Mexico. The rivers covered by the WGRFC include:

- Brazos River

- Colorado River

- Guadalupe River

- Lavaca and Navidad Rivers

- Neches River

- Pecos River

- Rio Grande River

- Sabine River

- San Bernard River

- San Antonio River

- San Jacinto River

- Trinity River

3.7.3 Climatic Characteristics

A significant diversity of climates exists across the WGRFC area of responsibility. The eastern portion is classified to have humid mesothermal, temperate, with no dry season. In the central portion of the area covered by WGRFC, the climate gradually changes from middle latitude prairieland in the north and subtropical prairieland in the south. In the far western portions, climates are highly localized with respect to elevation and range from subtropical desert in the south to middle latitude steppe and highland climates in the north. In the eastern two-thirds parts of the area, significant precipitation events can crop up during any month of the year, but in the western third they are more concentrated around the summer/early fall thunderstorm season. There are heavy winter snowfalls in the Rocky Mountains portion of the area. Hourly records gathered by the WGRFC herald that heavy precipitation events can occur at any time of the day.

Most of the eastern portion of the WGRFC area is flat or low hills, sloping gradually to the southeast. The western portion of the area is subjugated by high mountain ranges separated by wide, semi-arid valleys. In the northwest porton fo the RFC area, the headwaters of the Rio Grande rise in the Rocky Mountains, with some peaks exceeding 14,000 feet (4,300 meters).

3.7.4 Hydrologic Characteristics

Hydrologic events are usually caused by excessive rainfall or occasionally by spring snowmelt from the Rocky Mountains. The central and eastern portions of the RFC area are especially vulnerable to storms tapping the abundant moisture of the Gulf of Mexico, and heavy, short-duration and medium-duration events frequently occur. Because of this reason flash flooding is a common problem of the entire area.

4. STUDIES USING NEXRAD DATA

NEXRAD data has been used for studies in various fields for hydrologic purposes. Some of the studies using this kind of data are as follows:

- After the devastating Tropical storm Allison flood, which caused well over $5 billion in total damages and 50,000 damaged structures, in Houston, flood warning and flood alerts became an important aspect which came to public attention (Bedient et al., 2003). Initially gauge based flood warning systems provided notification to the people but with the advent of GIS technology and NEXRAD, it is assumed that, reliability can be based on an efficient and more accurate approach. The data from the radar can be used to determine peak flows for a given basin using different hydrologic models. Bedient et al., 2003, developed and illustrated the design, operation and performance of an advanced flood warning system with the use of NEXRAD data. This system developed by the Texas Medical Centre (TMC) successfully determined hydrologic predictions for the Brays Bayou watershed in Houston, Texas.

- Seann and Maidment, 2004, developed GIS based programs GENHARP.f and GENHARP.aml to integrate NEXRAD rainfall data with Digital Elevation Models (DEM) to extract rainfall runoff modeling parameters. A need for such programs came into being because researchers at the U.S. Army Corps of Engineers Hydrologic Engineering Center (HEC) have proposed to develop "Next Generation Software" designed to replace HEC1, HEC2, and other similar codes. They have been actively evaluating methods for using NEXRAD stageIII product as input to the "Next Generation Software". Seann and Maidment (2004) projected using a bespoke version

of the Clark unit hydrograph method to incorporate NEXRAD rainfall data into their streamflow forecasting projects. For fulfilling this proposition there is a need to estimate the information about the area of each rainfall cell falling within each modeled subbasin and the average flow length from each rainfall cell to the corresponding subbasin outlet. Seann and Maidment, 2004, integrated NEXRAD rainfall data and USGS DEM's to determine rainfall-runoff modeling parameters for a particular subbasin. Using GIS they amalgamated a gridded NEXRAD precipitation surface with a gridded description of surface topography from a DEM to generate an input for runoff models which were spatially distributed. Using these programs distributed precipitation estimates are translated into improved streamflow forecasts and significant drawbacks previously associated with rainguages can be overcome by the use of NEXRAD data.

- Moon et al., 2004, used a new alternative in high resolution radar rainfall data, NEXRAD data and compared it to the ground data at every rain gauge location to evaluate the radar data's accuracy and validity. Their main objective was to check the use of spatially distributed rainfall on stream flows by taking NEXRAD data as the input for the SWAT model for the Trinity river basin in northeast Texas. The results obtained by using radar data were compared to the results obtained from the ground data. Moon et al., 2004 found that the efficiency estimation for both the models were similar but NEXRAD provided a better flow estimate. They concluded that NEXRAD captured rainfall for localized events which was often missed by ground rain gauges and so it was a good alternative to rain guage data and could be extremely important in large watershed areas having sparse gauge coverage (Moon et al., 2004).

- Some bay areas, like Tampa Bay area in Florida, in U.S. rely primarily on groundwater to meet the needs of its population (Glenn et al., 2001). Glenn et al., 2001, evaluated the effects caused by present and projected pumping of groundwater using existed and improved numerical methods. According to them, overpumping of the groundwater leads to burden on the groundwater system and thus proves to be detrimental in the long run. One of the important factors which have to be taken care of, as a result of the study, was defining accurate recharge for the system. Estimation of recharge involves accurate measurement of precipitation. They used NEXRAD data for finding precise and accurate precipitation patterns over the watershed (Glenn et al., 2001). This study shows remarkable improvement can be achieved in the dynamics of groundwater hydrology, over traditional methods, by using radar data (Glenn et al., 2001).

- Since highly temporal and spatial variability in rainfall is common in the areas of Brays Bayou watershed and White Oak Bayou watershed of Houston, flooding conditions have greatly increased over the past thirty years (Bedient et al., 2000). Bedient et al., 2000, studied the effects of Allison over Houston. NEXRAD Level II data was used in the study to estimate rainfall rates over the two watershed areas. They compared the traditional rainguage data with the radar data. Similar hydrologic modeling studies have been used to create real-time hydrologic forecasting capabilities of the Rice University - Texas Medical Center Flood Alert System (www.floodalert.org) (Bedient et al., 2000). The system, in place since 1998, serves the largest medical center in the world and uses WSR-88D rainfall averaged over the entire basin to make flood forecasts (Bedient et al., 2000).

- The National Oceanic and Atmospheric Administration's National Severe Storms Laboratory leads the way in investigations of all aspects of severe and hazardous weather (NSSL, 2004). Substantial improvements in severe and hazardous weather forecasting by the NSSL, has led to increased warning lead times to the general public. One of the prominent historical accomplishments of the NSSL is the invention of the Doppler radars to improve detection and warning of the severe weather (NSSL, 2004). Due to the success of these Doppler radar all over the country for providing improver thunderstorm and tornado warnings NSSL started the Next Generation Weather Radar (NEXRAD) program that resulted in the WSR-88D operational network of Doppler radars for the U.S. The Department of Commerce presented the NSSL with a Gold medal for its contribution of the NEXRAD program (NSSL, 2004).

- Heavy flooding events which occur during the rainy seasons cause extensive property damage and loss to human life (Smith and Bradley, 1994). Real-time data processing and flood forecasting can work towards minimizing these damages (Hadley and Srinivasan, 2002). Reliable rainfall data with good spatial and temporal coverage play a vital role in flood forecasting. Since the state of Texas has experienced some of the largest rainfall and flood events (Hadley and Srinivasan, 2002) in the United States it is important to develop a near real-time runoff estimation. The use of NEXRAD data for developing this has been proposed by Hadley and Srinivasan, 2002. This study will provide information useful for flood mitigation, reservoir operation, and water resource management practices. The use of Soil and Water Assessment Tool (SWAT) is also proposed by them. As suggested by them this study will involve the use of NEXRAD data, the USGS Multi- Resolution Land Characteristics (MRLC) data set and USDA-

NRCS State soil geographic (STATSGO) database. Daily runoff calculations will be made using SCS Curve number method and runoff depths will be estimated from NEXRAD measurements. Daily surface runoff maps of Texas will be developed at a resolution of 4 km x4 km.

- Vivoni and Sheehan, 2004, designed a distributed model which couples a runoff generation subcomponent based on the Soil Conservation Service (SCS) approach and a DEM-based Travel Time routing method. Different aspects of model calibration and evaluation were considered along with data analysis and encapsulation of a GIS model. Two storm events, the June 1998 Squannacook River basin, MA event and the January 1998 Peachcheater creak, OK storm event, which produced high flow conditions, were analyzed. NEXRAD data used was calibrated and validated by using telemetered stream gauge data obtained from USGS. The driving reason for utilizing NEXRAD data in a distributed hydrologic model is the spatial coverage and variability offered by the radar rainfall data (Vivoni and Sheehan, 2004). Spatially distributed rainfall maps obtained from StageIII NEXRAD data were used to derive the watershed response for the two basins. The raster-based, distributed hydrologic model captures the spatial distribution and variability of the incident rainfall and integrates the input into a time-varying prediction of river flow at the basin outlet (Vivoni and Sheehan, 2004).

- Hoblit et al., 2003, used a variety of GIS procedures for a study in which discontinuities in the coverage of NEXRAD data, for the state of Florida, were eliminated. Quality control was carried out and the ground clutter was suppressed, which yielded a seamless map of unadjusted radar rainfall estimates. More than 400 rain gauges located throughout the state were used for quality control and spatial

adjustment. With the help of this approach the volumetric rainfall estimates from the rain gauges were retained along with preserving the spatial nature of the rainfall. The use of this technique significantly improved gauge adjusted radar rainfall estimates (Hoblit et al., 2003).

- Nelson et al., 2000, carried out a rainguage network design study in the Mountainous regions of the Catskill Mountains of New York state using NEXRAD precipitation estimates. This raingage network design is intended to be implemented for water quality modeling studies performed in the WOH watershed as mandated by the Environmental Protection Agency (EPA) (Nelson et al, 2000). The main objectives of this study are to use NEXRAD radar for rainguage network design and compare the results obtained with the standard National Climatic Data Center (NCDC) data and then use a simulation approach for the network design. This simulation approach is used to analyze random, stratified, and site specific networks. Data from mean monthly and annual precipitation are used to evaluate long term climatological biases and storm events are used for carrying out error analysis.

- Huebner et al., 2003 conducted a study in south Florida for the development and use of NEXRAD database for Water management for the South Florida water management District which is responsible for managing water resources in a 46,439 square-kilometer (17,930 square-mile) region which extends from Orlando to Key West and from the Gulf Coast to the Atlantic Ocean and contains the country's second largest lake (Huebner et al., 2003). NEXRAD data was used for modeling, operating, planning, analysis and reporting by the district for water management practices. Huebner et al., 2003, designed the database by integrating with the corporate database and established

access methods for data verification and for applications of the NEXRAD data, for water resource management, for weather reporting that targets operational issues.

• In another study by Bedient et al., 2000, NEXRAD data was used to estimate the areal and spatial distribution of rainfall for three major storms over the Brays Bayou watershed in Houston for hydrologic modeling purposes. According to the results of the study NEXRAD radar estimates were well in conjunction with the point rainfall measurements at the rain gauges for the largest storm in October, 1994. Two HEC-1 models were run using the unadjusted NEXRAD data and rain gauge network and then for the three events the modeled outflow hydrographs were compared. It was found that some of the results from the radar data were even more accurate than the results obtained from the rain gauge model while estimating hydrologic parameters like volume, time of peak, and peak flow. These results are being used to generate local flood warning system for the Brays Bayou watershed (Bedient et al., 2000).

• In another study by Marchionno and Wise, 2002, a stochastic model was developed for the spatial and temporal distribution of rainfall using historical rain gauge data in conjunction with data from the Next Generation Radar (NEXRAD). By using spatial analysis of NEXRAD data along with temporal analysis of rain gauge data, a better understanding of the stochastic description of the precipitation is sought in this study. Such a development could ultimately lead to more accurate assessment and quantification of flood risks (Marchionno and Wise, 2002).

- Radar-Rainfall Estimation in the Catskill Mountains was also carried out by Bradley et al., 2000. This was done as accurate measurement of rainfall duration, timing, location and accumulations are critical for assessing the water quality and water supply in these mountains (Bradley et al., 2000). And since space –time variations in the rainfall can be provided by weather radar, NEXRAD data was used for this study.

- Near Real-time flood prediction using hourly NEXRAD rainfall data for the State of Texas is being carried out by Bakkiyalakshmi and Srinivasan, 2004. Rainfall runoff values are being estimated by the use of NEXRAD rainfall values for spatial resolution of 1sq. km. to 4 sq. km. which greatly reduces the uncertainty exerted by the spatial variability of point measured rainfall. This study will use SWAT model with NEXRAD data as the input data for calculating distributed hydrologic modal parameters like streamflow, evapotranspiration and infiltration. The main objectives of this study are to predict near real time hourly runoff estimation using high resolution NEXRAD rainfall estimates in a basin scale for the state of Texas and then to evaluate and improve the Green & Ampt Infiltration algorithm in SWAT for hourly flood prediction analysis (Bakkiyalakshmi and Srinivasan, 2004). Flood prediction for each of the 23 river basins in the Texas region can be predicted on an hourly basis at a resolution of 4 km x 4 km. This study will further open doors for assessing other water quality parameters.

- Vieux et al., 1998, investigated the effect of spatial aggregation of the rainfall maps on runoff simulation. This was done by aggregating the NEXRAD radar data from a 0.5 to 6 km radar and then simulating the impact of spatial resolution on storm runoff simulation in a 1200 sq. km. river basin in Oklahoma. GIS and "r.water.fea", an

internally integrated hydrologic simulation model, was used to process the radar data and to simulate storm runoff using rainfall distributed maps.

- Burgess et al., 2001, developed a System Wide Model (SWM) for long term weather flow management and planning for analysis, of the Metropolitan Sewer District of Greater Cincinnati (MSDGC). It was calibrated using gauge-corrected radar rainfall as input, which was taken from 29 storm events that occurred during the period of February thru June 2001 over Cincinnati. The radar data, for calibration, was collected from $1km^2$ grid resolution and 5 minute temporal resolution using NEXRAD installation in Wilmington, Ohio. Burgess et al., 2001, evaluated the variability in precipitation depths for various basin sizes using the data collected for model calibration. The results of this study were a set of reduction factors which represented the ratio of basin average precipitation to maximum basin averaged precipitation as a function of basin size. This analysis suggested that there is little variability of precipitation distribution across areas less that 2 sq. km. However, for basin areas roughly between 2 sq. km. and 10 sq. km., basin precipitation decreases to approximately 85% of the rainfall depths observed for the smaller basin areas. For areas larger than roughly 10 sq. km., no clear trend applies as the size of the area increases. After determining the reduction factors they also studies the wet-weather sanitary sewer flow conditions. Finally, guidance was also provided for developing design storm protocols.

- Vieux et al., 2002, checked the rainfall accuracy of radar-rain gauge networks for rainfall runoff modeling. They suggested that since it is not feasible to install sufficient rain gauges over a sewer system, therefore, a combination of rain gauge and

radar monitoring offers advantage for scrutinizing both rainfall and runoff in urban areas. Runoff simulated using gauge corrected radar is evaluated for a series of tropical and convective storms over Brays Bayou in Houston. They were able to demonstrate that accurate rainfall derived from a combined system of radar and rain gauges reduces the model input and output errors, that are not representative of the drainage areas being modeled.

- Different software used for the analysis of the NEXRAD data are available as of today.University Corporation of Atmospheric Research (UCAR) (2004) developed Plan Position Indicator Mesoscale and Microscale Meteorology package which is a program to display and analyze radar measurements taken at spherical coordinates (range, azimuth, and elevation). Priegnitz (2004) developed IRAS (Interactive Radar Analysis Software) package which is used for analyzing and displaying WSR 88D data. It is an X-Windows based software tool and been used exclusively as a research tool to play back base level data from a number of research radars. WXP (The Weather Processor) developed by Unisys (2004) is analyzing and visualization software developed by the Purdue University. SKYVIEW95 developed by Unysis (2004a, 2004b) is a NEXRAD Level III Product Visualization Software for the PC display Level III products which was developed by National Climate Date Centre (NCDC). FasTrac and NexTrac models developed by Baron Services (2004a) ingest the National Weather Service's NEXRAD data, providing crisp, detailed storm imagery atop high-resolution topography and maps. One of the most widely used software all over the world today is TITAN. TITAN stands for Thunderstorm Identification, Tracking, Analysis and Nowcasting and was developed by Dixon and Weiner (1993). It is used to identify

storms within three dimensional radar data and to check them as physical entities. The data produced is suitable for scientific analysis for understanding and subsequently forecasting the physics involved in storm development and movement. TITAN undertakes real-time automated identification, tracking and short term forecasting of thunderstorms based on volume scan weather radar data.

5. DATA USED AND STUDY AREA

5.1 STAGE III DATA

5.1.1 About NEXRAD Stage III Data

Stage III data is basically generated from Digital Precipitation Array (DPA) products also referred to as hourly digital precipitation products (HDP) products, which are, in turn, generated by the PPS and operational hourly rain gauge data (NOAA, NWS, 2005). The Hydrometeorological Analysis and Service (HAS) forecasters at the River Forecast Center (RFC) interactively quality control the main ingredients in the Stage III data. These DPA products are radar estimates of hourly accumulation of rainfall on a 4x4 km HRAP (hydrologic rainfall analysis project) grid. As discussed earlier in Section 3 (Weather Radar Data) the accuracy of these products is determined by the following factors:

1) Radars sensitivity to detect precipitation

2) Radar hardware calibration

3) Accurate estimation of the different precipitation parameters like hail cap, Z-R relationship etc.

4) Sampling errors in the radar measurements

5.1.2 Format of NEXRAD Stage III Data

NEXRAD Stage III data is stored in the form of XMRG format which is a type of binary format. Codes to read this format are provided by the National Weather Service

<http://www.nws.noaa.gov/oh/hrl/dmip/nexrad.html>. There are two different types of codes which can be used for Little Endian - describes a computer architecture in which, within a given 16- or 32-bit word, bytes at lower addresses have lower significance (the word is stored 'little-end-first'). The *PDP-11* and *VAX* families of computers and Intel microprocessors and a lot of communications and networking hardware are little-endian (catb.org, 2005) and Big Endian Machines-describes a computer architecture in which, within a given multi-byte numeric representation, the most significant byte has the lowest address (the word is stored 'big-end-first'). Most processors, including the IBM 370 family, the *PDP-10*, the Motorola microprocessor families, and most of the various RISC designs are big-endian (Catb.org, 2005).

5.1.2.1 Code to Read XMRG File on a Big Endian Machine

- "read_xmrg.c"

This is a code written in C language. This utility reads an XMRG file and writes it to an ASCII vector file. The format of the output file is as follows:

Column# || Row# || Cell value (data in mm).

The (0, 0) element is the located in the lower left corner of the grid.

Executables can be created using the standard UNIX commands. After running the program the output file will be a ".out" file. More information on the utility can be found in the header comments of the "read_xmrg.c"

5.1.2.2   Code to Read the XMRG File on a Little Endian Machine

5.1.2.2.1   read_xmrg_lin.c

This is also a code written in C language. It is a modified version of read_xmrg.c to work on Little Endian machines. This utility reads an XMRG file and writes it to an ASCII vector file. The format of the output file is as follows:

Column# || Row# || Cell value (data in mm).

The (0, 0) element is the located in the lower left corner of the grid.

Executables can be created using the standard Linux commands. After running the program the output file will be a ".out" file. More information on the utility can be found in the header comments of the "read_xmrg_lin.c"

5.1.2.2.2   reverse_byte_order.c

This is a utility which reverses the ordering of the bytes in each 4-byte word of an integer array. The need fo this utility arises from the differences in the memory architecture across different computers. For more explanation see the header comments of the program.

The XMRG data values can be defined by the HRAP (Hydrologic Rainfall Analysis Project) co-ordinate system. Explanation on the conversion into Lat/Long is provided in the header comments of read_xmrg. A FORTRAN subroutine is provided by NOAA and can be downloaded from NOAA website.

5.1.3 Basic Description of the File Name of NEXRAD Data

The data is encoded in binary format. The naming scheme for the data is as follows:

"**xmrg**mmddyyhh"

where mm-2 digits of month-00 to 12

dd-2 digits for day-   01-31 for january,march,may,july,august,October,December

01-30 for feb,april,june,September,November

01-28 for feb -non leap year

01-29 for feb –leap year

yy-2 digits for year-   97-04

hh-2 digits for hour   00-23

The following notation applies.

mm   two-digit month number (01-12)

dd   two-digit day of the month (01-31)

yy   two-digit year (00-99)

yyyy   four-digit year (beginning 2002)

hh   two-digit hour in UTC (00-23)

RFCID   two character River Forecast Center identifier"

5.1.4 Specification of the Different NEXRAD Formats

NEXRAD data can be found in different formats. These are the general formats which have been used by the WGRFC to distribute this data.

5.1.4.1.1 Prior to September 1997 the NEXRAD Data Was Represented by the

Following Notation

xllcorner — polar ster (HRAP): -671512.5 (260)

yllcorner — polar ster (HRAP): -7620000.0 (1)

Cell size 4762.5 m, number of columns 455, and number of rows 500

Monthly tar data format: SiiimmyyWG.tar

Daily tar data format: SiiimmddyyWG.tar

Hourly data format: xmrgmmddyyhhz.Z

After transferred to ASCII file: xmrgmmddyyhhz.out

where xllcorner is the lower left corner of the HRAP grid (260), yllcorner is the lower

right corner of the HRAP grid (10), other terminology is the same as above.

5.1.4.2   September 1997 to December 1998

xllcorner — polar ster (HRAP): -671512.5 (260)

yllcorner — polar ster (HRAP): -7620000.0 (1)

Cell size 4762.5 m, number of columns 455, and number of rows 500

Monthly tar data format: SiiimmyyyyWG.tar

Daily tar data format: SiiimmddyyyyWG.tar

Hourly data format: xmrgmmddyyhhz.Z

After transferred to ASCII file: xmrgmmddyyhhz.out

5.1.4.3   1998 to 2002

xllcorner — polar ster (HRAP): -528637.5 (290)

yllcorner — polar ster (HRAP): -7577137.50 (10)

Cell size 4762.5, number of columns 425, and number of rows 390

Monthly tar data format: SiiimmyyWG.tar

Daily tar data format: SiiimmddyyWG.tar

Hourly data format: xmrgmmddyy_hhz.Z

After transferred to ASCII file: xmrgmmddyy_hhz.out

5.1.4.4   Subsequent to 2002

xllcorner — polar ster (HRAP): -528637.5 (290)

yllcorner — polar ster (HRAP): -7577137.50 (10)

Cell size 4762.5, number of columns 425, and number of rows 390

Monthly tar data format: stage3_mmyyyy_RFCID.tar

Daily tar data format: stage3_mmddyyyy_RFCID.tar

Hourly data format: xmrgmmddyy_hhz.Z

After transferred to ASCII file: xmrgmmddyy_hhz.out

5.1.5 Steps for Untarring and Uncompressing the NEXRAD Data Files

Data for each year was downloaded from the NOAA website <http://dipper.nws.noaa.gov/hdsb/data/nexrad/wgrfc_stageiii.html>. Each yearly file is in the form of a tar file which has a set of 12 more tar files in it. The 12 tar files represent one file for each month. Inside each monthly tar file there are 30-31 more daily tar files, one for each day. Each daily tar file contains 24 more zipped files. Each of these is for hourly rainfall data for each day.

Here is a method for dealing with the data:

- look for files of Siii[mm][yy]WG.tar

- for each month untar each file to Siii[mm][dd][yy]WG.tar

- for each day untar each Siii[mm][dd][yy]WG.tar to xmrg[mm][dd][yy][hh]z.Z

- for each hour xmrg[mm][dd][yy][hh]z.Z uncompress it to xmrg[mm][dd][yy][hh]z

- call the xmrgtoasc to transfer xmrg[mm][dd][yy][hh]z into xmrg[mm][dd][yy][hh]z.out (selecting hrap as the third argument.)

After this step, each monthly tar file will be compressed to hourly files (*.out), totally about 720 (30 x 24) files. Each year will be totally about 8760 (365 x 24) files. The size of each file is about 1.68 MB. So for one month will about 1.23 GB, and for one year will be about 15.33 GB.

5.2 MPE DATA

The other form of NEXRAD data used in this study is the Multisensor Precipitation Estimator (MPE) data. This is provided by the NWS West Gulf River Forecasting Center. Also called NEXRAD Stage IV data, these are available for 1-, 6-, and 24-hour total precipitation summaries for the standard HRAP grid for the whole of US. These data are montaged from local, 4 km polar-stereographic grids for each of the 12 regional River Forecast Centers (RFCs) in the continental U.S. The nominal ground spacing is approximately 4 km throughout, but fluctuates with actual NEXRAD coverage and distance from the radar installation. Orographic effects may also cause this number to change a slight bit. MPE data are derived from the Stage III precipitation products which have been generated by the different RFCs. Each grid point in the MPE

product provides accumulated precipitation in mm measured for a particular span of time.

The MPE data has replaced the previously used Stage2/Stage3 data at the various RFCs and WFOs. The main purpose for the creation of the MPE data was to create hourly gridded precipitation estimates which could be used to produce MAPX time series for input into the National Weather Service River Forecasting System (NOAA, 2005). The main steps involved in creating the multisensor estimate include creating a multi-radar mosaic, mean field bias adjustment, and merging this information with gage observations. The multi-radar mosaic is generated by using radar estimates from individual radars, such that for any grid box, the radar which provides coverage at the lowest height above sea level is used to fill that box (NOAA, 2005). The MPE data is hence an integration of rain gauge, radar and satellite data.

NEXRAD hourly rainfall accumulations are stored within individual Digital Precipitation Array (DPA). At different NWS River Forecasting Centers (RFCs) these are statistically coalesced with gauge and satellite data to fabricate Multisensor Precipitation Estimates (MPE). MPE offers a versatile and integrated platform and a robust scientific algorithm suite for multisensor precipitation estimation using the benefits of rain gauges, radars and satellite data (Seo, 2003). MPE data for this study was supplied by West Gulf River Forecasting Centre (WGRFC) of the NWS Hydrologic Research Laboratory (HRL). The data can be downloaded from:

http://dipper.nws.noaa.gov/hdsb/data/nexrad/wgrfc_mpe.html

The MPE data available for the study extends for a period of 3 years (2000 thru 2002). Table 1 gives a summary of the availability of data for these years.

Table 1. MPE Data Availability

Year	Data Available No. of Months	Data Not Available No. of Months
2000	7	5
2001	10	2
2002	12	0

While carrying out this research it was noted that there were a lot of data missing in the data archives. For the year 2000 the months of January, February, August, September and December were among the missing data. Data for the months of January and February was not available for the year 2001. For months with available data, sometimes five or more days of data were missing. There were about three months in the year 2000 in which more than five days of data were missing. Also in the year 2001 around two months had more than eight days of data missing.

In general the MPE values were found to be higher than the Stage III data for almost all HRAP grid cells. There was a large variation in the difference between the two values. Sometimes the MPE values were one and half times greater than the Stage III values but at times the recorded MPE values were almost three times higher than the Stage III values. Table 2 gives a quick glance on this aspect. In terms of unrecorded data, MPE estimates were found to be better, as there were only a very few days with unrecorded data as compared to Stage III data. For Stage III data if the precipitation values were very small, the radar generally was not able to capture them and so there

were gaps in the recorded values. But this was not the case with MPE data. No matter how small the estimate is, it is recorded and made available in case of MPE data. This aspect can be explained as follows: sometimes, due to the topography of certain areas – generally orographic effects, setting up a closed knit network of rain gauges is practically impossible. Also, in these areas the coverage of radar is not complete as the microwave beams are not able to completely cover the entire regions due to obstructions etc. But satellite coverage of such areas is possible. And so MPE estimates, being an amalgamation of gauge, radar and satellite data, are helpful in overcoming this problem and detecting rainfall at such places. Using the MPE data, the local bias corrected satellite estimates are mosaicked with the radar estimates to fill gaps in the radar field and then these are further merged with the rain gauge to capture the benefits of all the sources. This is the reason why, at places where Stage III data are not available, MPE recordings are still possible. It is important to state at this point that even though the improvement in the data will be most apparent in the areas where there are significant gaps in the radar coverage but in areas where there are not enough gauges, to bias correct satellite estimates, the validity of the MPE data depends upon the quality of the satellite estimates themselves and hence this can be an area of concern while using the MPE data (Seo et. al., 2003).

Table 2. MPE Value Greater Than Stage III

Column	Row	Stage3 Value	MPE Value
178	0	-999	9
179	0	-999	7
180	0	-999	6
181	0	-999	9
182	0	-999	18
183	0	-999	26
184	0	-999	29
185	0	-999	25
186	0	-999	25
275	0	36.43	51.69
276	0	44.56	63.23
277	0	25.94	31.69
278	0	37.71	63.89
279	0	20.26	73.78
280	0	32.23	49.2
281	0	44.56	92.68
282	0	35.77	60.18
283	0	61.16	127.2
284	0	30.19	45.13
284	0	25.43	30.12
291	0	25.37	31.1
292	0	34.29	42.19
293	0	68.42	84.19
294	0	54.34	66.87
295	0	45.72	62.95
329	18	37.46	62.62
330	18	43.26	128.61
331	18	35.37	59.43
332	18	24.71	43.41
333	18	32.96	56.25
334	18	41.44	41.37
335	18	25	43.83
336	18	22.98	51.32
337	18	25.05	38.22
338	18	29.34	87.75
339	18	26.11	147.32
340	18	25.05	156.04
341	18	25.79	62.12
342	18	25.05	51.41
343	18	37.63	60.82
344	18	51.49	62.18
345	18	54.38	95.86

It was noted that the MPE values were, not always, higher than the Stage III values. Table 3 shows some regions, selected randomly, where the recorded MPE values were lower than the Stage III values. The descipencies in the data can also be as a result of mosiacking of data for a particular region from different radars. If the areas of coverage overlap the rainfall estimate used is the lowest unobstructed i.e. free from significant beam blockage and uncontaminated volume i.e. free from ground clutter and using this lowest over lapping value can result in underestimation (local bias >1) . This was especially noted during the heavy rain events. It can be due to the fact that heavy rain events are often localized and are not uniform over larger areas and so, MPE data representing the uniform distribution of rainfall over the entire gap, showed lower values. The precipitation is being distributed over a larger area, in other words much localized precipitation is smeared out to a larger area by the precipitation algorithm. These effects cannot be accounted for by the MPE estimation algorithm and so there are discrepancies in the values. Higher or lower values of MPE data can also be accounted for by significant precipitation surplus, especially in the up wind areas of the mountainous areas. In these areas orographic effects on the precipitation strength are not properly considered and so sometimes there is strong underestimation of values. Other areas of concern are that since satellite uses infrared technique to estimate the precipitation, values from relatively low clouds at warm fronts cannot be described to be accurate due to the limited range of the IR rays. Also proper merging of satellite data with rain gauge/radar and bias information sharing with the other WFOs are among the other problems faced by WGRFC as state by Allen, 2003.

Table 3. MPE Values Lower Than Stage III

Column	Row	Stage3 Value	MPE Value
112	0	15.17	12.23
179	1	21.25	12.12
187	6	36.23	6.21
207	25	13.45	11.12
209	116	57.88	23.57
218	0	43.71	18.23
272	64	21.56	11.29
286	235	24.57	10.15
186	113	13.75	6.72
275	250	36.43	27.61
276	317	37.71	27.23
277	6	25.94	14.78
278	268	44.28	6.27
279	26	59.16	13.78
280	96	36.23	14.15
281	128	47.29	29.68

Table 3 shows the difference in Stage3 and MPE value, for a grid cell, recorded during a given time. As can be seen from the tables there are a lot of discrepancies in the results obtained.

Table 4. Inconsistent MPE and Stage III Values

Column	Row	Time	Stage3 Value	MPE Value
280	84	10/23/02,09h	32.41	42.71
281	84	10/23/02,09h	37.42	49.32
212	85	10/22/02,06h	44.66	73.47
344	189	07/13/02,23h	23.91	38.35
32	298	10/26/02,21h	8.71	9.66

As can be seen, Table 4 shows the inconsistency in the MPE and Stage III values.

While carrying out the research it was also found that Stage III and MPE values give inconsistent results while finding the 1 hour annual maxima. As can be seen from Table 5, incongruent values of annual maxima are recorded for the same HRAP grid cells at different times. Occurrence of 1 hour annual maxima is predicted at different times with the two sets of data. Also there is a lot of variation in the annual maxima values.

Table 5. Inconsistent Annual Maxima Values

Column	Row	Time_Stage3	Stage3 Value	Time_MPE	MPE Value
336	189	12/23/02,16h	26.55	10/20/02,00h	24.78
421	189	11/04/02,01h	28.91	10/03/02,17h	40.69
34	190	09/10/02,21h	14.12	08/11/02,01h	14.09
219	191	09/09/02,23h	16.69	09/10/02,02	28.73
26	298	05/19/02,21h	3.37	10/26/02,21h	9.18

The multisensor estimates can reflect a significant amount of human interaction, with the forecasters at the RFCs being responsible for their assembly (Durrans et al., 2003). They may decide to alter seemingly suspect gauge reports or insert "pseudo gauges and reports" (Durrans et al., 2003). Part of human interaction may involve making changes to account for quality control of raw data and its analysis. Certain adjustment may also be carried out which include draw in and deletion of precipitation amounts and areas. Also sometimes, certain manual "reruns" i.e reanalysis of the data can lead to alterations alter in the data. Unfortunately, archives of alterations have not been maintained and therefore it is very difficult to detect the changes in the original records (Durrans et al., 2003).

It is recognized from the study that the available data records are much too short to enable reliable verification of the MPE data. An explanation for the difference between the Stage III data and the MPE data is not clear. Short data records and the kind of algorithm used in the processing of the data may be partly to blame.

Problems may lie with the radars or with the PPS processing algorithms because annual maximum precipitation values maybe systematically biased as a result of noise reduction or other factors like volume averaging. This leaves room for future research for the isolation of these problems and implementation of corrective measures to rectify these problems.

But all said and done MPE data, if correctly quality controlled, not only reduces small scale errors caused by rain gauges and radars but also account for spatial variability in precipitation climatology (Seo, 2003). It also fills the data for the missing areas and hence gives a near complete coverage of watershed area due to the fact that satellite data fill in radar-data void areas. Ongoing improvements these days include quality control using rain gauge and objective merging of satellite derived precipitation estimates with radar and gauge data which will help in better estimation of the precipitation estimation.

5.3 STUDY AREA

5.3.1 Area and Major Cities

The state of Texas is under consideration in this research study. Texas is the second largest state in the United States and covers a total area of 268,601 sq. miles (Texas facts, elearning, 2004). It is located in the south central part of the country and includes major cities like Austin, Houston, San Antonio, Dallas, Fort Worth, Galveston etc. Figure 9 shows the major cities of Texas.

Figure 9. Study Area- Texas (Pearson Education, 2005).

5.3.2 Major River Basins

The NEXRAD Data distributed by the WGRFC, used in the study, covers 23 major river basins in Texas. The river basins of Texas vary greatly in size, shape, and stream patterns (Wermund, 1998). The largest, the Rio Grande, differs markedly with the smallest, the San Jacinto River, in both size and length. The Red, Colorado, and Brazos Rivers have similar areas, but the Brazos River is 25 percent longer than the other two (Wermund, 1998). The major river basins of Texas include the following:

- Canadian River Basin

- Red River Basin

- Sulphur River Basin

- Cypress River Basin

- Sabine River Basin

- Neches River Basin

- Neches-Trinity River Basin

- Trinity River Basin

- Trinity-San Jacinto River Basin

- San Jacinto River Basin

- San Jacinto-Brazos River Basin

- Brazos River Basin

- Brazos-Colorado River Basin

- Colorado River Basin

- Colorado-Lavaca River Basin

- Lavaca River Basin

- Lavaca-Guadalupe River Basin

- Guadalupe River Basin

- San Antonio River Basin

- San Antonio-Nueces River Basin

- Nueces River Basin

- Nueces-Rio Grande River Basin

- Rio Grande River Basin

Figure 10 shows a map of the major river basins in Texas.

Figure 10. Major River Basins in Texas (TWDB, 2004).

5.3.3 Topographical Regions of Texas

According to the climatic variability and other topographical features the state of Texas can be broadly divided into seven regions namely:

- Panhandle Plain

- Prairies and Lakes

- Pineywoods

- Gulf Coast

- South Texas Plains

- Hill Country

- Big Bend Country

Figure 11 shows the location of the different regions in Texas.

Figure 11. Texas Regions Chart **(**TPWD, 2004).

5.3.3.1 Panhandle Plains

Region 1- Pandlehandle Plains
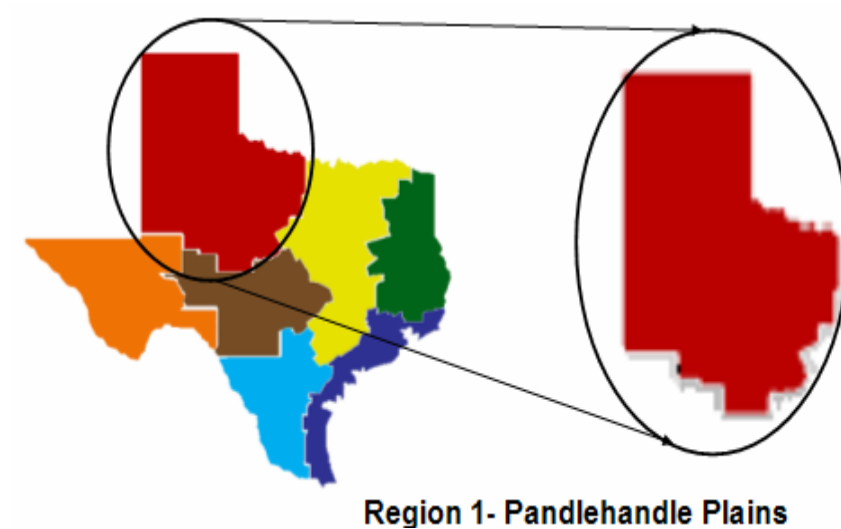
Figure 12. Region 1 – Panhandle Plains.

Figure 12 shows the Panhandle Plains. The panhandle region is made up of the geographic regions known as the "Rolling Plains" and the "High Plains". It roughly occupies an area of 81,500 sq. miles with an average rainfall of 15-17 inches/year (TPWD, 2004). The topography varies form rolling to moderately rough. The major cities in this area include Amarillo, Abilene, Lubbock, Wichita Falls etc. Rainfall variation in this region ranges from a maximum of approximately 29 inches in Perryton, which is at an elevation of 2,942 ft., to a minimum of 14 inches in Odessa, which is at an elevation of 2,891 feet (TPWD, 2004). The panhandle region is generally flat, sloping gently towards the southeast, with the maximum elevation of 3,889 ft. at Muleshoe and a minimum elevation of 946 ft. at Wichita Falls (TPWD, 2004). The

climatic conditions vary from very warm to hot summers and cool winters (Wildernet, 2004). Rainfall is lowest in winter and mid-summer and highest in April/May and September/October.

5.3.3.2 Prairies and Lakes

Region 2- Prairies and Lakes
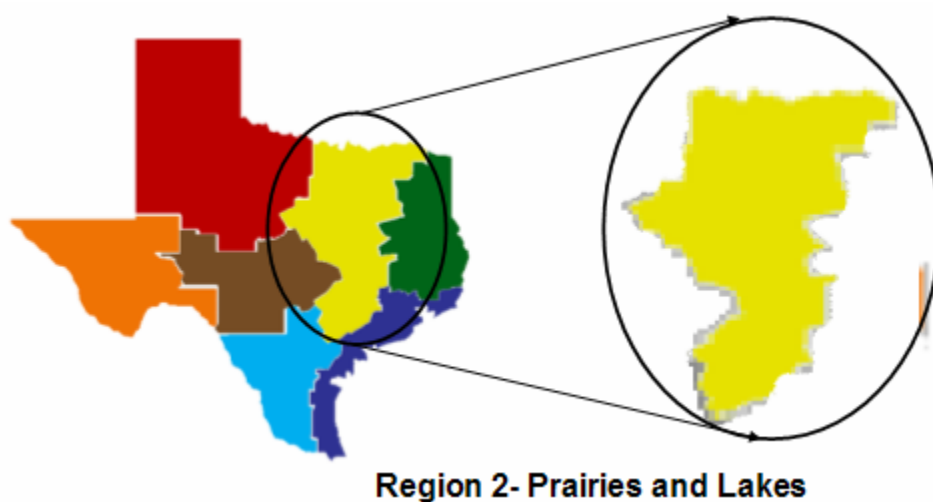
Figure 13. Region 2 – Prairies and Lakes.

Figure 13 shows the Prairies and Lakes. This region covers a considerable amount of northeast and central Texas including the cities of Dallas and Fort Worth. Topography of this region ranges from flat to gently rolling to hilly. Elevations range from 300 to 800 ft. above sea level (TPWD, 2004). The region experiences annual rainfall averages of 20-40 inches per year with month of May or June bringing in the maximum rainfall (TPWD, 2004). The south central part gets uniformly distributed

rainfall through out the year. The general trend in rainfall is that it increases from west to east. The region experiences hot humid summers and mild to cool winters. Mexia, in the east, experiences maximum rainfall in the whole region, which is as high as 41 inches per year, whereas Sequin, receives the least amount of rainfall, approximately touching a low of 21.52 inches per year (TPWD, 2004).

5.3.3.3 Pineywoods

Region 3- Pineywoods
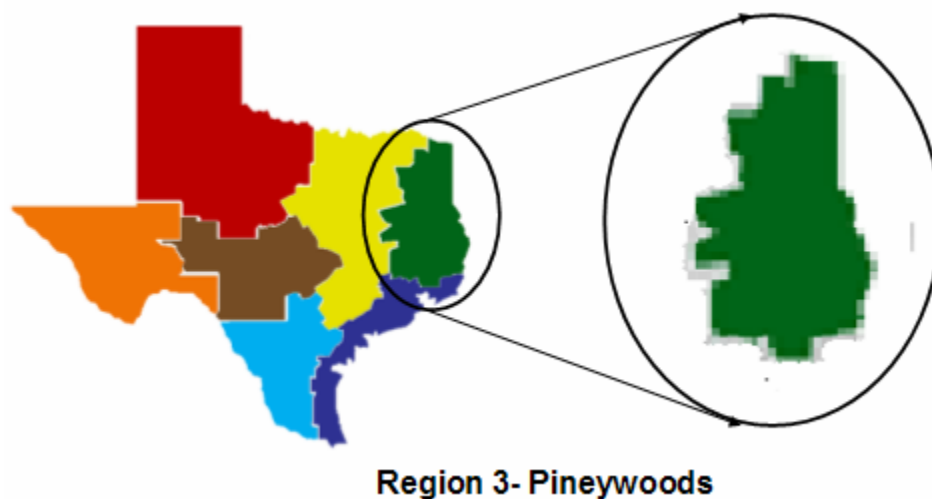
Figure 14. Region 3 – Pineywoods.

Figure 14 shows the Pineywoods region. The Pineywood region covers the Northeast Texas. The area covered by this region is 23,500 sq. miles (Wildernet, 2004). This region is part of a pine-hardwood forest which extends eastwards into Louisiana, Arkansas and Oklahoma. It has a rolling terrain covered with pine and oak trees.

Elevations in this region of Texas range from 200 to 500 ft above sea level. The region experiences an average rainfall of about 36-50 inches in a year. This rainfall is fairly uniformly distributed throughout the year. Temperatures are generally high and the region experiences a lot of humidity. The Texarkana region experiences maximum rainfall of about 58 inches per year and Canton, which is at a much higher elevation than Texarkana, experiences the lowest amount of rainfall of about 38 inches per year (Wildernet, 2004).

5.3.3.4 Gulf Coast
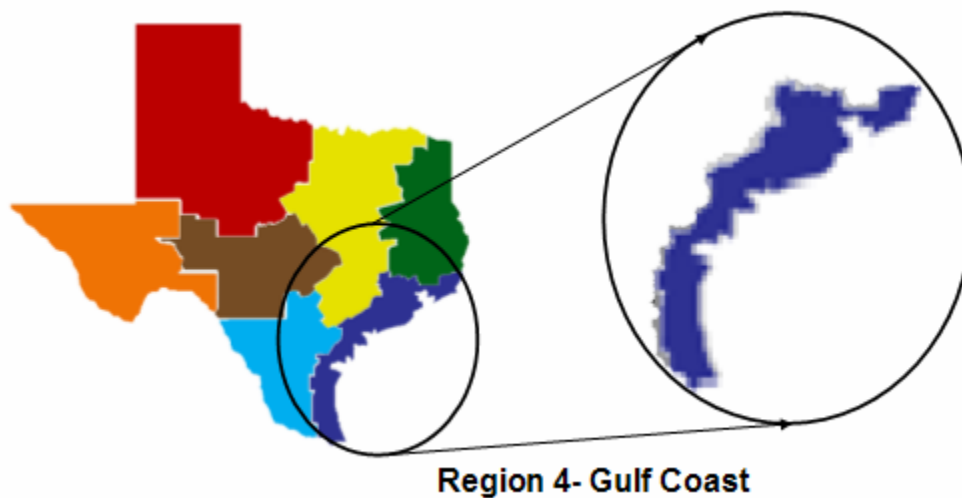
Region 4- Gulf Coast

Figure 15. Region 4 – Gulf Coast.

Figure 15 shows the Gulf Coast region. This nearly level, slowly drained plain region, less than 10 feet in elevation is dissected by streams and rivers flowing into the

Gulf of Mexico. The Gulf Coast, 21,000 sq. miles in area, experiences an average rainfall of 30-50 inches per year. It includes the cities of Houston, Galveston, Corpus-Christi, Brownsville and South Padre Islands. This region lies along the gulf coast and extends from Louisiana in the north to the Mexico border in the south. This region experiences high temperatures and humid climate. This region is a low lying area with maximum elevation of 104 ft. in Richmond and a minimum elevation as low as 5 ft. in South Padre island. The largest city in this region, Houston, is at an elevation of 55 ft. above sea level and experiences almost 51 inches of rain in a year (TPWD, 2004).

5.3.3.5 South Texas Plains
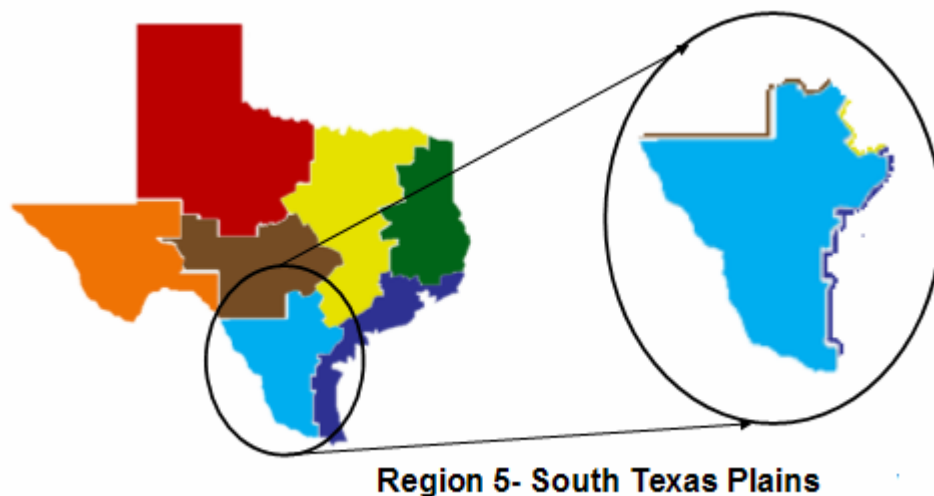
Figure 16. Region 5 – South Texas Plains.

Figure 16 shows the South Texas Plains. This region covers south Texas stretching from the San Antonio region, south to Laredo and the Rio Grande basin. The

total area it covers is about 28,000 sq. miles (Wildernet, 2004), with an average rainfall, not too high, of about 20-30 inches per year. This rainfall increases from west to east with rainfall being lower during winters than during summers and fall. Temperatures are very hot with high evaporation rates during the summers. Major cities include Alice, Mc Allen, and Laredo etc. Variation in elevation is from as low as 122 ft. in Mc. Allen to 797 ft. in Eagle Pass (TPWD, 2004).

5.3.3.6 Hill Country

Region 6- Hill Country
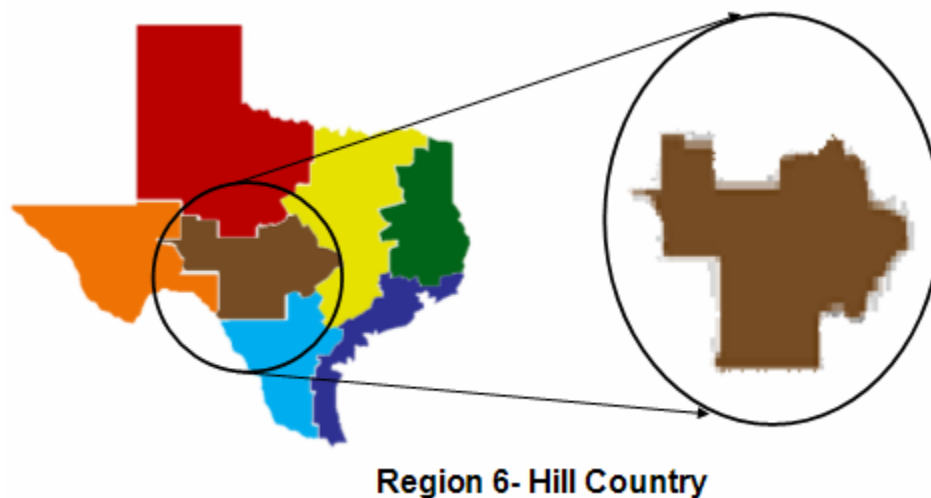
Figure 17. Region 6 – Hill Country.

Figure 17 shows the Hill Country region. This region is located in central Texas. It consists of two regions- the "Edward Plateau", covering an area of 31, 000 sq. miles and "llano Uplift", covering a small area of about 5000 sq. miles. The hill country

region generally consists of springs, stony hills and steep canyons. Average rainfall ranges from 15-32 inches per year with rainfall being highest in May/June and September. Landscape is rolling to hilly and elevations range from 825 to almost 2,250 ft. above sea level (TPWD, 2004). Several rivers run into this region creating a rough and well drained landscape. Climatic conditions are generally hot and humid in summers to mild in winters. This includes the areas around Austin and Fredericksburg.

5.3.3.7 Big Bend Country

Region 7- Big Bend Country
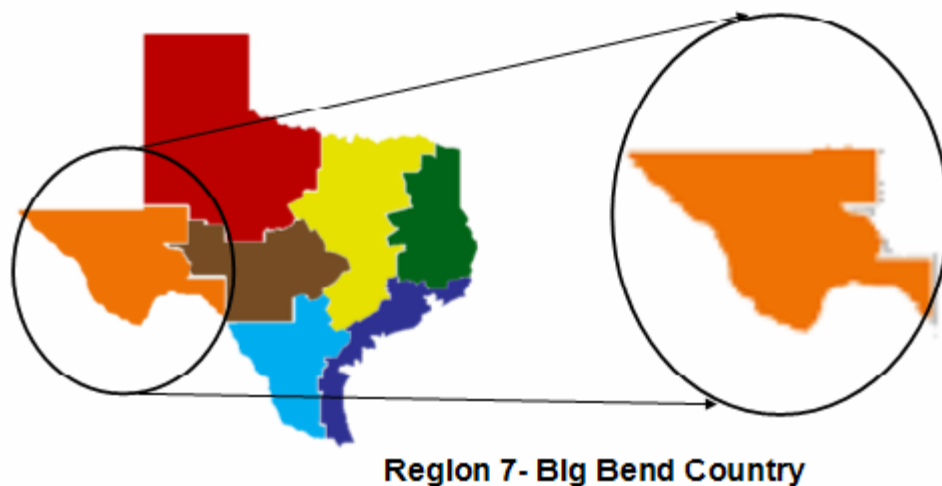
Figure 18. Region 7 – Big Bend Country.

Figure 18 shows the Big Bend Country which covers most of western Texas. This region covers an area of 38,000 miles with elevations ranging from 2000 ft. to as high as 8749 ft. at the Guadalupe peak (Texas Freeway, 2004). The rainfall patterns are

generally very low with average annual rainfall ranging from 10 to 18 inches per year. The area consists of rugged plateaus and wooded mountain slopes. Elevations generally rise from south to north and east to west.

6. METHODOLOGY

6.1 OBTAINING AND MANAGING DATA

NEXRAD radar-rainfall data were obtained for the present study by the NWS Hydrologic Research Laboratory (HRL). The data employed are Stage III data (for the years 1995 thru 2004) and MPE data (for the years 2000 thru 2002) for the West Gulf River Forecasting Centre (WGRFC). Monthly tarred data was downloaded from the NOAA website. This kind of data was used because they are the longest and best documented records available from the WGRFC. Monthly tarred files of Stage III data and MPE data can be downloaded from West Gulf River Forecast Centre (WGRFC). The links to download them are given:

http://dipper.nws.noaa.gov/hdsb/data/nexrad/wgrfc_stageiii.html- Link for Stage III data, and http://dipper.nws.noaa.gov/hdsb/data/nexrad/wgrfc_mpe.html- Link for MPE data. For a detailed description on data availability and missing records refer to Section 3 'Weather Radar Data'.

The following is the format in which the data were stored:

- A separate directory was made for each year which was named as "yyyydata" where yyyy stands for the year eg. 2003data, 2002data etc. Then twelve sub directories were made (one for each month) and they were named as follows: Siiimmyyyy where, Siii stands for Stage III, mm- 2 digits for month, yyyy- four digits for the year. MPE data were also handled in the same way only difference being the files named were in the following manner yyyydata_MPE and MPEmmyyyy.

- All the monthly files were downloaded in that their respective sub-directories. The monthly files were named in the following manner: SiiimmyyyyWG.tar where, Siii stands for Stage III, mm- 2 digits for month, yyyy- four digits for year, WG-name of the RFC. Due to a different format of the NEXRAD data the files for the years 2002, 2003 and 2004 were named as stage3_mmyyyy_WG.tar.

- These files were untarred using standard UNIX utilities. These subdirectories were further unzipped to obtain daily files which were in turn unzipped to get hourly data files. For each directory there were about 8,760 files, depending on whether the data for the year was complete and whether the year was a leap year. The hourly files were in the following format xmrg_mmddyyyy_hhz_WG.

- The hourly files were in binary format and had to be converted to ASCII format. Using the utilities provided by NOAA these daily hourly files were converted into ASCII files. A description of how to do this is given in Section 5 "Data Used and Study Area"

- After all the files had been converted to ASCII format, an archive for each year was made and the data was again tarred and zipped into a file. The file was stored with a ".tar.gz" extension. This was done in order to deal with the large amount of space the unzipped files occupied.

- Finally there were zipped files for each year which contained hourly ASCII precipitation data.

6.2 EXTRACTION OF ANNUAL MAXIMA

The next step was to find the annual maxima value for each cell in the HRAP grid. As discussed earlier there were 425x390 cells in the whole grid. For finding the

ARF ratios it was important to find the annual maximum values for each cell and then calculate the ratios with its surrounding concurrent precipitation values. For this all the hourly files for a particular year were taken and then a C program "Annualmaxima.c" was written which read all the values for a particular cell from the 8760 files and replaced the cell value with a higher value until it got the highest value for a particular cell. This was done for all the cells in the grid, scanning all the cells, row by row. Finally a grid was obtained which had the maximum value for each cell. The grid file was named as "maxgrid_yyyy.dat". The attributes of the file were:

PathGrid || Column || Row || Value

where, Path is the absolute path of the directory, Grid is the name of the grid (or file) from where the maximum value came from, Column- cell's column number, Row- cell's row number, Value – annual maximum value of the cell.

There was one "maxgrid" for each year. Figure 1 shows the structure of the file for more clarity.

6.3 DIVIDING GRID INTO 5x5 BLOCKS

The next step was to divide the entire grid in blocks of 5x5 blocks as can be seen in Figure 19. The idea of doing this stemmed from findings in literature (Asquith and Famiglietti, 2000) that ARF's may vary significantly from one geographical region to another. And so it was mandatory to find ARF ratios which covered the entire region. At the same time it was perceived that finding ARF for each cell would be unnecessary effort and time consuming as places which lie at a distance of about 20 km from one

another would be climatically similar. So a judgment was made that ARF ratios would be found for blocks of 5x5 cells.

The arrangement of the blocks was as follows as shown in Figure 19:
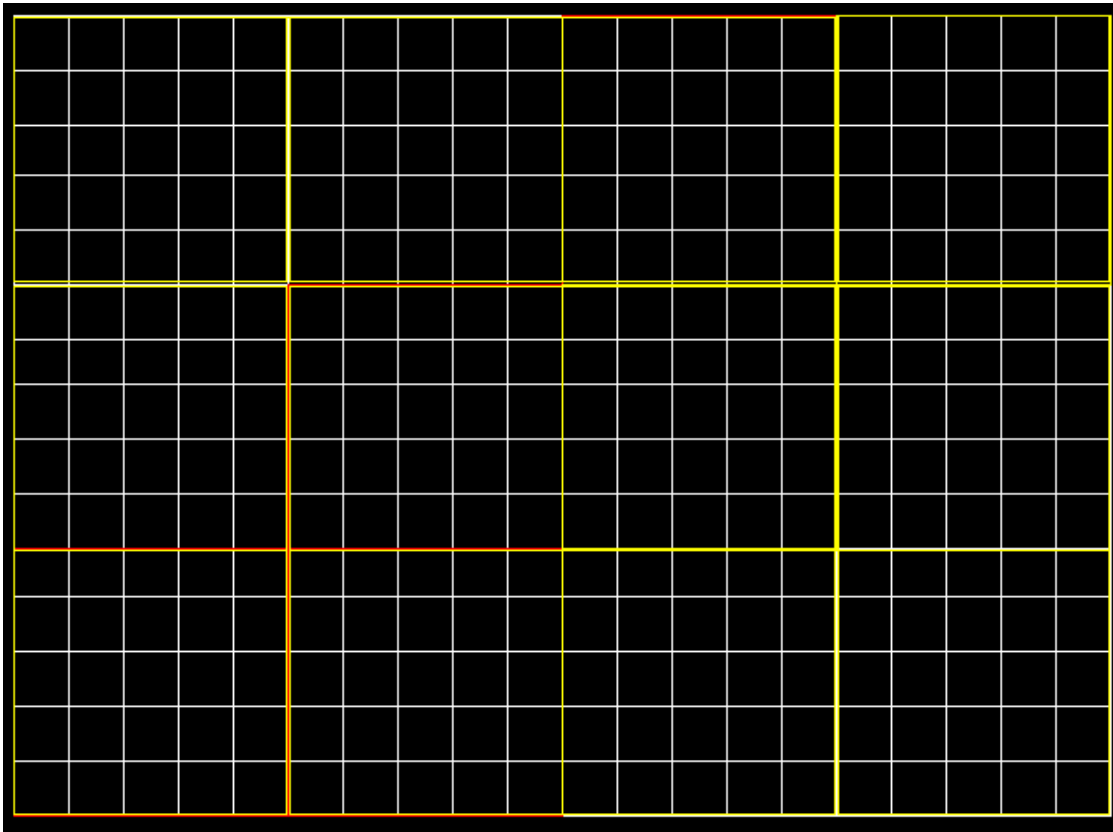
Figure 19. Arrangement of 5x5 Blocks.

6.4 FINDING MAXIMUM VALUED CELL

After the whole grid had been divided into 5x5 cells, the next step was to find the cell in the block having the maximum annual value. **NOTE**: If the cell with the

maximum value was belonging to the following rows or columns (which were the edges of the HRAP grid) then the next higher valued cell was taken into consideration.

Rows 0, 1, 2, 387, 388, 389

Column 0, 1, 2, 422, 423, 424

This was done because if these cells were selected then it was not possible to find all the six ARF values explained later in the section. The cell having the maximum value in each block was taken to be the central cell and the ARF ratios were calculated with these and their surroundings cells. In total we had 6630 5x5 blocks after dividing the whole grid and so there were 6630 number of central cells. Once the central cell for each block was identified the next step was to identify the grid (file) this cell value came from. The attributes of the file were checked and the corresponding grid was identified.

6.5   FINDING ARF RATIOS

Once the central cell and the grid (file) from which it obtained that value was identified ARF ratios were calculated with the surrounding cells and concurrent precipitation values. The following is the arrangement in which the different ARF values were calculated.

- RS1 = Average of precipitation values of the 3x3 square window around the central cell/point precipitation value of the central cell.

In other words:

RS1 = Average of precipitation values for cells 1 to 9 / precipitation value of cell 5.

- RC1 = Average of precipitation values of the equivalent 3x3 circular window around the central cell/point precipitation value of the central cell.
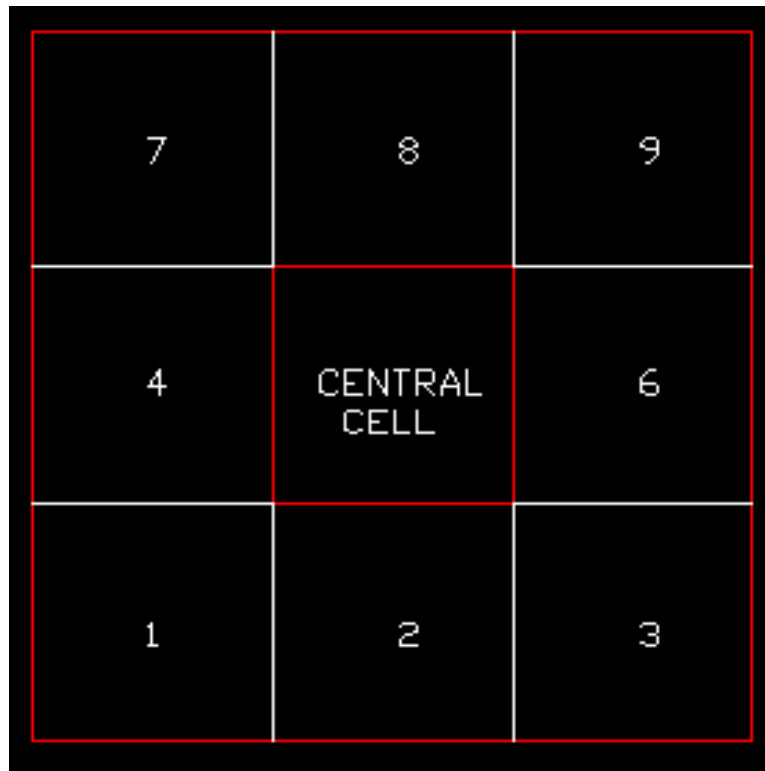
Figure 20. Arrangement of 3x3 Window (9 Cells-144Sq. Km.).

Figure 20 shows the arrangement of the 3x3 window.

- RS2 = Average of precipitation values of the 5x5 square window around the central cell/point precipitation value of the central cell.

In other words:

RS2 = Average of Precipitation values for cells 1 to 25 / Precipitation value of cell 13.

- RC2 = Average of precipitation values of the equivalent 5x5 circular window around the central cell/point precipitation value of the central cell.

21	22	23	24	25
16	17	18	19	20
11	12	CENTRAL CELL	14	15
6	7	8	9	10
1	2	3	4	5

Figure 21. Arrangement of 5x5 Window (25 Cells-400 Sq. Km.).

Figure 21 shows the arrangement of the 5x5 window.

- RS3 = Average of precipitation values of the 7x7 square window around the central cell/point precipitation value of the central cell.

In other words:

RS3 = Average of Precipitation values for cells 1 to 49 / Precipitation value of cell 25.

- RC3 = Average of precipitation values of the equivalent 7x7 circular window

around the central cell/point precipitation value of the central cell.

Figure 22. Arrangement of 7x7 Window (49 Cells-784 Sq. Km.).

Figure 22 shows the arrangement of the 7x7 window.

From now the following terminology will be used in this study:

RS1- square ARF representing an area of 144 Sq. Km.

RC1- circular ARF representing an area of 144 Sq. Km.

RS2- square ARF representing an area of 400 Sq. Km.

RC2- circular ARF representing an area of 400 Sq. Km.

RS3- square ARF representing an area of 784 Sq. Km.

RC3- circular ARF representing an area of 784 Sq. Km.
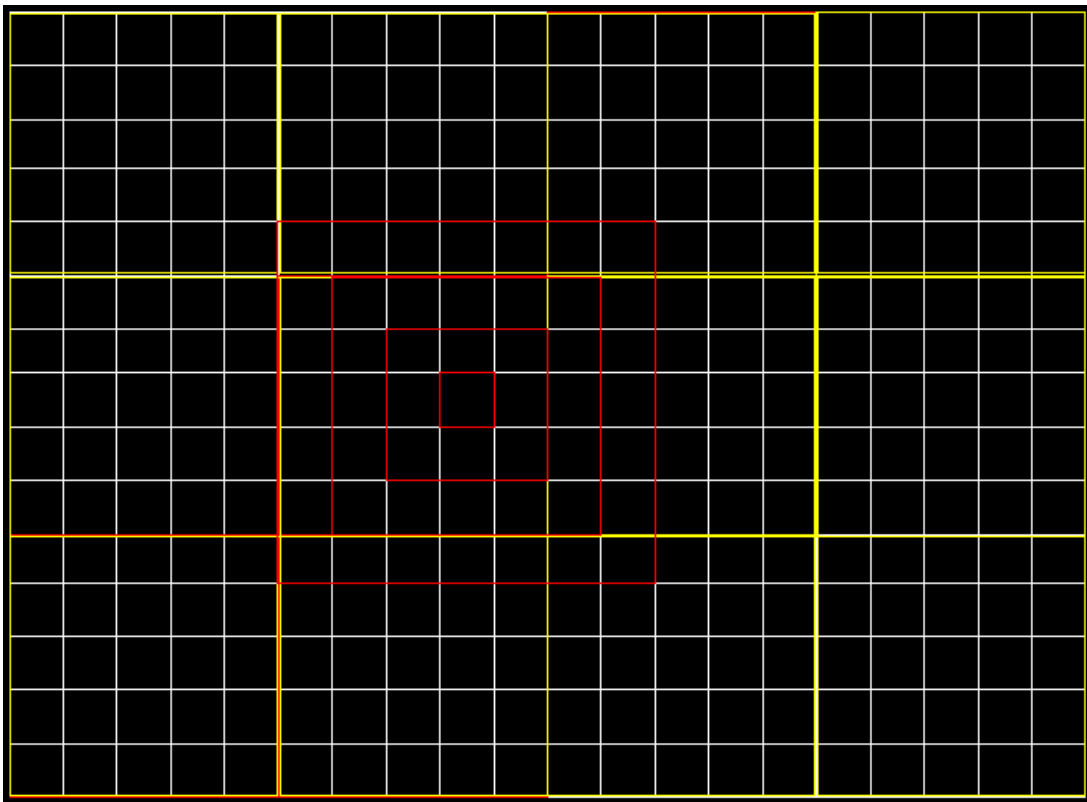
Figure 23. Arrangement of the Various Windows Around the Central Cell.

Figure 23 shows the arrangement of the windows around the central cell. While carrying out the study it was found that there were certain discrepancies in the values of the ARF ratios obtained. These ratios did not truly represent the ARF for a particular area

and so there were some cases which had to be flagged and filtered out. The following cases have been flagged in the study:

- Sometimes there were cells which had the annual maxima value as -999. This value has been given to cells by NOAA when there is no data recorded. Therefore a cell with a   -999 value means that the radar was not able to capture any value for that cell and the cell value is represented as -999. In very rare cases there was no recorded value for a cell and so the annual maximum for that particular cell was found to be -999. Such cases were seen, mostly, towards the lower left corner of the HRAP grid. These cases were flagged as nan, not a number, values.

- In such cases the ARF ratios were calculated by using the surrounding cells and filtering out that cell. For example, if there was one such cell in a 3x3 window then the RS1 value was calculated based on eight cells by using the rest of the eight cells. If there we two such cells then the ARF ratio was calculated using seven cells and so on.

- The results show that the values of the ARF lie between a range of 0 to1. In the study it was found that the values of ARF always range between 0 and 1 i.e. $0 \leq ARF \leq 1$. This can be verified by that fact that ARF values are calculated with the 1hour annual maxima as the central cell and all the values around it were less than the central cell value. Therefore after taking the average of all the cells the ARF value can never exceed 1. TP-29 also places this kind of restrictions on the ARF values, i.e. ARF ≤ 1.

In some cases, however, it was noticed that the values of the ARF were greater than unity. This was due to the fact that the annual maxima calculated in a given block did not coincide with the centre of the storm and so there was another value in the next

block which was greater than this value, which actually would have been the centre of the storm. In such situations, the ARF values calculated did not correctly represent the ratios for that particular area. Because of the cell in the next block being of higher value, the average value was sometimes (not always) less than the point precipitation value and so the ratios added up to a value which ended up being great than one. But this was not always the case. Sometimes even though the values in the next block were greater than the previous block, the difference in the two values was not significant to raise the average and, hence, the ARF values to be greater than one. Therefore it was important to flag all these values as they did not truly represent the ARF ratios. These values have been flagged in this study and these ratios have not been used to determine the results as they would have caused certain discrepancies in the final outcome. It was generally noted that the cells lying at the edges caused such problems. Therefore cells having annual maxima values which were located at the edges were checked for such conditions and filtered out if they met this requirement.

The sample ratios plotted represent a small and random subset of the entire grid. As can be seen from the figure it is evident that the variability of the ratios is large. With larges distances it can be seen that the ratios decrease and tend to reach zero. This case is more likely to occur when the area of the watershed increases. As explained above ratios larger than one are not uncommon. This can also be explained by the fact that matches the physical reality that locations other than the point coincident with the annual maxima for a particular block can have larger concurrent depths.

7. RESULTS AND DISCUSSIONS

7.1 VARIATION OF ARF WITH AREA AND COMPARISON WITH THE STANDARDS

The reduction factors derived from this analysis show, in general, decay in the ARF values with respect to an increase in the area. As can be seen from the figures in this section, these ARF values are the highest for smaller areas and, as the size of the watershed increases, these values decrease. However, no particular trend was found in the decay of the values. The results obtained by this study are in close approximation to the ones obtained from previous studies, but certain discrepancies can be seen in ARF values for larger areas. It was found that ARF values were location specific so ARF values for various regions have been compared to the standard values. Composite ARF values were calculated for each region and then these were plotted along with the standard results for the comparison.

Figures 24 (a) thru (g) illustrate the decay in square ARF values for various regions over the different years.
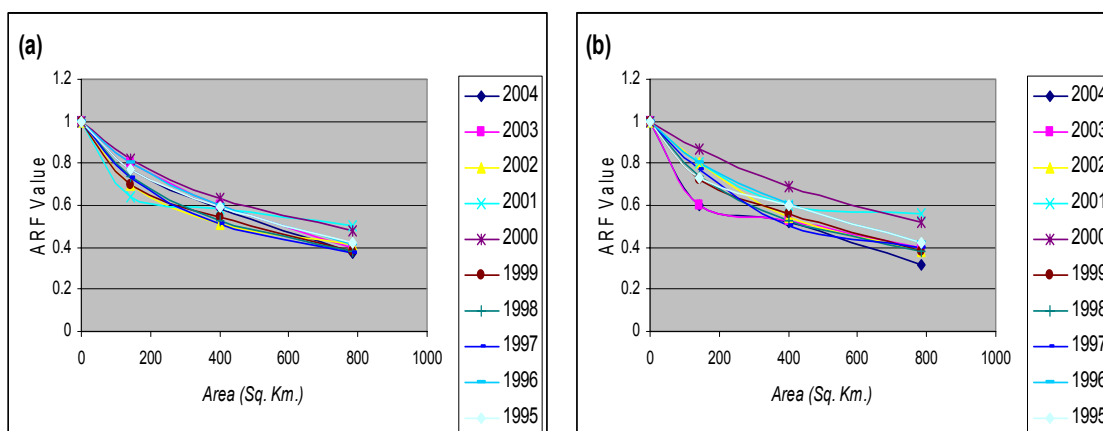
Figure 24. Variation of ARF Values with year for (a) Region 1 (b) Region 2.
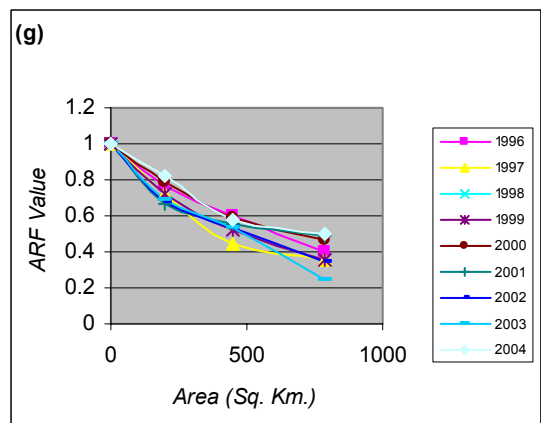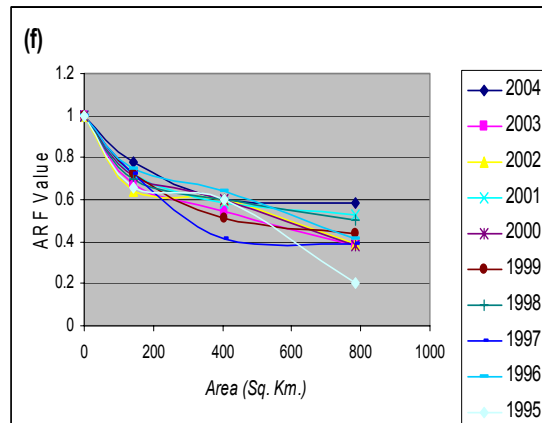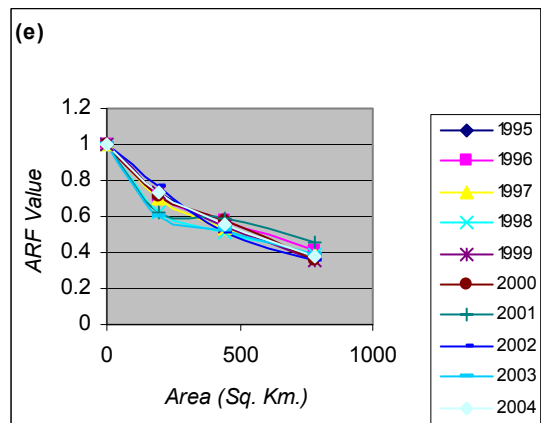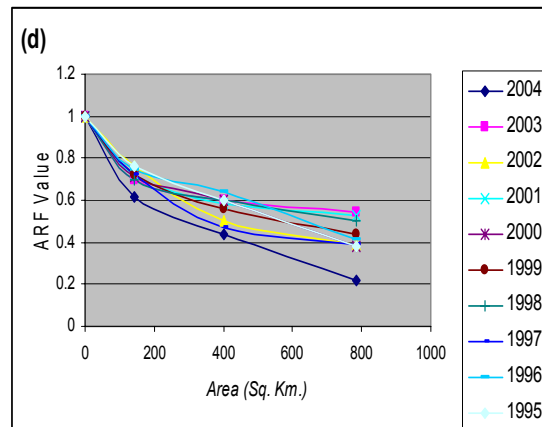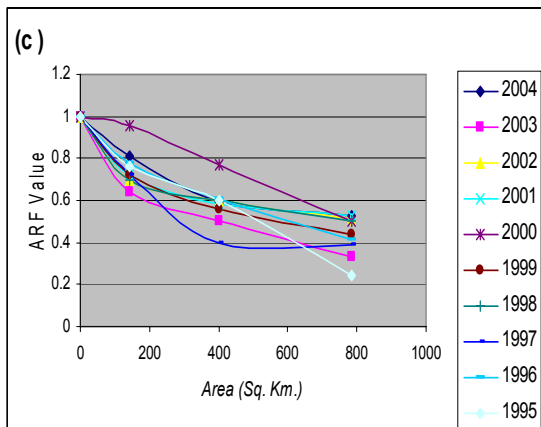
Figure 24. (continued) (c) Region 3 (d) Region 4 (e) Region 5 (f) Region 6 and (g) Region 7.

Similarly decay was also found in the circular ratio values. For clarity purposes these have not been shown here with the square plots. As can be seen from all the figures ARF values tend to be almost the same for smaller areas but as the size of the watershed increases certain incongruity can be noticed.

Since the NEXRAD data has shown improvement over the years so variations in the ARF for two time intervals (1994-1999 and 2000-2004) also shown. Figures 25 (a) thru (g) illustrate the variation in the average ARF values for 1995-1999 and 2000-2004.
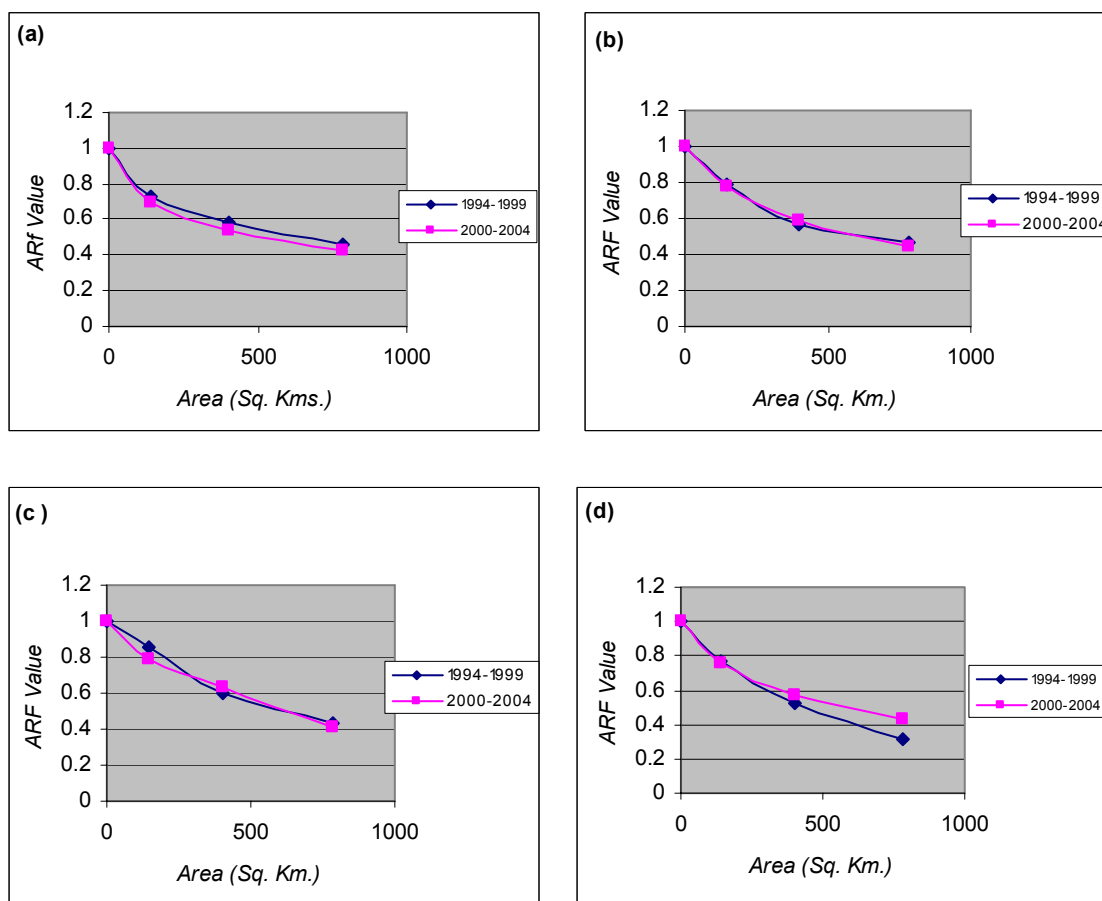
Figure 25. Variation of ARF Values for Pre 1999 and Post 1999 Cases for (a) Region 1 (b) Region 2 (c) Region 3 (d) Region 4.
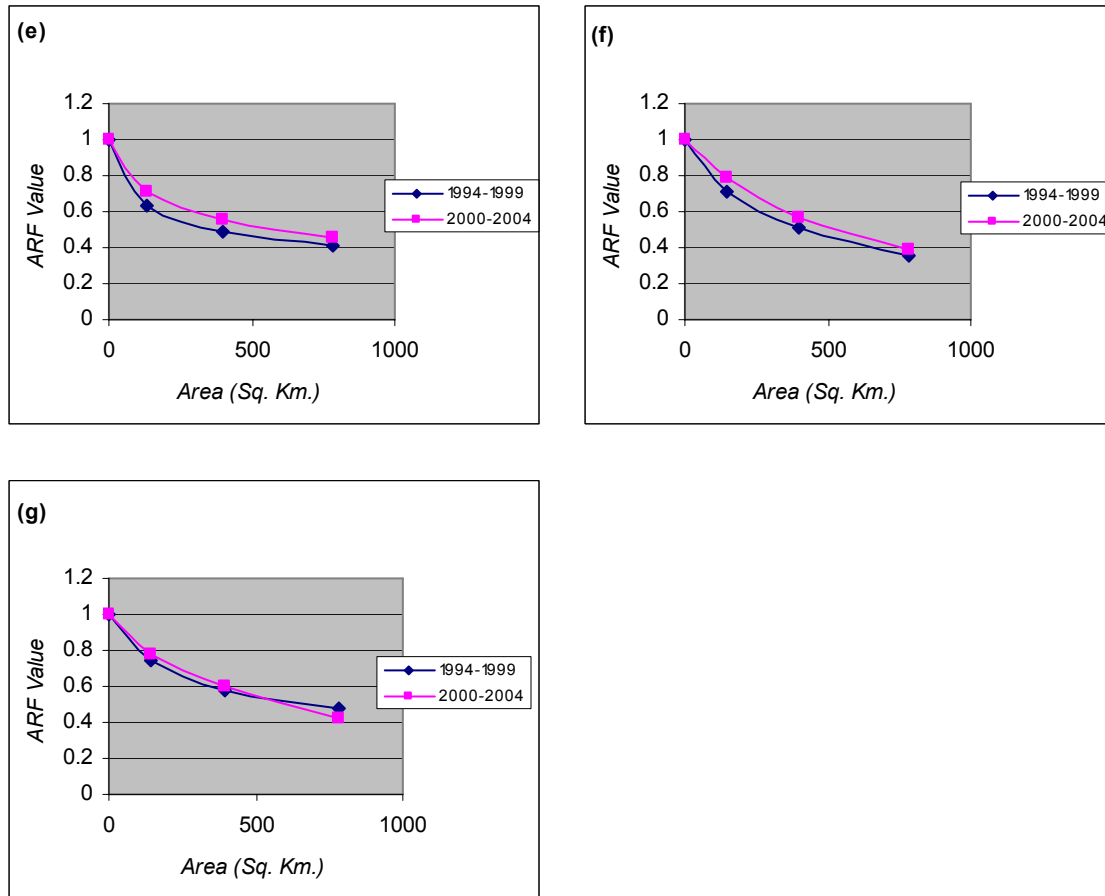
Figure 25. (continued) (e) Region 5 (f) Region 6 and (g) Region 7.

Table 6 shows the values of the composite ARF for the different years, for various regions, for which the study was carried out. There was a general decrease in the ARF values with increasing area. For operational purposes it is assumed that the areal reduction in areas smaller than the size of the storm cell is negligible and hence ARF value is taken to be unity. For operational purposes it is observed that for very small areas ARF values are at or near unity. This means that the average areal precipitation is almost equal to point precipitation. For this reason the ARF ratio for

very small area is taken to be unity and there is no reduction in the amount of point precipitation value in order to convert it to areal average value.

Table 6. Calculated ARF Values for Various Regions

Area Sq. Km.	Region 1 ARF Range	Region 2 ARF Range	Region 3 ARF Range	Region 4 ARF Range	Region 5 ARF Range	Region 6 ARF Range	Region 7 ARF Range
0	1	1	1	1	1	1	1
144	0.83-0.64	0.90-0.60	0.97-0.69	0.72-0.60	0.77-0.60	0.80-0.62	0.82-0.64
400	0.62-0.41	0.68-0.50	0.72-0.40	0.62-0.47	0.60-0.50	0.63-0.41	0.62-0.41
784	0.51-0.34	0.52-0.28	0.60-0.23	0.54-0.20	0.49-0.36	0.60-0.19	0.53-0.28

Figures 26 (a) thru (g) show the comparison of the calculated ARF values with some of the standards used in present studies. Composite ARF values are calculated for each region and then compared with the standards. The composite ARF values were calculated by finding the mean of all the values for a specific region.
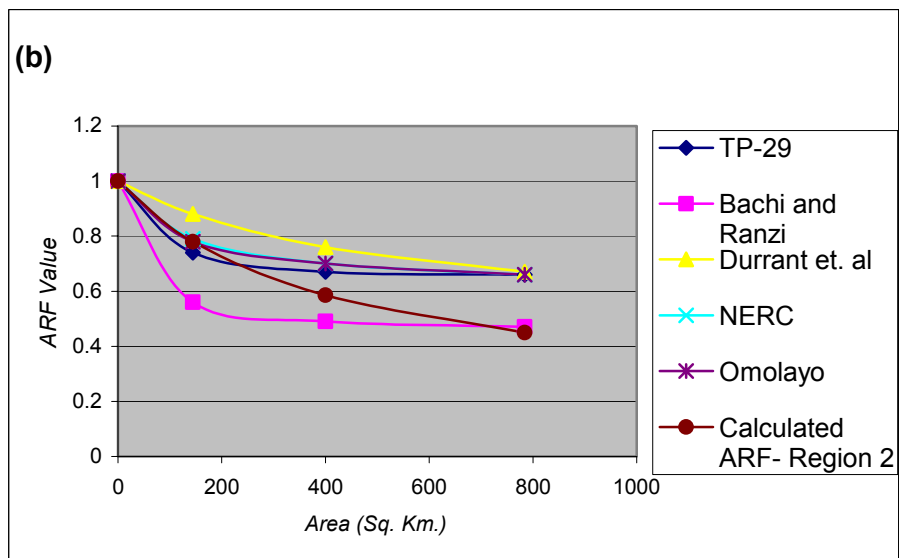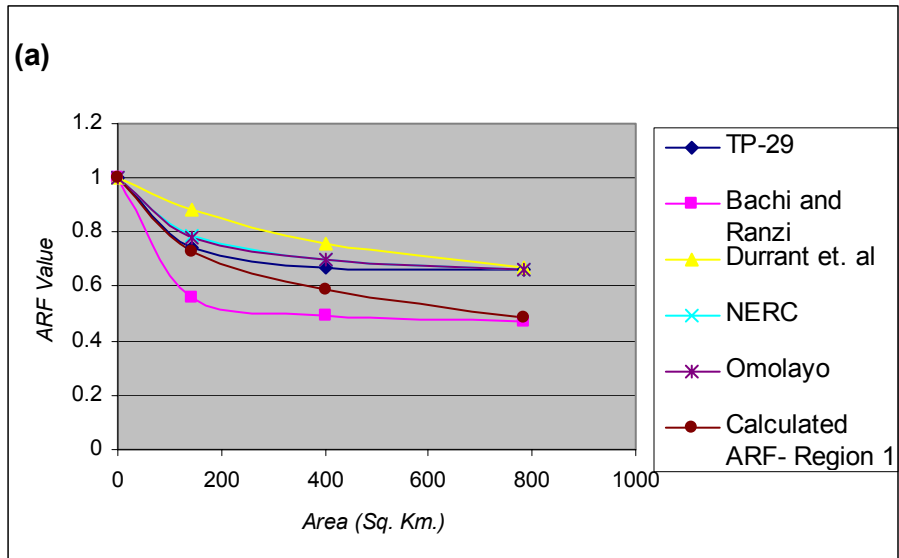
Figure 26. Comparison of ARF Values with Standards for (a) Region 1 (b) Region 2.
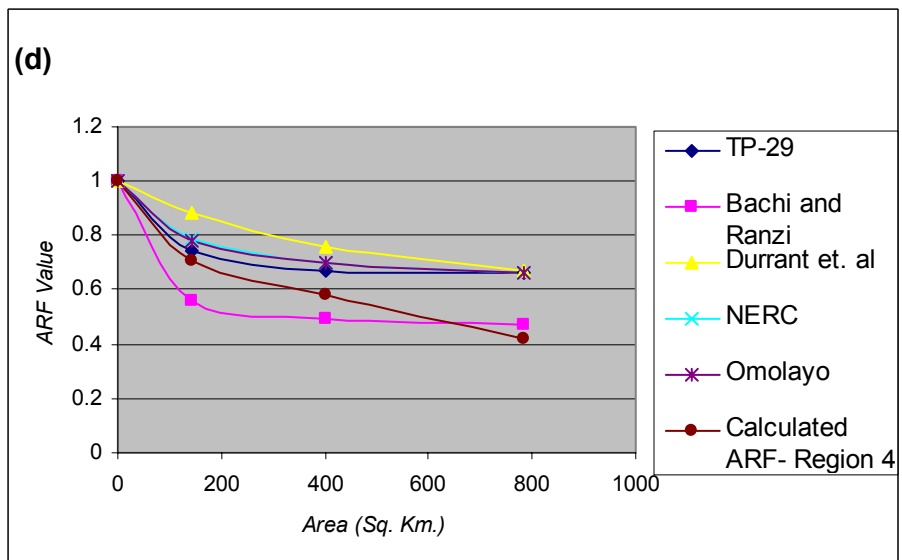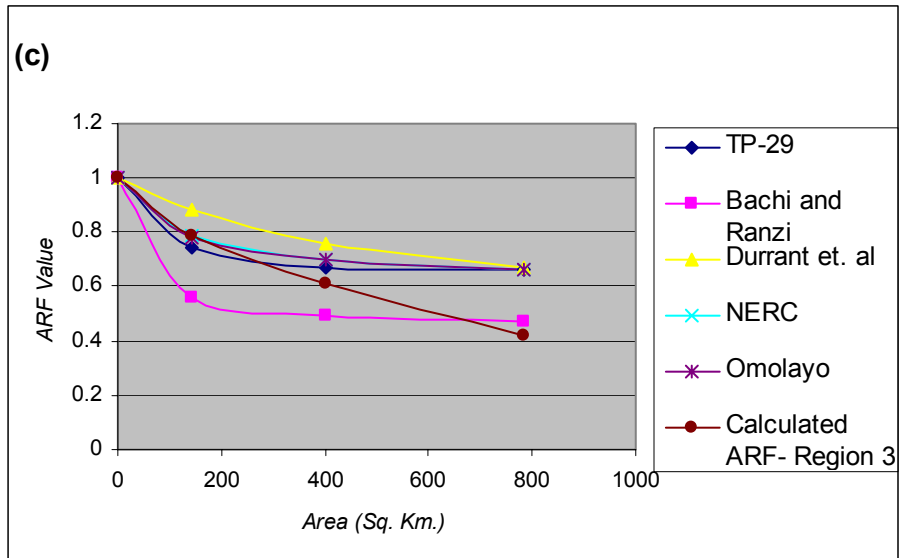
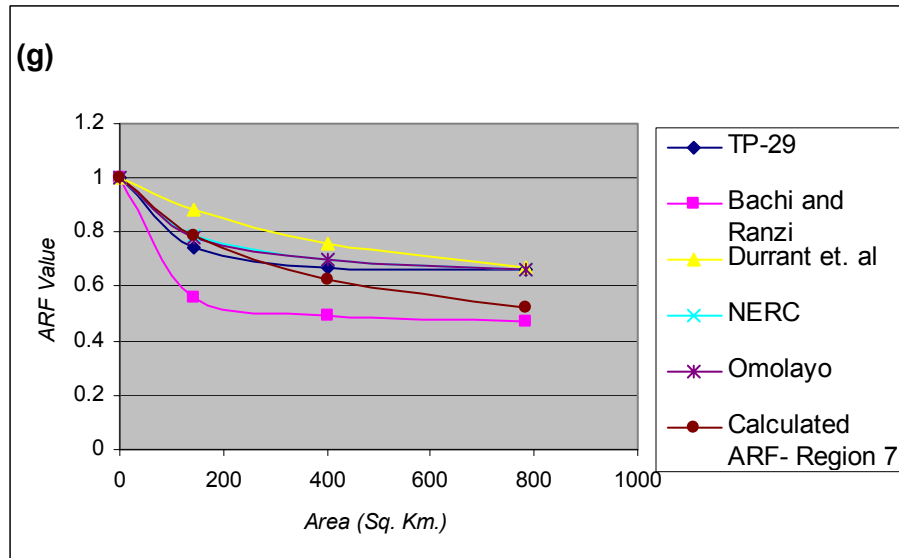**Figure 26.** (continued) (c) Region 3 and (d) Region 4.
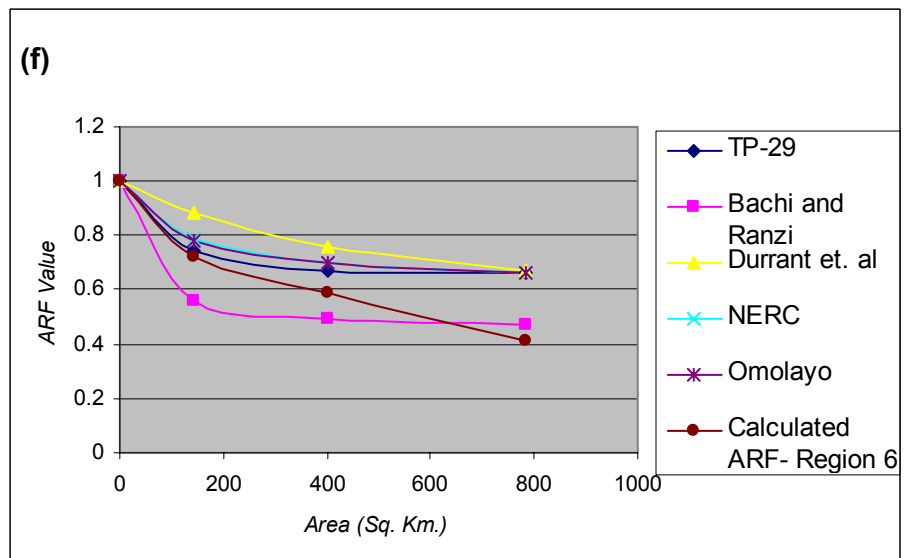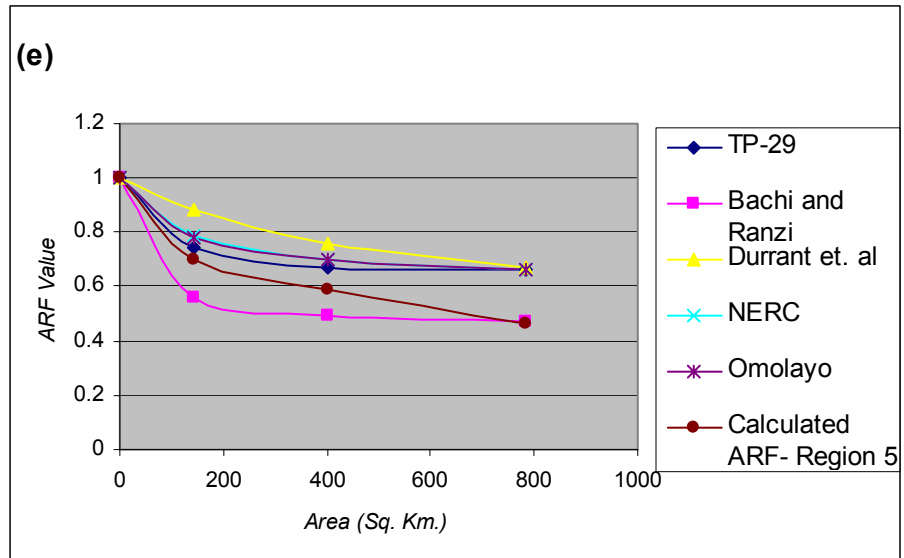
Figure 26. (continued) (e) Region 5 and (f) Region 6.

Figure 26. (continued) (g) Region 7.

The study is consistent with the findings of TP-29 and other such standards that area under consideration is a major factor affecting the reduction factors. One important thing to note here is that it was found that the decay in the values for larger area was much more than the standard studies. Slope of the decay is not much as predicted by standards but as can be seen from the above figures this slope is much higher for this study.

The study also showed, discussed later, that geographic location was an important factor, and could not be neglected while calculating the ARFs. Therefore ARF values cannot be taken as generalized values and used everywhere. Further, records available were too short to study the effect of the return period on the ARFs. For carrying out the statistical analysis 10 years of data are not sufficient as at least 30-40 years of data are required to study the affect of return period on ARFs. As can be seen from above figure the ARF ratios presented are significantly smaller for larger area than those published in official studies. The decay in the ARF values for larger areas was found out to be more than expected, as indicated in previous studies. Depth area ratios are less than unity but are higher than those published in TP-29 1 hour curves and Bachi and Ranzi (1996). The analysis presented here, keeps the track indicated by Asquith, 2000 study, although some substantial modifications are introduced. Therefore the results are also compared to his study of 1day ARF values.

Table 7 shows the comparisons of the results obtained to some standard studies.

Table 7. Comparison of Results with the Standards

Values from Previous Studies		Area in Sq. Km.		
	0	144	400	784
TP-29				
30 mins.	1	0.62	0.57	0.56
1 hr	**1**	**0.74**	**0.67**	**0.66**
2 hr	1	0.84	0.72	0.68
3 hr	1	0.86	0.81	0.78
6 hr	1	0.90	0.84	0.83
24 hr	1	0.94	0.92	0.91
Asquith (2000) 1day				
Houston	1	0.85	0.73	0.69
Austin	1	0.76	0.69	0.66
Dallas	1	0.81	0.77	0.73
Bachi and Ranzi (1996)	1	0.56	0.49	0.47
Durrans (2003)				
1 hr	**1**	**0.88**	**0.76**	**0.67**
2 hr	1	0.89	0.70	0.69
4 hr	1	0.90	0.80	0.70
NERC	**1**	**0.79**	**0.70**	**0.66**
Omalayo(1986)				
1 hr	**1**	**0.78**	**0.70**	**0.66**
1 day	1	0.94	0.92	0.90
Calculated Texas ARF				
Region 1	1	0.73	0.59	0.49
Region 2	1	0.78	0.59	0.45
Region 3	1	0.79	0.61	0.42
Region 4	1	0.71	0.58	0.42
Region 5	1	0.70	0.59	0.47
Region 6	1	0.72	0.59	0.41
Region 7	1	0.79	0.62	0.52

Comparisons with some formulas that are widely used in the engineering practice show that the results are consistent for smaller areas. But as the area under consideration increases there is a larger decrease in the values as compared to other studies. Assuming the ergodicity of the rainfall processes, essential for the formulation of any statistical analysis, the reduction factors derived should be considered rather representative. Also this study does not take into account the frequency of the storm and duration of the storm and so these values do not exactly harmonize with the previous studies. The ARF factors presented in this study have been based on the assumption that the areal reduction factor does not vary with return period. Variation with return period needs to be investigated in order to make more valid conclusions. Furthermore, the ARF for areas smaller than 16 Sq. Km. are assumed to be unity. Both these areas can be a subject of further research. Also storm duration is another factor which can considerably affect the ARF values and so this is also a topic of future research. Further testing of the methodology based on the analysis of the different meteorological events and statistical analysis for frequency determination are certainly needed before the results of the study can be accepted for applications. Also research can be carried out to check the dependence of ARF values on climatic conditions. Due to the novelty of the radar data collection leads to the fact that the archived records of the radar data are very short (10 years in this case) and so they are not representative of long term behavior. With the acquisition and availability of sufficient additional data and deeper research, this study can be extended to longer storm durations and statistical frequency analysis. Continued research is necessary and would lead to significant improvements in the estimation of ARF values.

7.2 VARIATION OF ARF WITH LOCATION

It was found out during the study that the same ARF values calculated could not be used throughout Texas, as ARF values had a significant dependency upon the location of the area under consideration. Due to the variation in these values with respect to location, ARF values were calculated for the various regions. As already discussed in the earlier sections, Texas can be divided into seven different regions depending upon the topography and climatic conditions. ARF values were calculated for these seven regions and it was noted that these values were different for one another. Though there was no significant disparity, the difference in the values was considered rational enough to find area representative values for the various regions. Figures 27 (a) and (b), 28 (a) and (b) and 29 (a) and (b) show the variability of the ARF values for Region 1. As can be inferred from the plots most of the RS1 values for the region were found to lie in the range of 0.7 to 0.84. Values, as low as 0.46, were also found during the estimation of the ARF ratios. RC1 values were also found to follow the same pattern, though the values calculated were a little smaller than the RS1 values. Also, the RC1 values were distributed over a narrower range.
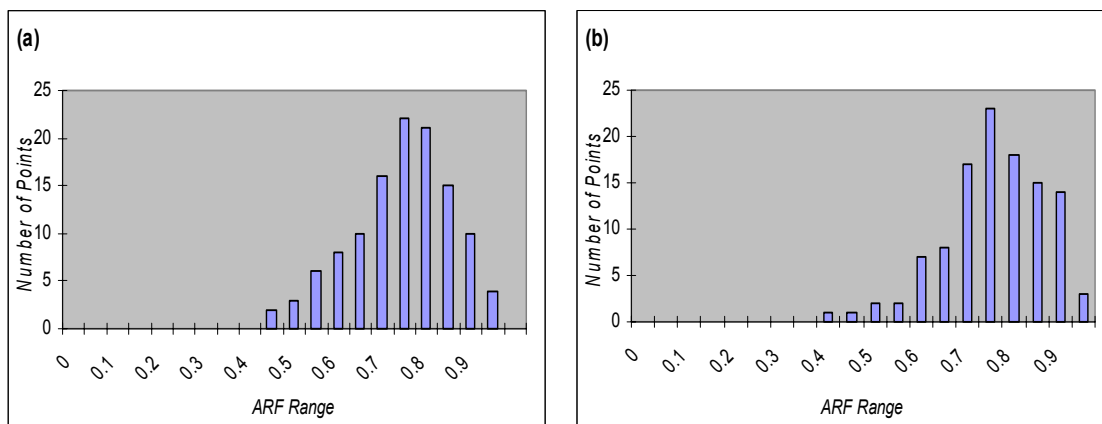
Figure 27. Variation of ARF Values for Region 1(a) RS1 Values (b) RC1 Values.

The RS2 values were found to be in the range of 0.04 to 0.8, with 0.68 being the average value. However, some extreme values were also found to exist. There was more uniformity in the RC2 values as compared to the RS2 values. The range for the values was much larger, with 0.62 being the average. Figure 28 shows the variation of RS2 and RC2 values Region 1.
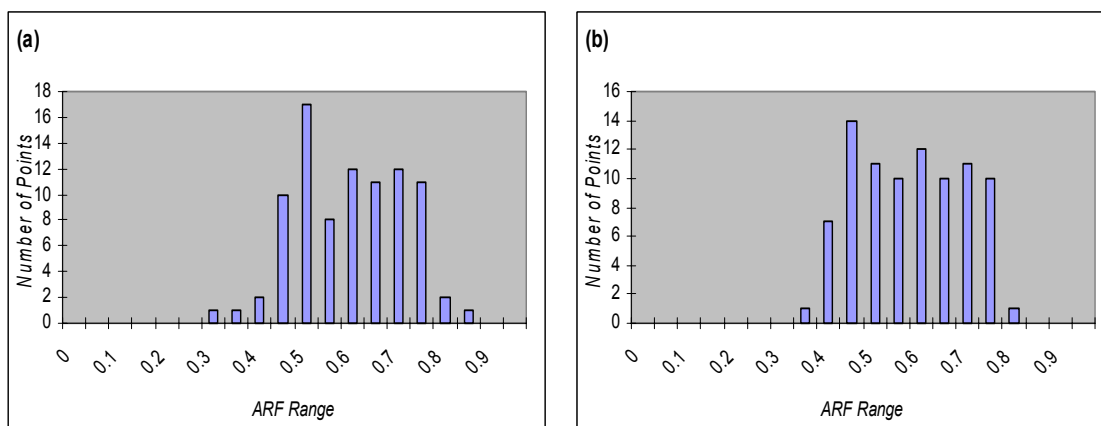

Figure 28. Variation of ARF Values for Region 1(a) RS2 Values (b) RC2 Values.

Figures 29 (a) and (b) show the variation of the ARF values for an area of 784 Sq. Km. As can be seen from the plot, the scatter in these values is much larger than for others. This can be explained by the fact that the storms are more localized and cover a smaller area and as the area of the watershed increases the storm, usually, might not be able to cover the whole of the area.
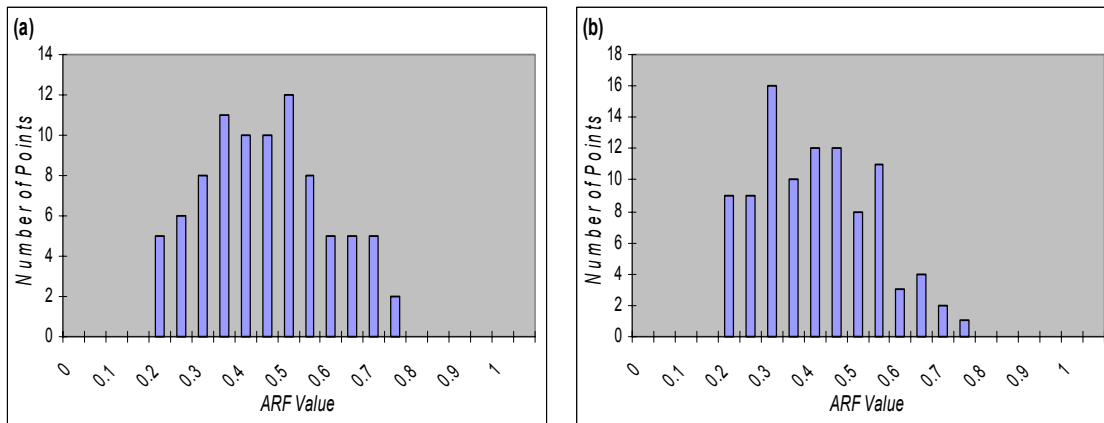
Figure 29. Variation of ARF Values for Region 1(a) RS3 Values (b) RC3 Values.

Figures 30 (a) thru (g) illustrate the variability of the RS1 ARF ratios (144 Sq. Km.) for different regions for the year 2000. Figures 30 (h) thru (n) illustrate the variability of the RC1 ARF values (144 Sq. Km.) for various regions for the year 2000. Curves for other areas are not shown along with these plots to make them more readable. For plots showing ARF ratios for other area (400, 784 Sq. Km.) refer to the appendix.
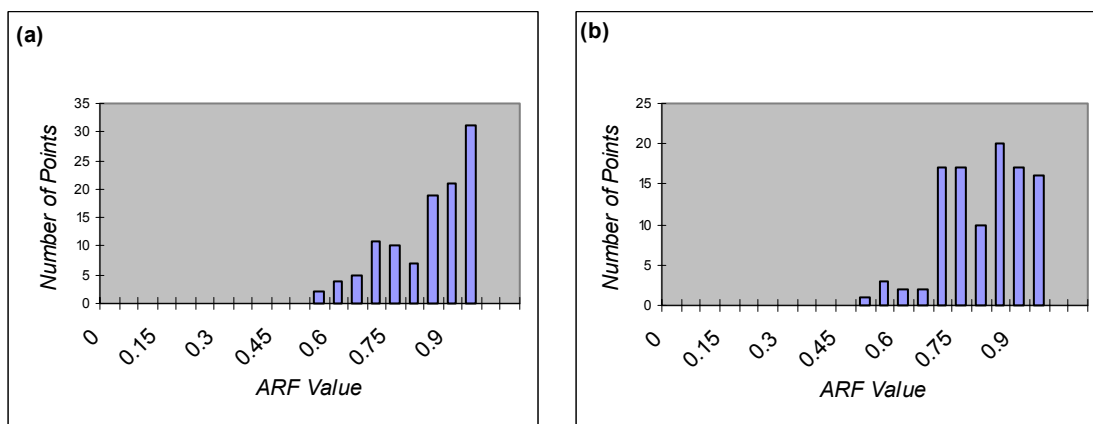
Figure 30. Variation of RS1 and RC1 for (a) Region 1 (b) Region 2.
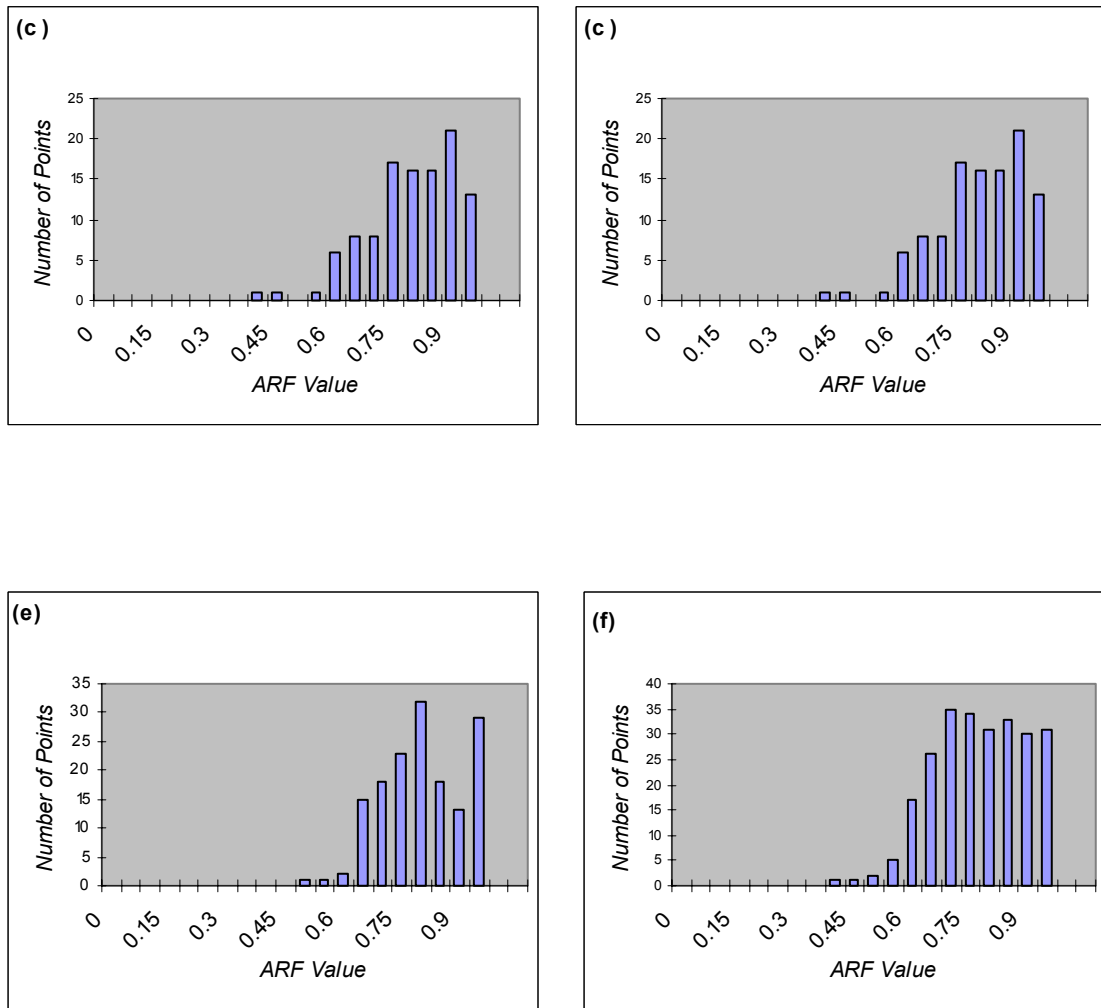
Figure 30. (continued) (c) Region 3 (d) Region 4 (e) Region 5 (f) Region 6.
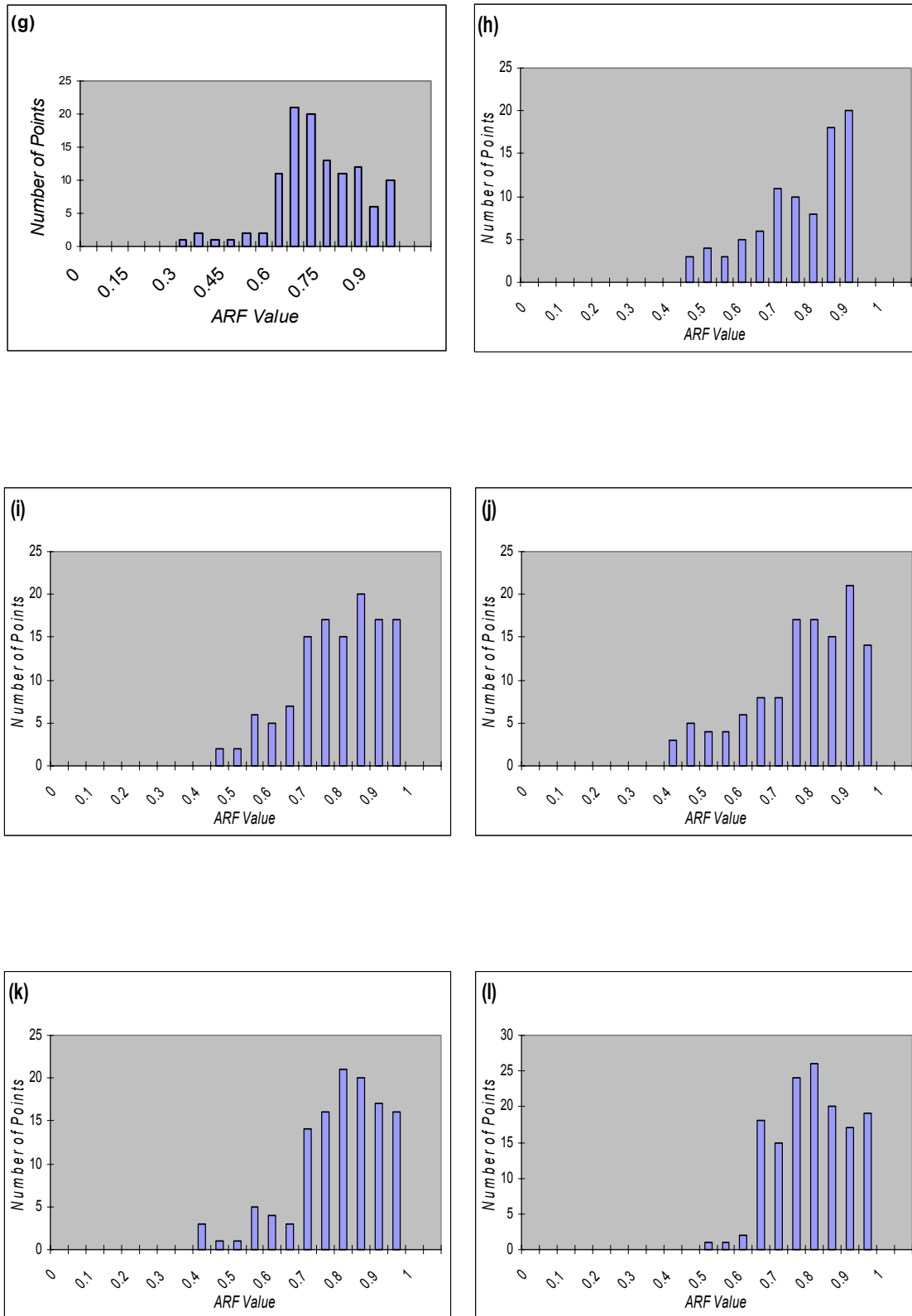
Figure 30. (continued) (g) Region 7 (h) Region 1 (i) Region 2 (j) Region 3 (k) Region 4 (l) Region 5.
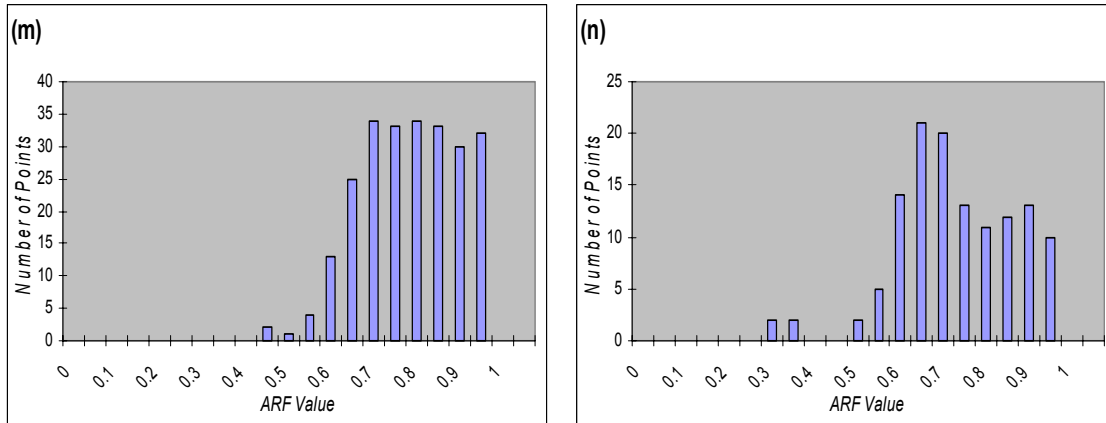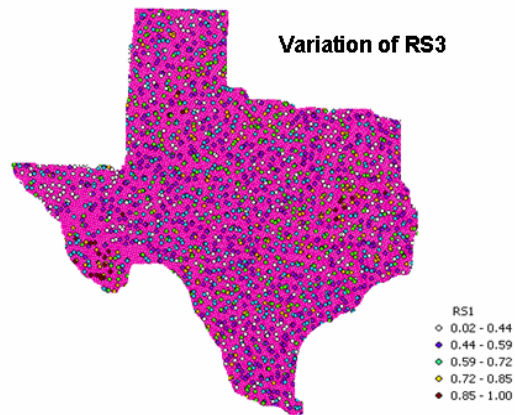
Figure 30. (continued) (m) Region 6 and (n) Region 7.

.

Figures 31 (a) thru (c) illustrate the variability of the square ratios throughout the area of study for 2002.
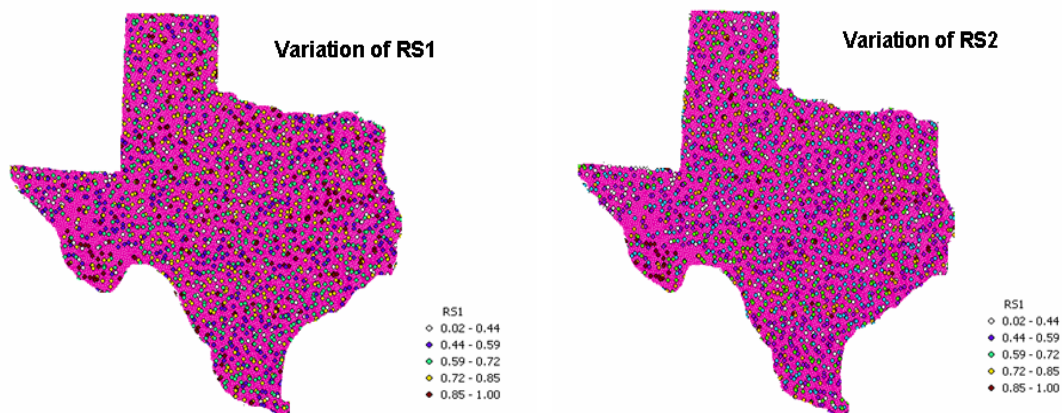
Figure 31. Variation for Region 1 (a) RS1 Values (b) RS2 Values.

Figure 31. (continued) (c) RS3 Values.

Variability of various ARF values (RS1, RC1, RS2, RC2, RS3, and RC3) for different years are also represented for various blocks. The blocks were chosen randomly and have nothing to do with any specific area of concern. As it is not feasible to show all the blocks in any particular region so it was assumed that by showing the values of the ARF for a central block in every region, one would get an idea as to how the values differ from one region to another. It must be reiterated here that these blocks are assumed to be representative and may/may not symbolize the true variation of ARF for a particular region. This was done to consolidate the finding that ARF pattern depends upon the geographical location of the watershed.

Figures 32 (a) thru (g) show the variation in ARF values for different years.
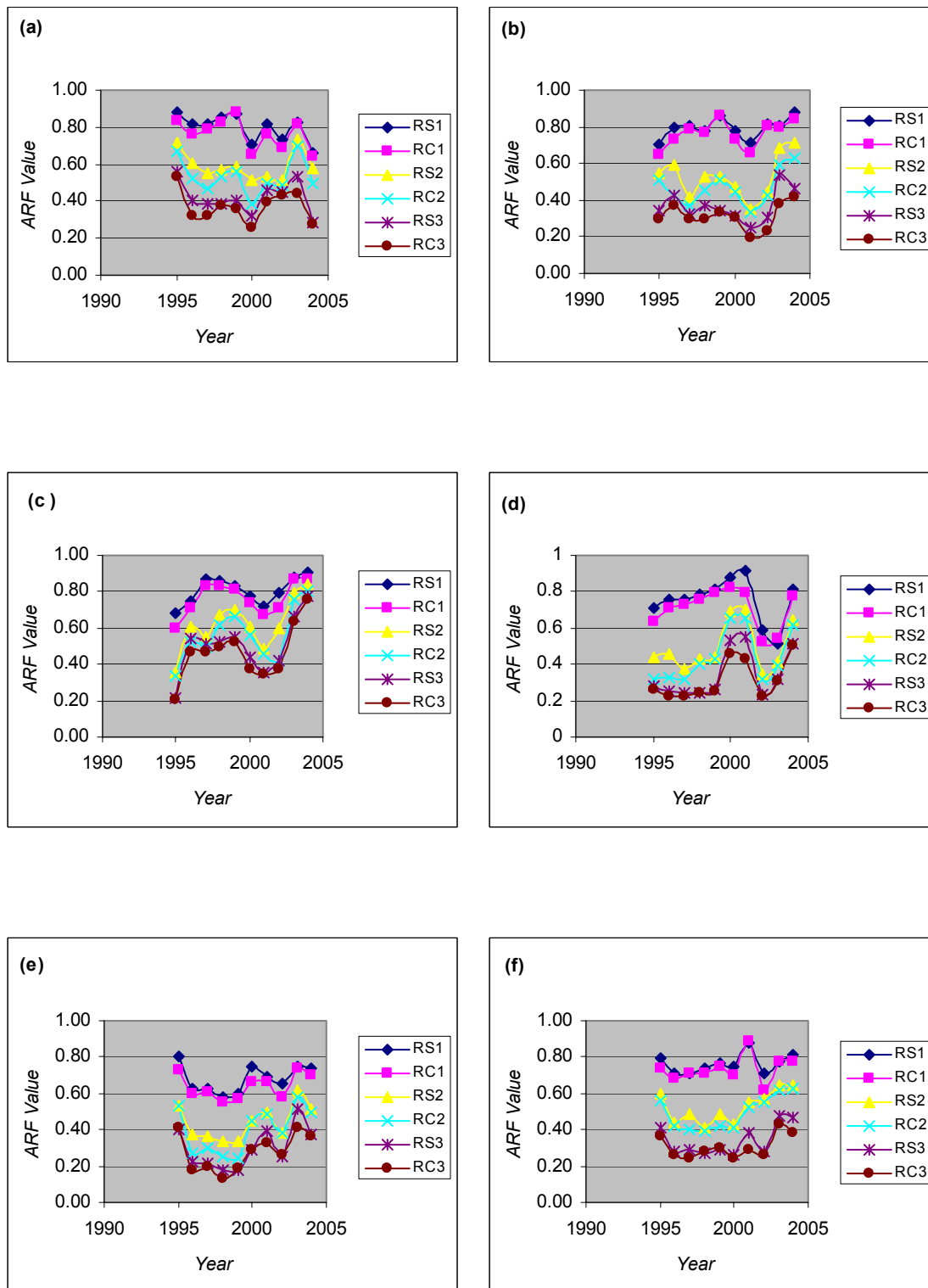
Figure 32. Variation of ARF Values for Blocks in (a) Region 1 (b) Region 2 (c) Region 3 (d) Region 4 (e) Region 5 (f) Region 6.
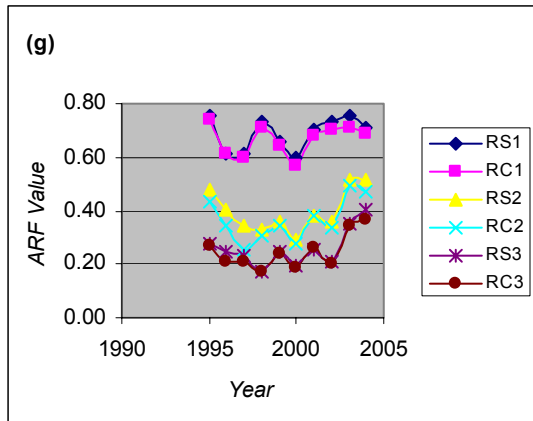
Figure 32. (continued) (g) Region 7.

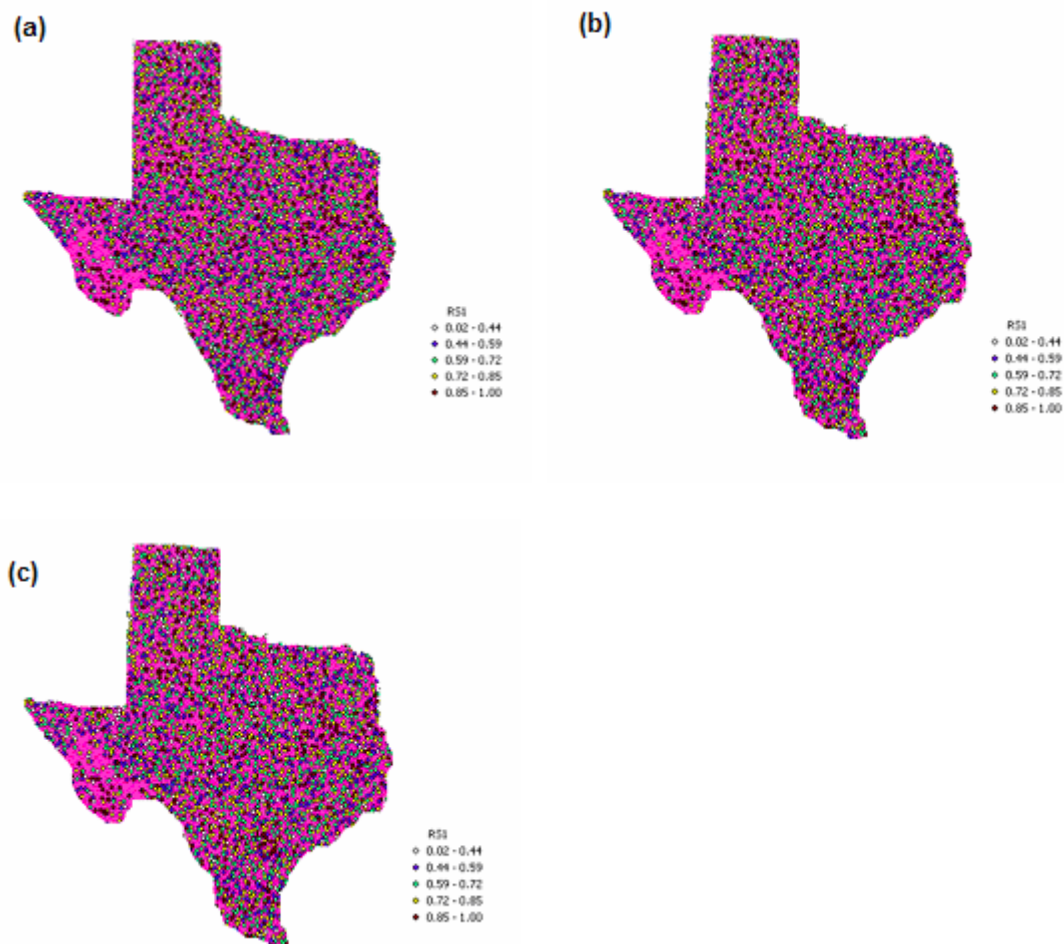Figures 33 (a) thru (i) show the variability of the RS1 ratios for Texas during various years.
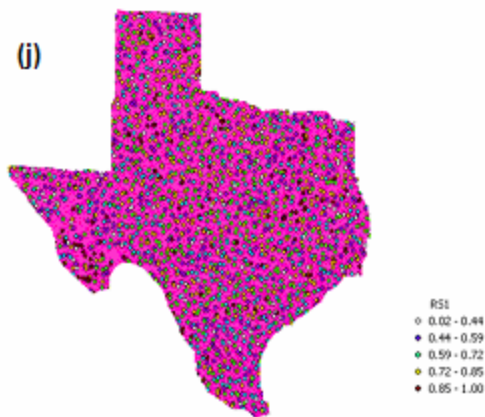

Figure 33. Variation of RS1 for (a) 1995 (b) 1996 (c) 1997.

Figure 33. (continued) (d) 1998 (e) 1999 (f) 2000 (g) 2001 (h) 2002 (i) 2003.

Figure 33. (continued) (j) 2004.

The reason for these differences in the values is not very clear but can be explained by the fact that the ARF values depend upon the time of the year when the annual maxima occurs. Also, for this study duration of the storm was not taken into account and so this can also be a leading factor in causing such inconsistency. These can also be attributed to random sampling variations or to certain irregularity in the radar data available. In general, a trend showing a decay in values as area increases can be found from the study. This fact is found to be consistent with the previous studies. Finally to conclude, it can be said with confidence, after looking at the results, that ARF values are dependent upon the location of the watershed and the values cannot be generalized and used everywhere. Specific values exist for specific locations and this point should be taken into consideration before actually using ARF values for a particular region.

7.3 VARIATION OF ARF WITH SHAPE OF WATERSHED

During the past studies, determination of representative shape of the watershed is taken to be arbitrary which in reality has certain implications. Part of this study was to see if the ARF values varied with the shape of the area under consideration. As can be seen from recent literature (Asquith and Famiglietti, 2000), the ARF values are said to differ with the watershed shape. In many of the earlier studies, the shape of the watershed is considered to be arbitrary. That is the ARF values are said not to depend on the shape of the area being considered. In TP-29, the shape factor is not taken into account and hence the same values of the ARF for a long narrow watershed and a circular watershed with the same area are assumed. In recent studies shape has been given importance (Asquith and Famiglietti, 2000) and hence in this study, square and circular shapes are taken into consideration when finding out the ARF values. ARF ratios are found for both square and circular shapes for areas of 144, 400, and 784 Sq. Km.

Figures 34 (a) thru (c) show the scatter plots of square and circular ARF values for Region 1 (Panhandle Plains) for the year 2003.
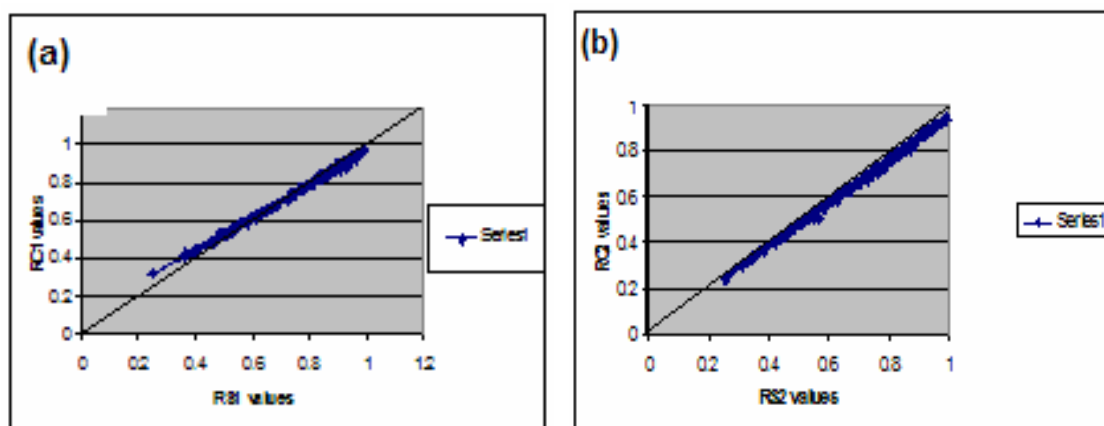
**Figure 34.** Scatter Plots for Region 1 (a) RS1 and RC1 (b) RS2.
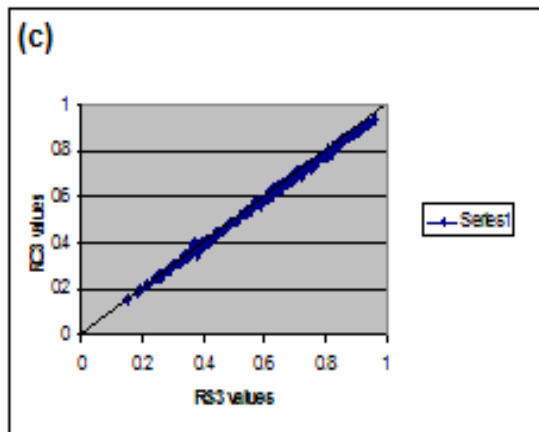
Figure 34. (continued) (c) RS3 and RC3.

As can be seen from the figures there is not much variation in the RS1 and RC1 values and there is a close scatter of these values around the 1-1 (45 degrees) line. This shows that for smaller areas (here up to 144 Sq. Km.), the ARF values for the square and circular shapes are almost identical and there is not much disparity in these values. On the other hand, these values tend to vary for larger areas. The square and circular ARF values become different from one another for areas of 400 and 784 Sq. Km. Circular values tend to be much smaller than the square values. The circular values better represent the ARF values for larger areas and so we can see that the ARF values are dependent upon the shape of the area being considered. The same trend can also be seen in the various regions.

Figures 35 (a) thru (f) illustrate the variation of RS1 and RC1 values for various regions.
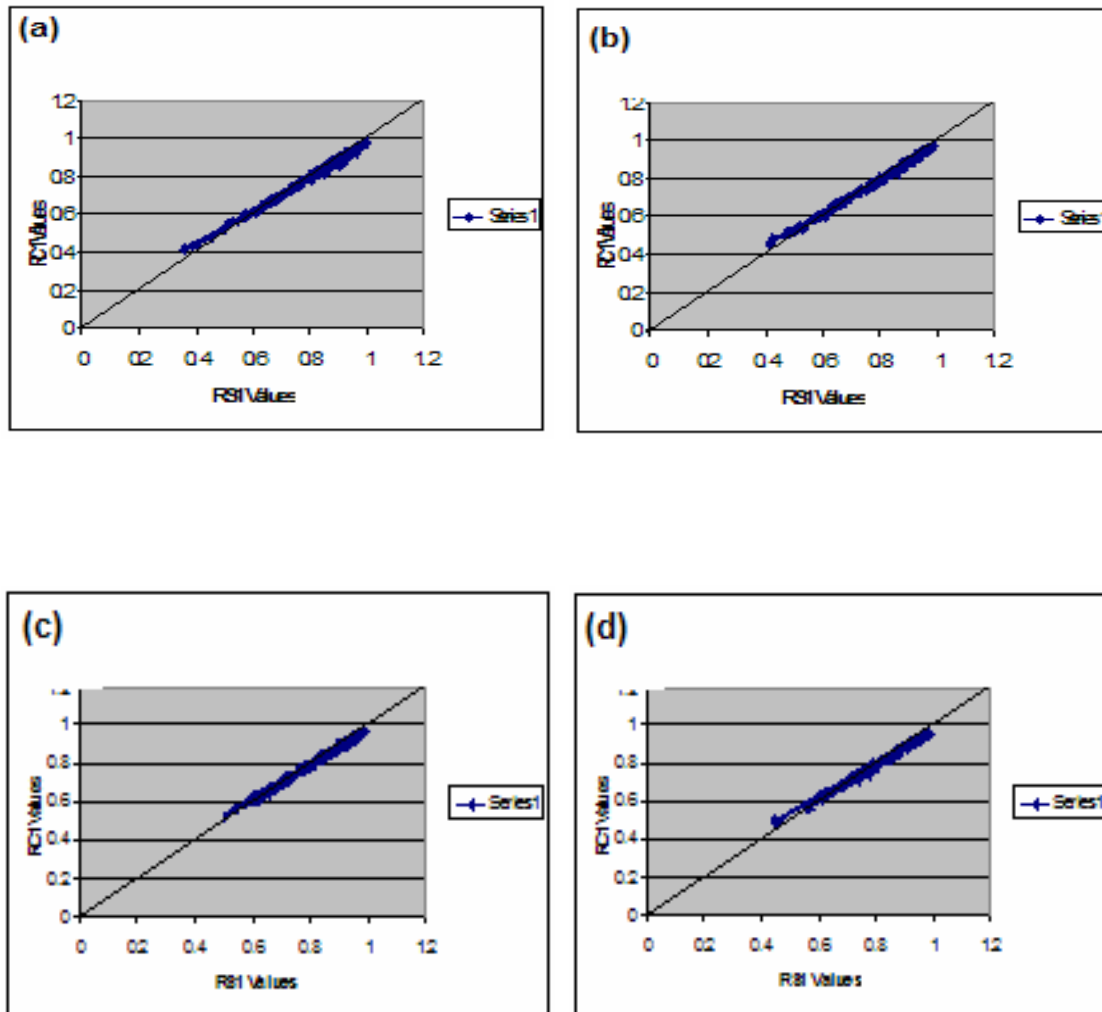

Figure 35. Scatter Plot RS1 and RC1 for (a) Region 2 (b) Region 3 (c) Region 4.
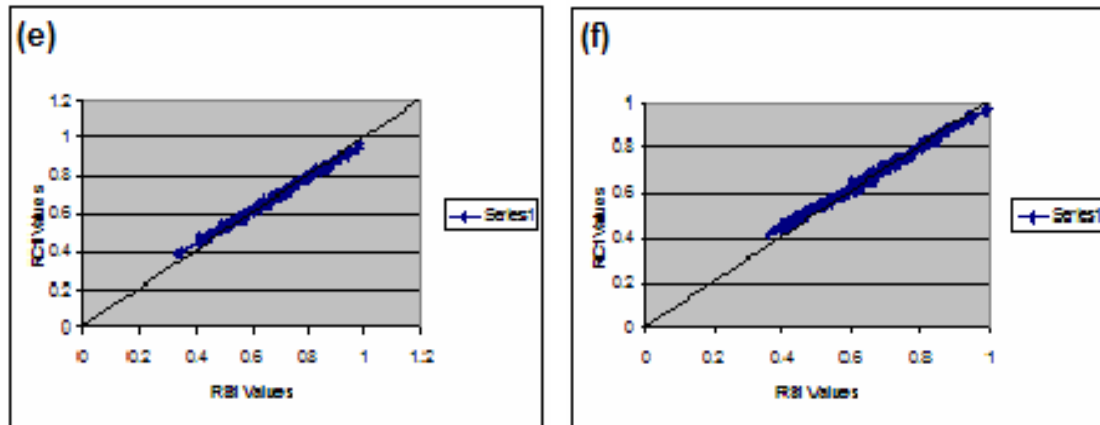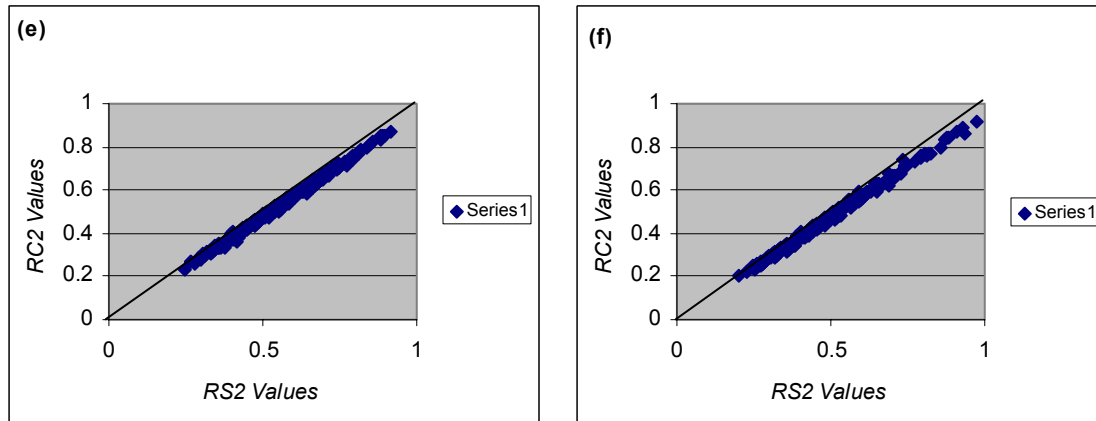
Figure 35. (continued) (e) Region 6 and (f) Region 7.

As can be seen from the above figures there was a strong linear relationship between the square and the circular ARF values. Close scatter around the 1-1 (45 degrees) line shows that for smaller areas the ARF values are almost similar for the square and circular regions. The values for both the shapes showed consistency with respect to one another. Circular values were almost similar to the square values for all the regions. Hence it can be said, without doubt, that the shape of the area under consideration does not have much impact on the ARF values for small watershed areas.

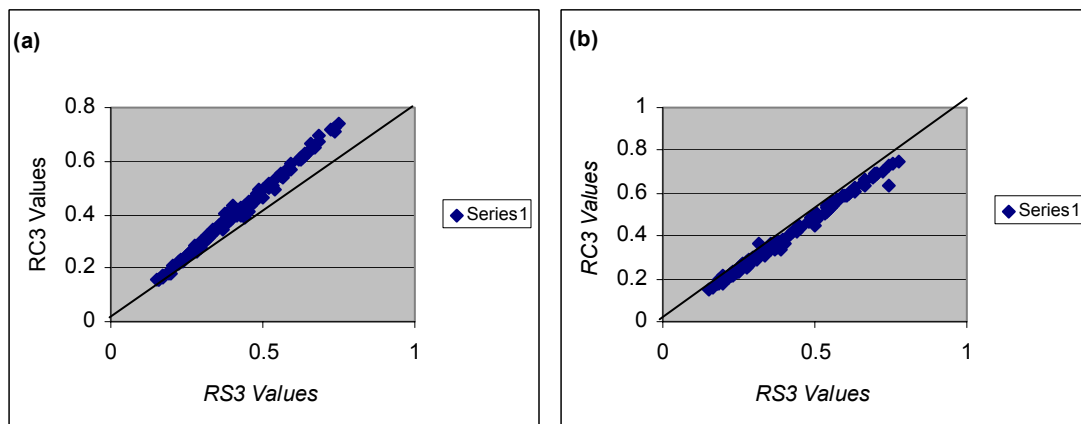Figures 36 (a) thru (f) illustrate the variation of RS2 and RC2 values for the various regions.
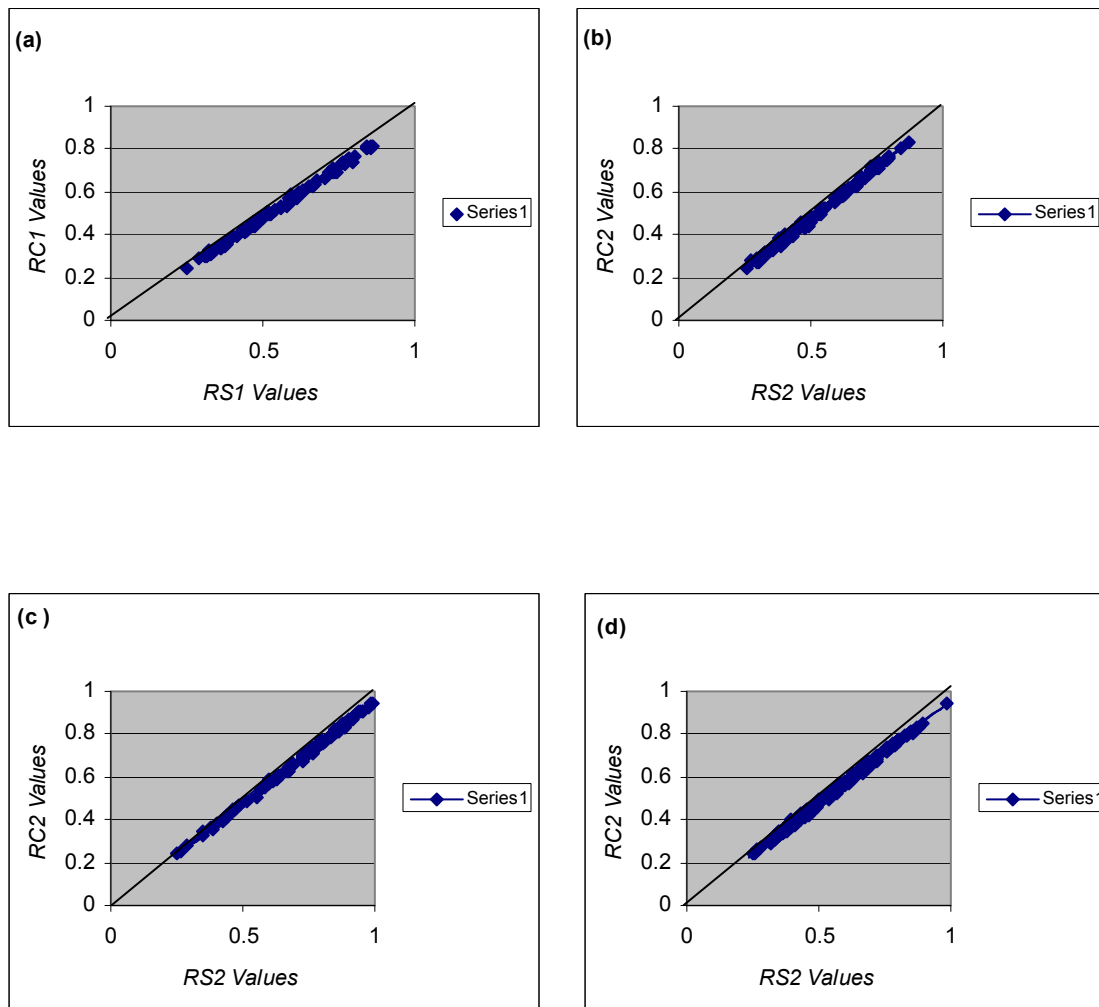
Figure 36. Variation of RS2 and RC2 values for (a) Region 2 (b) Region 3 (c) Region 4 (d) Region 5.
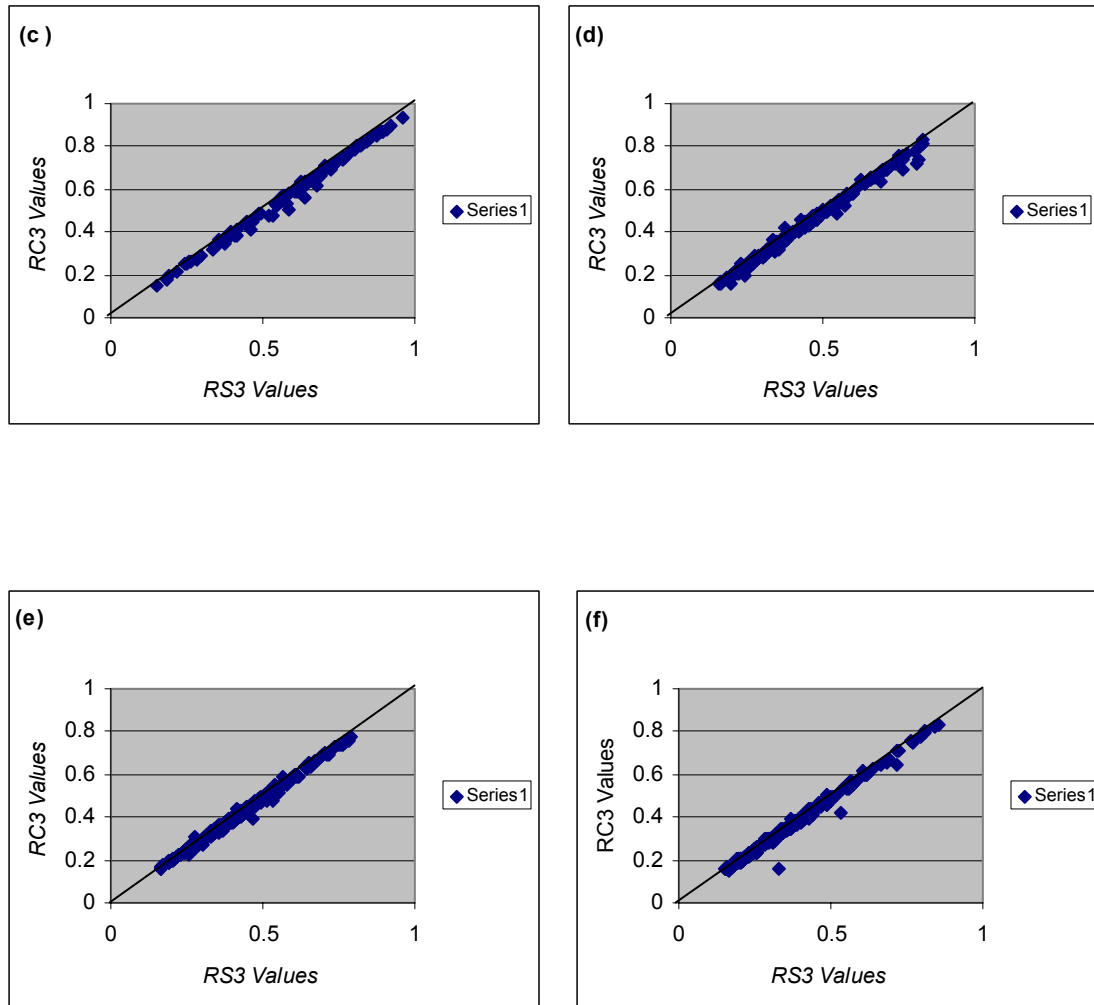
Figure 36. (continued) (e) Region 6 and (f) Region 7.

Figure 37 (a) thru (f) illustrate the variation of RS3 and RC3 values for the different regions.

Figure 37. Variation of RS3 and RC3 values for (a) Region 2 (b) Region 3.

Figure 37. (continued) (c) Region 4 (d) Region 5 (e) Region 6 and (f) Region 7.

The above figures illustrate that as the area under consideration increases, the shape of the area has an impact on the ARF values. In general, the scatter of the plots increases with increasing area, which shows the influence of shape on the ARF values. The general trend is that the circular values better depict the ARF values. It can be seen from the study that circular ratios were generally smaller than the square ratios. In is assumed that the circle gives a better estimate of the ARF values as the circular shape

being a typical shape does not have to deal with sharp corners. Generally, it is found that watersheds are not perfect shapes with sharp corners and therefore a circular shape can be assumed to be a better representative of its shape than a square one. Moreover, the circular shape, in our study covers more number of cells, with lesser extent of each cell. So a larger number of cells are accounted for which is not the case in square shape, where the full extent of the cell is covered and not part of it. Differences in the values were found from the study and it is inferred that circular shapes better represent the area. But due to no strong relationship between the two kinds values, finding one ratio will not help in determining the value of the circular ration for the same area. So these values should be considered representative. For future research, this study can be carried out for different shapes like an ellipse, with variation in the ratios or the minor and major axis, which is thought to best represent the shape of a storm. These differences may be clear and profound for these other shapes like ellipse etc. This study does not tell us clearly as to which shape better represents the estimation of the ARF. With future studies based on other shapes it is expected that the dependence of ARF on shape of the watershed can be clearly predicted and also the dependence of one kind of ARF value on another can be found. This study illustrates that unlike the previous studies like USDC, 1963 this methodology cannot be generalized to relax the assumption of square and circular shapes of a watershed. The results derived although preliminary may find useful applications for the definition of design storms in urban catchments of a given shape of the watershed.

7.4 COMPARISON OF NEXRAD STAGE III AND MPE DATA

NEXRAD hourly rainfall accumulations are stored within individual Digital Precipitation Array (DPA). At different NWS River Forecasting Centers (RFCs) these are statistically coalesced with gauge and satellite data to fabricate Multisensor Precipitation Estimates (MPE). Evolution and development of MPE data over the years is described in detail by Young et al., 2000. MPE offers a versatile and integrated platform and a robust scientific algorithm suite for multisensor precipitation estimation using the benefits of rain gauges, radars and satellite data (Seo, 2003). For more information on MPE data refer to Section 4- Data Description. MPE data for this study was supplied by West Gulf River Forecasting Centre (WGRFC) of the NWS Hydrologic Research Laboratory (HRL). The data can be downloaded from:

http://dipper.nws.noaa.gov/hdsb/data/nexrad/wgrfc_mpe.html

The ARF values calculated from the Stage III data and the MPE data were compared in the study.

The following section shows the variation in these values for the various regions.
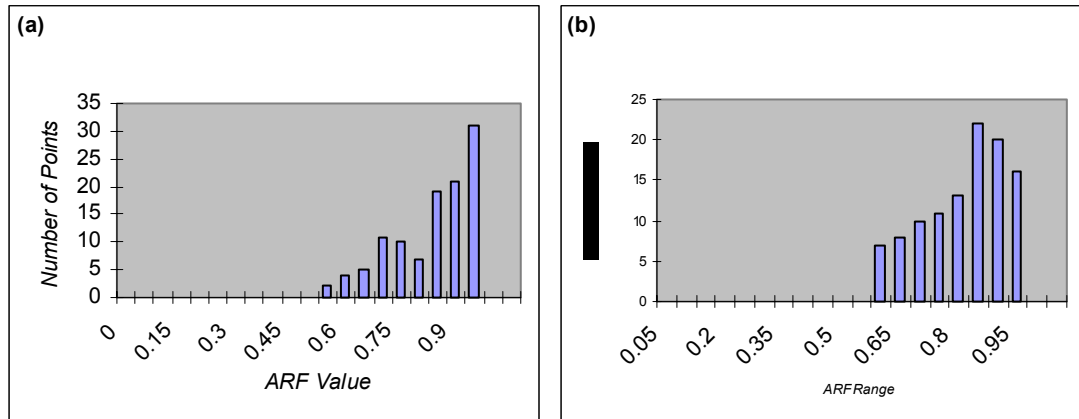
Figure 38. Comparison of RS1 Values for Region 1 (a) Stage III Data (b) MPE Data.

As can be seen from figures 38 and 39, majority of the RS1 values for the Stage III data for Region 1 were lying in the range of 0.85 to 1 and those for MPE data were lying in the range of 0.75 to 1. The standard deviation calculated for the points in this region was 0.22 for the Stage III data and 0.12 for MPE data. For the MPE data there were not too many RS1 with values of 0.9 and higher. Instead these values were distributed more uniformly, than the Stage III data, over a wider range.
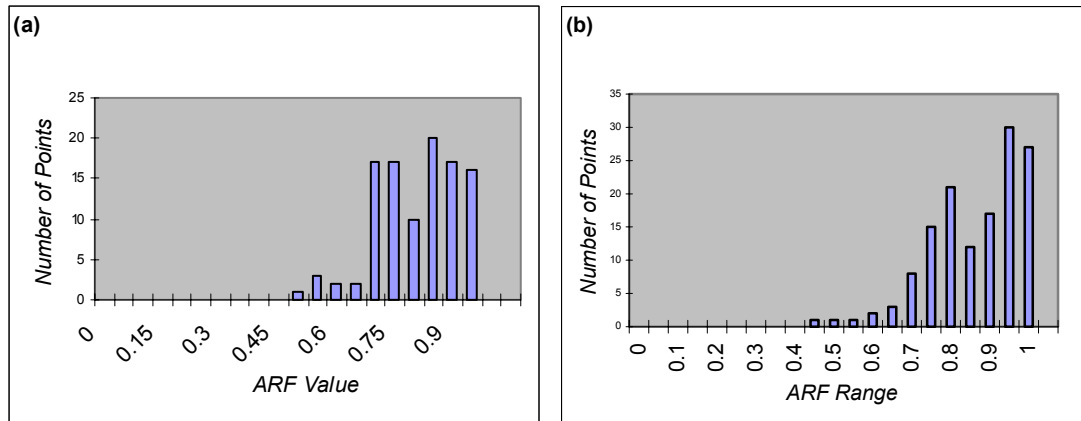
Figure 39. Comparison of RS1 Values for Region 2 (a) Stage III Data (b) MPE Data.

For Region 2, there was a uniform distribution of these values over a range of 0.7 to 1, for the Stage III data where as the distribution of the values obtained from the MPE data was non uniform. The standard deviation of points for the Stage III data was found to be 0.13 and that for MPE was 0.16

Figures 40 illustrate the variation of the RS1 ARF values for the various regions.
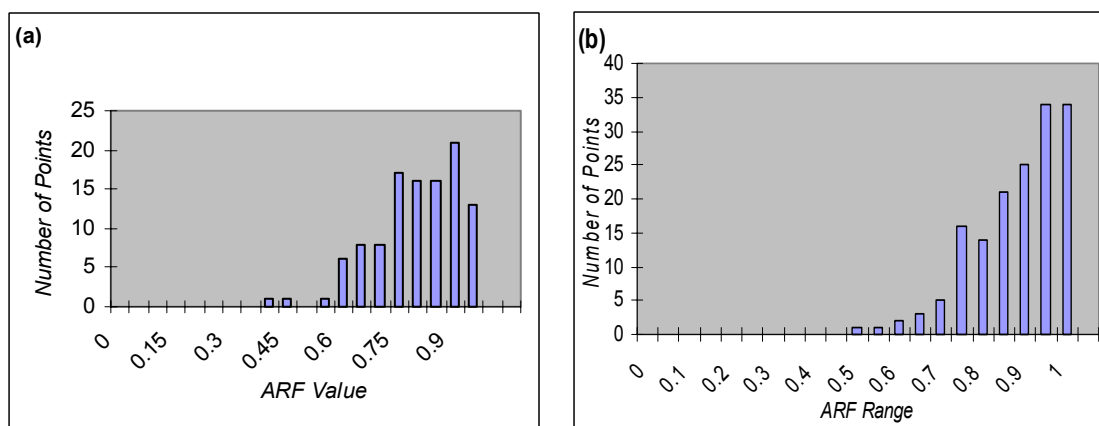
Figure 40. Comparison of RS1 Values for Region 3 (a) Stage III Data (b) MPE Data.
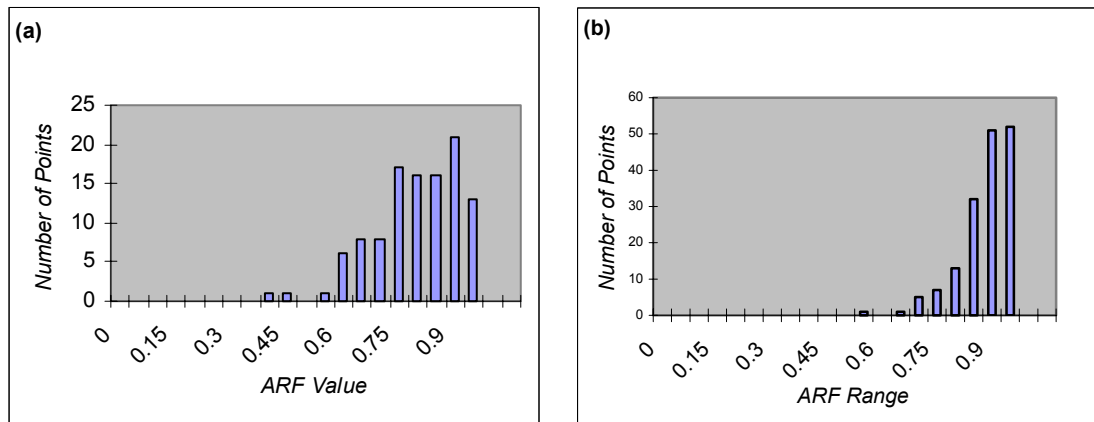
Figure 41. Comparison of RS1 Values for Region 4 (a) Stage III Data (b) MPE.

As can be seen from the figures 40 and 41, Stage III ARF values covered a wider range than the MPE ARF values. The standard deviation for MPE values was much lesser than the Stage III values.
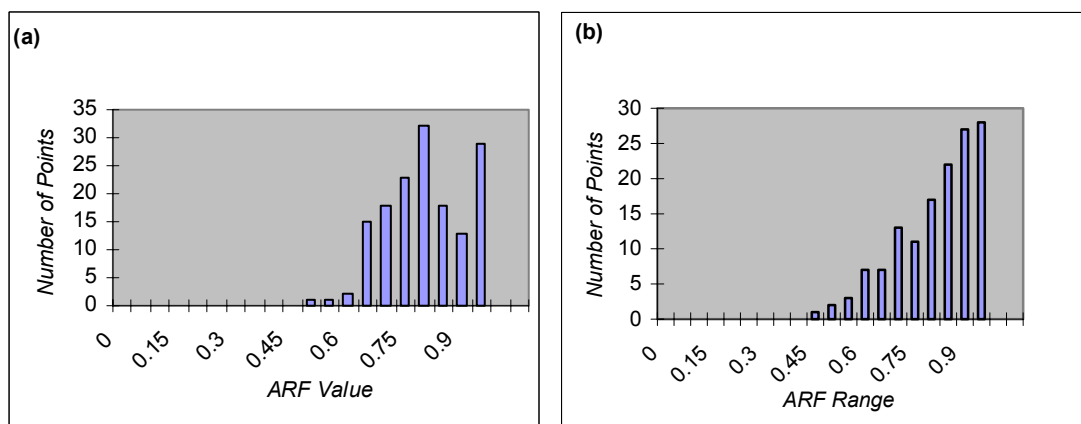
Figure 42. Comparison of RS1 Values for Region 5 (a) Stage III Data (b) MPE Data.

As can be seen from Figure 42, for Region 5 a general trend could be seen in the values obtained from the MPE data. There was an increase in the number of points as the ARF value increased. In other words there were more points with higher ARF values where as the number of points having low values were lesser. This trend could not be seen in case of Stage III data. For Stage III data there were a large number of points having the RS1 value between 0.8 to 0.85 and 0.95 to 1, whereas there were lesser number of points which lay in the range of 0.85 to 0.95.
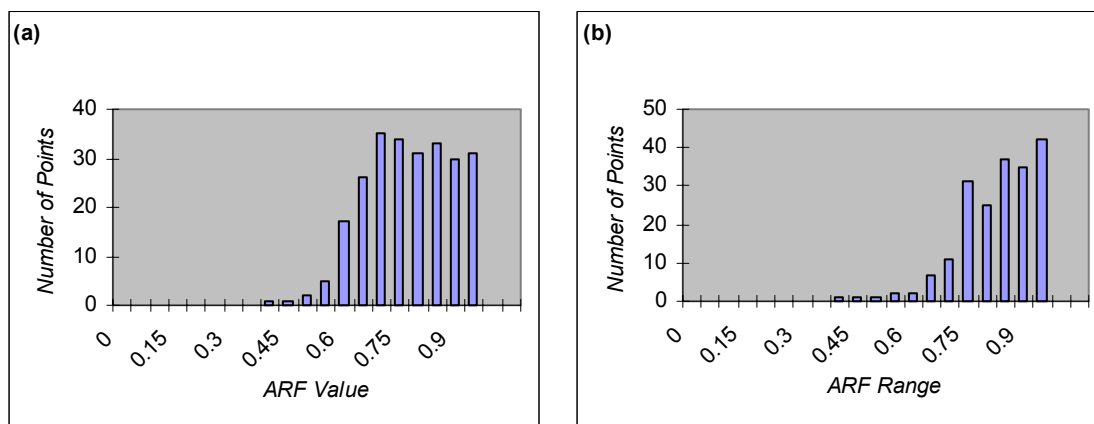
Figure 43. Comparison of RS1 Values for Region 6 (a) Stage III Data (b) MPE.

For Region 6, as can be seen from the Figures 43, RS1 values from Stage III data covered a range from 0.6 to 1 where as the values obtained from MPE data covered a narrower range from 0.75 to 1. Figure 44 illustrates the same trend for Region 7.
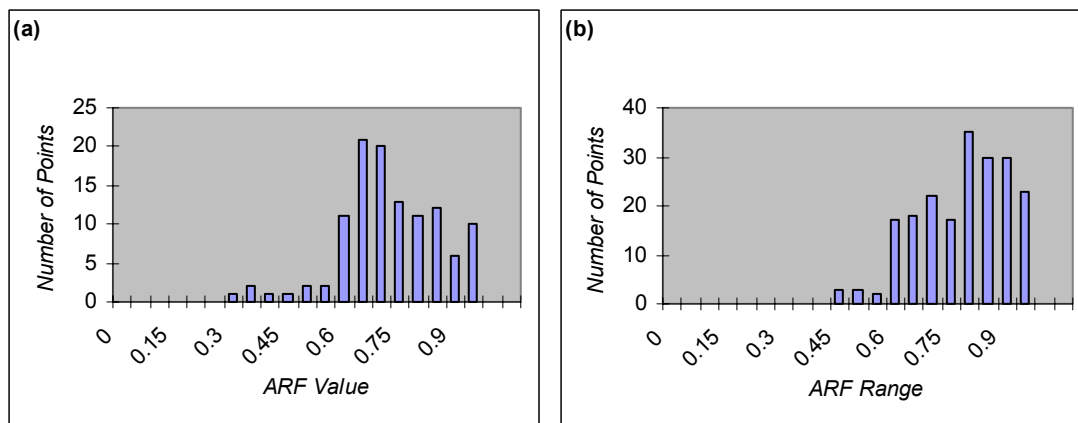
Figure 44. Comparison of RS1 Values for Region 7 (a) Stage III Data (b) MPE.

Values obtained from Stage III data were generally found to be spread over a wider range. Values, as low as, 0.33 could be found in Stage III data. There were lesser number of points having very high values in Stage III data whereas this was not the case with MPE data. A large number of values lay in the range of 0.9 to 1 for most of the regions for MPE data.

Comparison of the ARF values derived from the Stage III data and MPE data for various regions with respect to area is given by the following figures. ARF curves for the years 2002, 2001, and 2000 are plotted for both Stage III data and MPE data. Variation for other years is not shown here for clarity purposes.
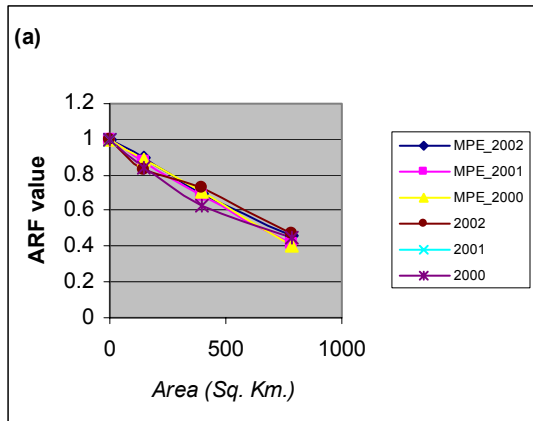
Figure 45. Comparison of Stage III and MPE Data for Blocks in (a) Region 1.

As can be seen from the figures 45 and 46 RS1 values lie in the range of 0.8 to 0.85, RS2 values in the range of 0.62 to 0.73 and RS3 values in the range of 0.38 to 0.49 for the block under consideration in Region 1. For the block in Region 2, range of RS1 is 0.78 to 0.88, RS2 is 0.63 to 0.71 and RS3 is 0.38 to 0.6.
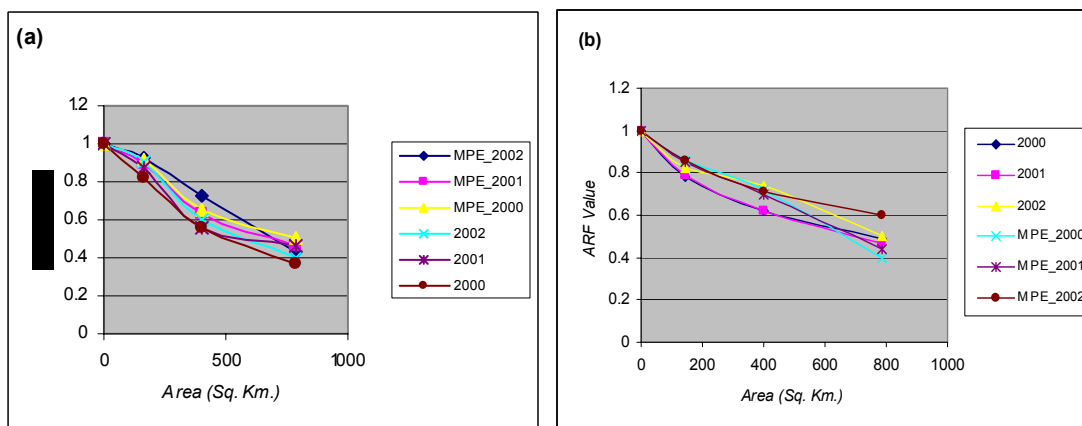
Figure 46. Comparison of Stage III and MPE Data for blocks in (a) Region 3 (b) Region 4.
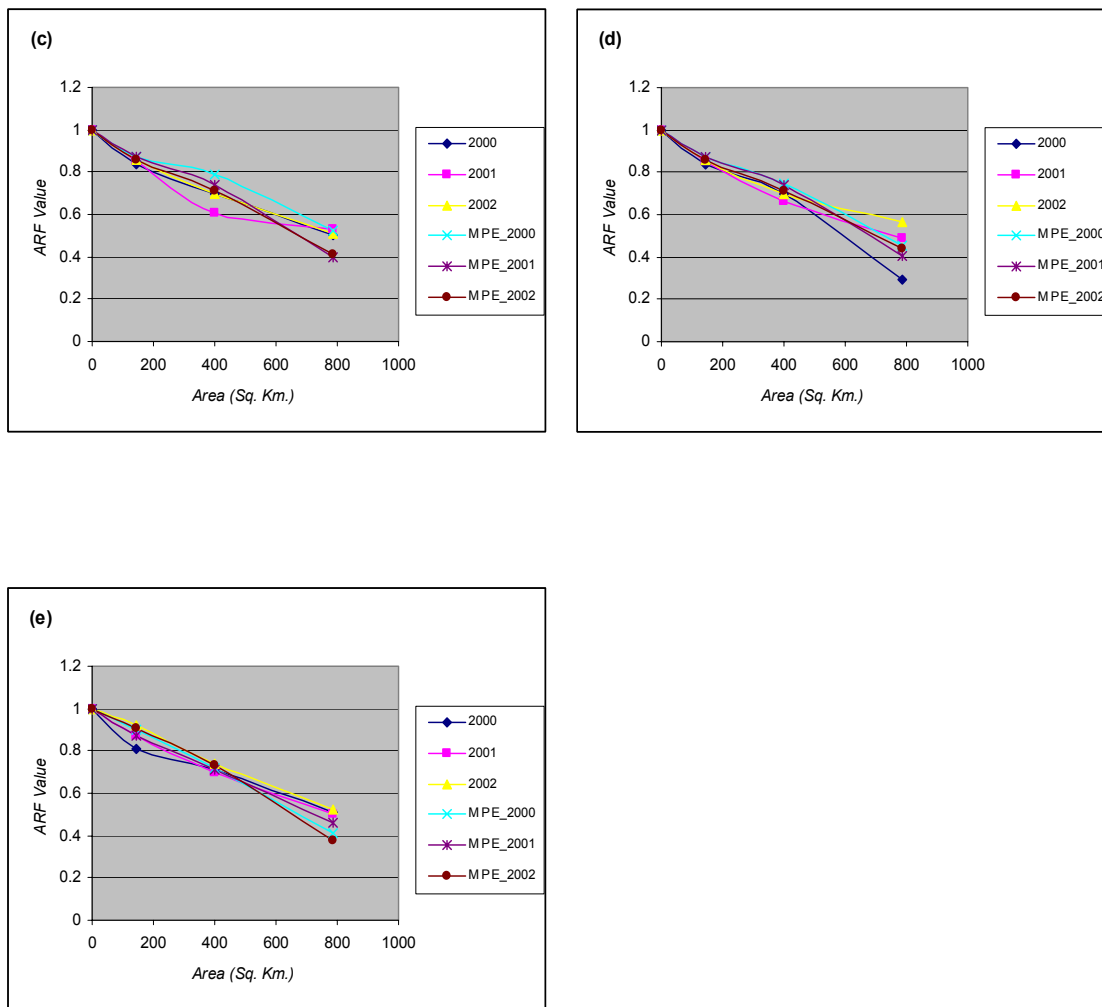
Figure 46. (continued) (c) Region 5 (d) Region 6 (e) Region 7.

7.5. SUBSTANTIAL DECREASE IN THE ARF VALUES FOR CELLS HAVING HIGH ANNUAL MAXIMA

While carrying out the study it was found that there was a substantial decrease in the ARF ratios for an area with central cell having higher annual maxima. This decrease in values became more subtle as the annual maxima value decreased. For higher annual maxima cells the RS1 ratios were much higher than the RS2 values

which were in turn higher than the RS3 values. The difference in the RS1 and the RS3 values was considerable for higher annual maxima values, where as for lower annual maxima values this difference was not that substantial. In other words, for extreme or large storms the ARF ratios are not as evenly distributed as for smaller, more frequent storms. This trend could also be seen in the circular ratios.

Table 8 below shows the variation of the annual maxima values for the different years. For the year 2001 the Maximum values were considerably higher than the rest of the years. High values for most of the years were around 112 and low values were around 9mm. The average values came out to be somewhere around 52.

Table 8. Variation of 1-Hour Rainfall Values for Different Years.

Year	Max.Value(mm)	Co-ordinate	Min.Value(mm)	Co-ordinate	Avg.Value(mm)
1995	114.21	351,234	9.38	69,370	47.27
1996	117.15	236,162	9.14	72,372	52.16
1997	108.61	298,115	9.18	116,215	53.01
1998	107.98	333,147	7.11	69,373	55.05
1999	110.11	333,54	6.11	70,315	55.82
2000	113.86	169,358	8.12	70,377	52.16
2001	183.02	299,116	7.10	58,123	52.03
2002	109.99	351,155	8.18	17,305	48.70
2003	110.98	231,158	14.53	94,158	37.88
2004	126.41	377,239	5.33	112,151	38.99

Figures 47 (a) thru (g) illustrate the distribution of the Square ARF values for all the seven regions for the year 2003.
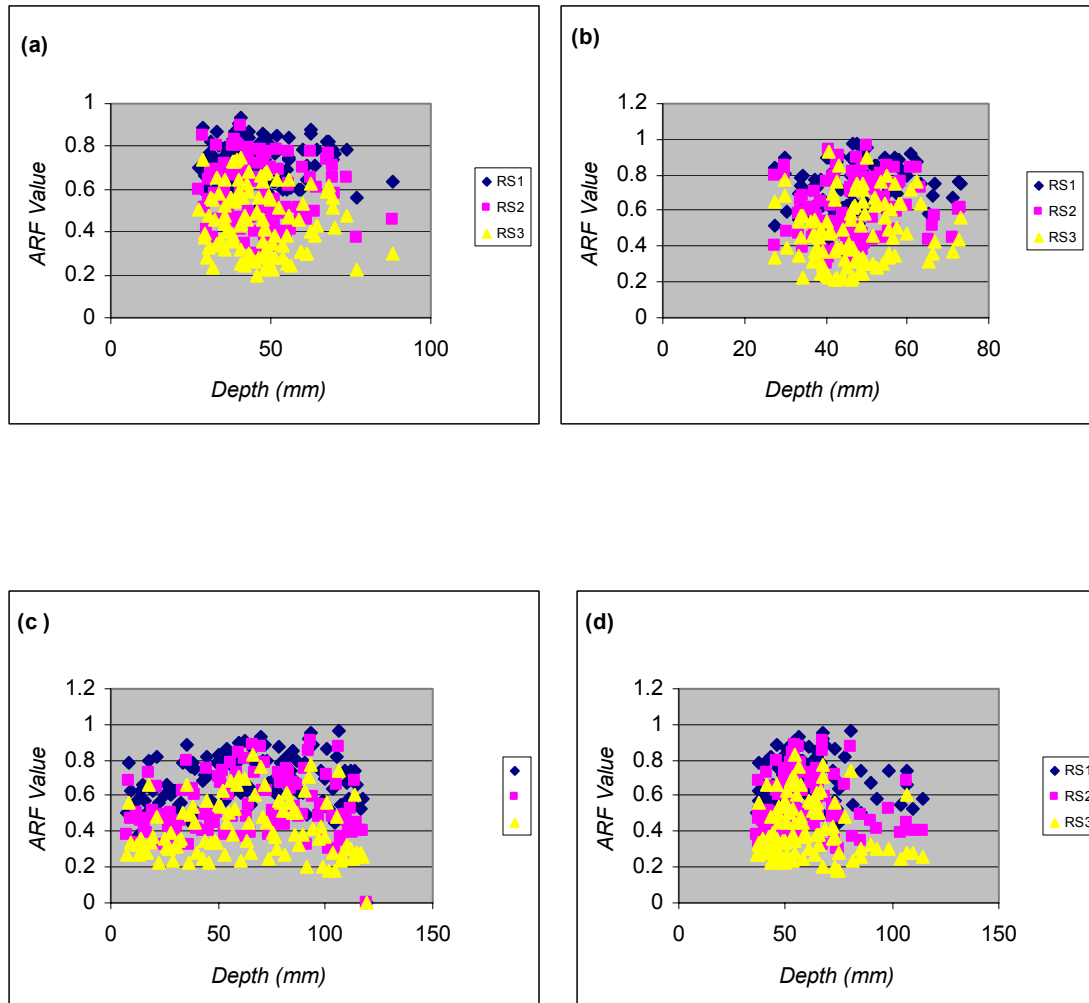
Figure 47. Distribution of Square Ratios for 2003 in (a) Region 1 (b) Region 2 (c) Region 3 (d) Region 4.
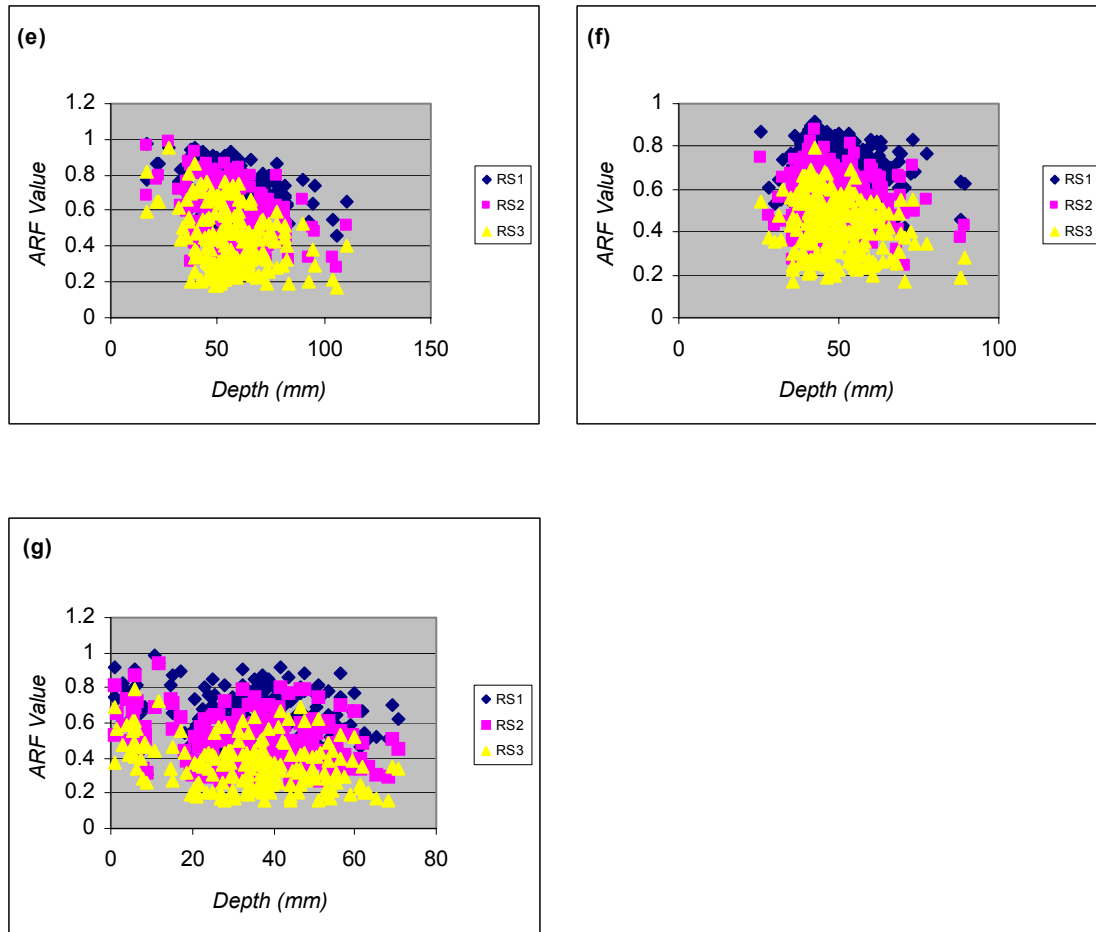
Figure 47. (continued) (e) Region 5 (f) Region 6 and (g) Region 7.

As can be seen from the figure Regions 3, 4 and 5 had high rainfall depths of upto 120 mm where as the other regions had comparatively lower depth values. Region 7 had rainfall depth values as low as 3mm where as for other regions the lowest values were around 25mm.

Table 9 below shows the percentage decrease in high square values for the year 2003.

Table 9. High Values (Square Ratios for 2003)

Column	Row	Value(mm)	Region	RS1	RS2	RS3	%Decrease
377	239	126.41	3	0.70	0.53	0.36	49.00
377	237	109.47	3	0.53	0.40	0.28	46.89
367	221	113.94	3	0.58	0.41	0.26	55.57
379	207	104.51	3	0.55	0.39	0.25	54.11
363	183	107.34	3	0.66	0.45	0.28	57.36

Table 10 below shows the percentage decrease in high circular values for the year 2003.

Table 10. High Values (Circular Ratios for 2003)

Column	Row	Value(mm)	Region	RC1	RC2	RC3	%Decrease
377	239	126.41	3	0.71	0.50	0.36	50.92
377	237	109.47	3	0.57	0.40	0.28	49.21
367	221	113.94	3	0.61	0.38	0.26	57.69
379	207	104.51	3	0.56	0.35	0.25	58.44
363	183	107.34	3	0.67	0.43	0.28	58.83

Table 11 below shows the percentage decrease in low square values for the year 2003.

Table 11. Low Values (Square Ratios for 2003)

Column	Row	Value(mm)	Region	RC1	RC2	RC3	%Decrease
113	147	8.38	7	0.55	0.53	0.47	14.99
112	151	5.33	7	0.55	0.50	0.48	12.11
114	148	8.38	7	0.55	0.52	0.49	10.97
140	148	5.94	7	0.90	0.88	0.80	11.37
150	148	7.92	7	0.93	0.93	0.85	8.17

Table 12 below shows the percentage decrease in low circular values for the year 2003.

Table 12. Low Values (Circular Ratios for 2003)

Column	Row	Value(mm)	Region	RC1	RC2	RC3	%Decrease
113	147	8.38	7	0.54	0.48	0.45	15.70
112	151	5.33	7	0.51	0.48	0.47	7.72
114	148	8.38	7	0.54	0.47	0.45	15.30
140	148	5.94	7	0.90	0.84	0.78	13.87
150	148	7.92	7	0.94	0.89	0.83	11.57

144

Table 13 below shows the percentage decrease in average square values for the
year 2003.

Table 13. Average Values (Square Ratios for 2003)

Column	Row	Value(mm)	Region	RC1	RC2	RC3	%Decrease
287	91	35.48	3	0.70	0.60	0.45	35.29
267	93	34.17	3	0.75	0.62	0.51	32.09
225	186	36.51	6	0.74	0.66	0.53	28.36
203	192	37.58	6	0.94	0.85	0.70	25.82
180	366	31.85	1	0.51	0.45	0.36	28.88

Table 14 below shows the percentage decrease in average circular values for the
year 2003.

Table 14. Average Values (Circular Ratios for 2003)

Column	Row	Value(mm)	Region	RC1	RC2	RC3	%Decrease
287	91	35.48	3	0.71	0.56	0.43	38.98
267	93	34.17	3	0.74	0.58	0.49	33.83
225	186	36.51	6	0.75	0.62	0.52	31.12
203	192	37.58	6	0.92	0.80	0.69	24.86
180	366	31.85	1	0.55	0.44	0.37	33.09

Same was the case with the year 2003. ARF ratio difference dropped from a
high of 46% for high values to about 57% for average values and reached to a
dwindling low of 11% for the low annual maxima values.

Table 15 below shows the percentage decrease in high square values for the
year 2004.

Table 15. High Values (Square Ratios for 2004)

Column	Row	Value(mm)	Region	RS1	RS2	RS3	%Decrease
182	120	109.01	3	0.86	0.63	0.45	47.84
231	158	110.98	3	0.56	0.37	0.21	62.10
239	159	107.08	3	0.47	0.34	0.26	45.15
264	102	101.39	5	0.68	0.43	0.33	51.55
265	103	110.53	5	0.76	0.51	0.34	55.36

Table 16 below shows the percentage decrease in high circular values for the
year 2004.

Table 16. High Values (Circular Ratios for 2004)

Column	Row	Value(mm)	Region	RC1	RC2	RC3	%Decrease
182	120	109.01	3	0.82	0.61	0.45	45.18
231	158	110.98	3	0.56	0.35	0.21	63.26
239	159	107.08	3	0.48	0.33	0.26	44.63
264	102	101.39	5	0.65	0.41	0.31	52.77
265	103	110.53	5	0.73	0.49	0.33	54.67

Table 17 below shows the percentage decrease in low square values for the year 2004.

Table 17. Low Values (Square Ratios for 2004)

Column	Row	Value(mm)	Region	RS1	RS2	RS3	%Decrease
94	158	14.53	7	0.82	0.80	0.71	13.41
102	158	16.53	7	0.93	0.91	0.81	12.22
113	159	18.80	7	0.84	0.84	0.76	10.43
165	186	19.57	7	0.87	0.84	0.76	12.59
139	193	19.36	7	0.80	0.80	0.66	17.58

Table 18 below shows the percentage decrease in low circular values for the year 2004.

Table 18. Low Values (Circular Ratios for 2004)

Column	Row	Value(mm)	Region	RS1	RS2	RS3	%Decrease
94	158	14.53	7	0.72	0.60	0.58	19.44
102	158	16.53	7	0.97	0.85	0.80	17.57
113	159	18.80	7	0.88	0.80	0.73	17.27
165	186	19.57	7	0.91	0.80	0.74	18.61
139	193	19.36	7	0.81	0.77	0.65	19.68

Table 19 below shows the percentage decrease in average square values for the year 2004.

Table 19. Average Values (Square Ratios for 2004)

Column	Row	Value(mm)	Region	RS1	RS2	RS3	%Decrease
358	270	36.14	3	0.83	0.66	0.53	35.96
366	270	39.87	3	0.67	0.53	0.42	36.39
378	277	36.58	3	0.89	0.75	0.63	29.12
308	263	37.58	2	0.45	0.38	0.32	28.54
323	270	33.65	2	0.92	0.79	0.65	29.32

Table 20 below shows the percentage decrease in average circular values for the year 2004.

Table 20. Average Values (Circular Ratios for 2004)

Column	Row	Value(mm)	Region	RS1	RS2	RS3	%Decrease
358	270	36.14	3	0.791	0.627	0.514	35.02
366	270	39.87	3	0.653	0.504	0.409	37.37
378	277	36.58	3	0.843	0.706	0.605	28.23
308	263	37.58	2	0.464	0.373	0.312	32.76
323	270	33.65	2	0.881	0.754	0.632	28.26

As can be seen from the tables the reduction in the square values for high values of annual maxima ranged from 45% to 62% and for circular ratios from 45% to nearly 63%. These values decreased to about 28% to 35% for average 1 hour annual maxima values and they were as low as 10% for low 1 hour annual maxima values.

This trend in the diminution of values can be accounted for by probability that the higher annual maxima values occurred due to an extreme event which covered only some part of the watershed area. And the area taken into consideration for the calculation of the second and third ratios was not being covered by the storm, as it was localized to a small area. The evenly distributed values resulting from average and low values indicate that these were recorded from smaller, more frequent storms. This trend in the values, at some places, could also result because of topography and seasonal variations.

8. CONCLUSIONS

The purpose of this study is to document estimation of Areal Reduction Factors for the state of Texas, using 1 hour rainfall accumulation NEXRAD data values. Although radar data are used, it is known however, that the performance of radar with respect to rain gauge is rather poor. Nevertheless, it is expected that the radar is more efficient than using rain gauge networks in capturing the internal and the spatial distributions of the rainfall pattern. Historically, ARF relationships have been developed on the basis of data derived from dense networks of recording gauges. However, with the ongoing availability of radar rainfall records, radar records represent an alternative to gauging data. This study intends to evaluate the potential of the NEXRAD rainfall-radar data for the development of geographically fixed ARFs by following the annual maxima centered approach. The objectives are to evaluate the use of radar–rainfall data for the development of the ARFs and identify potential obstacles that might hinder the use of such data. Therefore, from the perspective of the derivation of the ARFs ratios, not actual intensity values but the ratio between areal and point values are needed. Taking this into account the use of radar data should give at least as reliable results as those achievable by using only rain gauge data. Also the use of sophisticated radar data like MPE radar products, help in overcoming the shortcomings of the rain gauge and the radar.

This approach is a new development in the analysis of areal distribution of precipitation design. The approach is demonstrated by using radar data for the state of Texas and is believed to be the first study of such kind using NEXRAD data for the state of Texas. A simple method for modeling areal reduction factors, which are widely

used in reducing point rainfall to obtain areal average values for a specified area, of storm rainfalls is presented in this study. The study is an extension of the work carried out by Asquith and Famiglietti, 2000. The analysis presented here, somehow keeps the track indicated by Asquith and Famiglietti's study, although some substantial modifications are introduced. Work using radar data has been carried out by Durrans et. al, 2003 and my study attempts to link the previous approaches used for the derivation of ARF, based on the concept of concurrent precipitation surrounding and annual maxima, with the latest technology in the precipitation data. The approach, termed as annual maxima centered specifically considers the distribution of concurrent precipitation surrounding an annual precipitation maxima, which is a feature not common in other approaches (Asquith and Famiglietti, 2000). The approach is described and demonstrated in the spirit that it provides an alternative to approaches that are more computationally complex or are based on extensive statistical inference at the expense of requiring considerable databases (Asquith and Famiglietti, 2000). In this way it is expected that the estimation of the ARFs would be related to a sounder scientific basis and at the same time will be a result of the advancement in technology in the field of precipitation data. Hence, this study will also provide some guidance for new researches.

The reduction factors presented in this study have been based on the assumption that the ARFs do not vary with the return period. Further variation with the return period needs to be investigated in order to make more valid conclusions of the present study. Data analysis is needed to assess the variability of return period and different

storm durations with the ARF. With the acquisition of sufficient additional data, the results can be extended to longer storm durations and different return periods.

The results of the study significantly support the conjecture that watershed size holds for ARF values with increasing areas. The reduction factors derived from this analysis show decay in the ARF values with respect to increase in the area of the watershed, though the decay cannot be described with any set pattern. This result is consistent with the previous studies carried out on this topic. The approach produces ARFs that decay more rapidly for larger areas than those from TP-29 and other studies. This decay in the larger area ARF values is not the same as most of the studies but a reasonable approximation to the expected values of the ARF is proposed. Absence of the concept of return period and storm duration in this study, can be a major factor causing such disparity in the results. Table 21 below shows the range of calculated ARF values for various regions.

Table 21. ARF Range for Various Regions

Area Sq. Km.	Region 1 ARF Range	Region 2 ARF Range	Region 3 ARF Range	Region 4 ARF Range	Region 5 ARF Range	Region 6 ARF Range	Region 7 ARF Range
0	1	1	1	1	1	1	1
144	0.83-0.64	0.90-0.60	0.97-0.69	0.72-0.60	0.77-0.60	0.80-0.62	0.82-0.64
400	0.62-0.41	0.68-0.50	0.72-0.40	0.62-0.47	0.60-0.50	0.63-0.41	0.62-0.41
784	0.51-0.34	0.52-0.28	0.60-0.23	0.54-0.20	0.49-0.36	0.60-0.19	0.53-0.28

Finding the effect of the watershed shape was also one of the aims of the study. The study illustrates that the shape of the watershed affects the ARF values. It was shown that in general the circular ARF were found to be slightly smaller than the square shaped ARF. To better understand the dependency of shape on the ARF value, further research can be carried out to find how different shapes like ellipse cause a change in the ARF values for the same area. The results derived in my study although preliminary may find useful applications for the definition of design storms in urban catchments of a given size and duration having a given return period. It can also be inferred from the study that ARFs range from 0 to 1 and vary according to geographical location of the watershed.

Assuming the uncertainties associated with the use of radar data, essential for the formulation of any statistical analysis, the reduction factors derived should be considered rather representative. Hence this approach provides a reasonable line of attack to derive ARFs for hydrologic purposes.

In a nut shell it can be concluded that shortness of records and biases in the radar data are major factors limiting the dependence of ARF on return period and other aspects discussed above. The work carried out herein will help to identify some common problems associated with the use of radar data for further studies. Due to certain problems mentioned earlier, like non representative data (shortness of records or climatic variability) or characteristics of the radar precipitation algorithm the ARF values calculated can sometimes display unreasonable and/or unanticipated results. To sum up, even though radar rainfall data can be used for the derivation of the ARF

concept, due to the significant uncertainties, the results presented here are preliminary rather than representative and much additional research is needed.

REFERENCES

Allen, R.J., *Re-Evaluation of Extreme Rainfall Areal Reduction Factors.* M.S.Thesis, Cornell University, Ithaca, NY, 2003.

Asquith, W., and J.S. Famiglietti, Precipitation areal reduction factor estimation using an annual maxima centered approach*, Journal of Hydrology 230:* 55-69, 2000.

Austin, P.M., and R.A. Houze, Analysis of the structure of precipitation pattern in New England, *Journal of Applied Meteorology 11*: 926-935, 1972.

Bacchi, B., and R. Ranzi, On the derivation of areal reduction factors of storms*, Atmospheric Research 42*: 123-135, 1995.

Bradley, A.A., J.A. Smith, and C. Peters-Lidard, Radar-rainfall estimation in the Catskill Mountains, *IIHR Hydroscience and Engineering, Report 278*, 2000.

Baeck, M.L., and J.S. Smith, Rainfall estimation by the WSR-88D for heavy rainfall events*, Weather Forecasting 13*: 416-436, 1998.

Bakkiyalakshmi, P., and R. Srinivasan, A near real-time flood prediction using hourly NEXRAD rainfall for the State of Texas, *TWRI Project*, March, 2004.

Baron Services (2004a), FasTrac, NEXRAD analysis software, http://www.baronservices.com/Products/New_FasTrac/new_fastrac.html, 2004

Baron Services (2004b), NexTrac, NEXRAD analysis software, http://www.baronservices.com/html/nextrac.html, 2004.

Bedient, P., B.C. Hoblit, D.C. Gladwell, and B.E. Vieux, NEXRAD Radar for flood prediction in Houston, *Journal of Hydrologic Engineering 5,* 269, 2000.

Bedient, P., A. Holder, J.A. Benavides, and B.E. Vieux, Radar-based flood warning system applied to Tropical Storm Allison, *Journal of Hydrologic Engineering 8*(6), 308-318, November/December, 2003.

Bell, F.C., The areal reduction factors in rainfall frequency estimation, *NERC Report 35,* Institute of Hydrology, Wallingford, U.K, 1976.

Bell, T.L., A space–time stochastic model of rainfall for satellite remote sensing studies, *Journal of Geophysical Research 92*(D8): 9631-9644, 1987.

Bellin, A., and Y. Rubin, Hydro_gen: A spatially distributed random field generator for correlated properties, *Stochastic Hydrology and Hydraulics 10*: 253–278, 1996.

Bras, R., and Rodriguez-Iturbe, Rainfall generation: A non-stationary time varying multidimensional model, *Water Resources Research 12*(3): 450-456, 1985.

Chrisman, J.N, and C.A. Chrisman, An operational guide to WSR-88D reflectivity data quality assurance, *WSR-88D Operational Support Facility (OSF),* Norman, OK, 73072, January 25, 1999.

Crane, R.K., Space-time structure of rain rate fields, *Journal of Geophysical Research 95*: 2001–2020, 1990.

Dixon, M., and G. Weiner, TITAN: Thunderstorm identification, tracking, analysis and now casting - A radar based methodology, *Journal of Atmospheric and Oceanic Technology, 10*(6): 785-797, 1993.

Durrans, S.R., L.T. Julian, and M. Yekta, Estimation of depth area relationships using radar data, *Journal of Hydraulic Engineering, 7*(5): 356-367, 2003.

Einfalt, T., G. Johann, and A. Pfister, On the spatial validity of heavy point rainfall measurements, *Water Resource Technology 37*(11): 1998.

Frederick, R.H., V.A. Myers, and E.P. Auciello, Storm depth area relations from digitized radar returns, *Water Resources Research 13*(3): 675-679, 1977.

Fulton, R. A., J. P. Breidenbach, D. J. Seo, and D. A. Miller, The WSR-88D rainfall algorithm, *Weather Forecasting, 13*: 377-395, 1998.

Glenn, S., C. Moreno-Earle, B. Wise, and P. Bedient, Modeling effects of groundwater overpumping on water levels near Tampa, Florida: Building a base for accurate water balances through the use of NEXRAD and GIS, *ASCE Conf. Proc. III, 89,* 2001.

Gupta, V.K., and E.C. Waymire, A stochastic kinetic study of subsynoptic space-time rainfall, *Water Resources Research 15*(3): 637-644, 1979.

Gupta, V.K., and E.C. Waymire, A statistical analysis of meso-scale rainfall as a random cascade, *Journal of Applied Meteorology 32*: 251–267, 1993.

Hadley, J., and R. Srinivasan, Real-Time distributed runoff estimation using NEXRAD precipitation data, *TWRI Project, Feb,* 2002.

Hershfield, D.M., Rainfall frequency atlas of the United States for durations from 30 mins to 24 hours and return periods from 1 year to 100 years, *Tech. Paper No. 40,* U.S. Department of Commerce, Washington, D.C, 1961a.

Hershfield, D.M., Estimating the probable maximum precipitation, *Proceedings ASCE, Journal of Hydraulics Division 87*: 99-106, 1961b.

Hoblit, B.C., C. Castello, L. Liu, and D. Curtis, Creating a seamless map of gage-adjusted radar rainfall estimates for the state of Florida, *ASCE Conf. Proc. 118*, 215, 2003.

Hudlow, M.D., and V.L. Patterson, GATE radar rainfall atlas, *NOAA Special Report, 155,* U.S. Department of Commerce, Washington, D.C., 1979.

Hudlow, M.D. NEXRAD precipitation products, http://www.tucson.ars.ag.gov/icrw/Proceedings/Hardegree.pdf, 1991.

Huebner, R. S., C. Phatak, and B. C. Hoblit, Development and use of a NEXRAD database for water management in south Florida, *ASCE Conf. Proc. 118*, 216 2003.

Klazura, G. E. and D. A. Imy, A description of the initial set of analysis products available from the NEXRAD WSR-88D system. *Bull. Amer. Meteorol. Soc.*, *74,* 1293-1311, 1993.

Kessler, E., Radar meteorology at the National Severe Storms Laboratory, Radar in Meteorology, *D. Atlas, Ed., Amer. Meteorol. Soc., 44*:53, 1990.

Koutsoyiannis, D., A probabilistic view of Hershfield's method for estimating probable maximum precipitation, *Water Resources Research 35*(4): 1313-1322, 1999.

Leclerc, G., and J.C. Schaake, Derivation of hydrologic frequency curves, *Cambridge, MA, MIT, Report 142,* 151, 1972.

Lovejoy, S., and D. Schertzer, Generalized scale invariance in the atmosphere and fractal models of rain, *Water Resources Research 21*(8): 1233-1250, 1985.

Marchionno, A., and W. Wise, Stochastic modeling of rainfall using historical point based data with NEXRAD spatial data*, Journal of Undergraduate Research, 11,* University of Florida*,* 2002.

Michele, C.D., T.K. Nathabandu, and R. Rosso, The derivation of areal reduction factor from its scaling properties, *Water Resource Research 37*(12), 3247-3252, 1999.

Miller, J.F., R.H. Frederic, and R.J. Tracey, Precipitation frequency atlas of the conterminous western United States, *NOAA Atlas 2,* U.S. Department of Commerce, National Oceanic and Atmospheric Administration, National Weather Service, Silver Springs, MD, 11, 1973.

Moon, J.,R.Srinivasan, and, J.H.Jacobs, Stream flow estimations using spatially distributed rainfall in the Trinity River basin, Texas, *Transactions of ASAE,Vol 47*(5):1445-1451, 2004.

Myers, V.A., and R.M. Zehr, A methodology for point to area rainfall frequency ratios*, NOAA Technical Report*, National Weather Service, Silver Springs, MD, U.S. Department of Commerce, National Oceanic and Atmospheric Administration, NWS 24, 1980.

Natural Environmental Research Council (NERC), *Flood Studies Report 1,* Meterological Studies, Swindon, England, 1975.

Nelson, B.R., A. Allen Bradley, C. Peters-Lidard, C. Bryan Young, and J. A. Smith , Raingauge network design in a mountainous region using NEXRAD WSR-88D precipitation estimates, *IIHR Hydroscience and Engineering, Report 276*, 2000.

NOAA, National Weather Service, NEXRAD Radars, http://dipper.nws.noaa.gov/hdsb/data/nexrad/nexrad.html, 2004a.

NOAA, National Weather Service, NEXRAD Radars, http://www.srh.noaa.gov/wgrfc/resources/about_us.html, 2004b.

NOAA, NWS, NEXRAD Site in USA, http://weather.noaa.gov/radar/national.html, 2005.

NSLL, NEXRAD Data, http://www.nssl.noaa.gov/accomp/major.html, 2004.

Omolayo, A.S., On the transposition of areal reduction factors for rainfall frequency estimation*, Journal of Hydrology 145*: 191-205, 1993.

Osborn, H.B., L.J. Lane, and V.A. Myres, Rainfall/watershed relationships for southwestern thunderstorms*, ASAE 23*: 82-91, 1980.

Over, T., and V. Gupta, A space-time theory of mesoscale rainfall using random cascades, *Journal of Geophysical Research 101*: 26, 319, 1996.

Priegnitz, D., Interactive Radar Analysis System (IRAS) software, NEXRAD analysis software, http://lwf.ncdc.noaa.gov/oa/radar/iras.html, 2004.

Rakhecha, P.R., and C. Clark, Areal PMP distribution for one-day to three-day duration over India, *Applied Meteorology 9*: 399-406, 2002.

Rodriguez-Iturbe, I., D. R. Cox, and V. Isham, Some models for rainfall based on stochastic point processes*, Proceedings of Royal Society of London, Series A, 410*: 269–288, 1987.

Rodriguez-Iturbe, I., and H.M. Mejia, Design of rainfall networks in space and time, *Water Resources Research 10*(4): 713-728, 1974a.

Rodriguez-Iturbe, I., and H.M. Mejia, On the transformation of point rainfall to areal rainfall, *Water Resources Research 10*(4): 729-735, 1974b.

Seann and Maidment, NEXRAD success stories, http://www.ce.utexas.edu/prof/maidment/gishydro/seann/nexrad.htm, 2004.

Seo, D.-J., Real-time estimation of rainfall fields using radar rainfall and rain gage data, *Journal of Hydrology 208*:37-52, 1998.

Sivapalan, M., and G. Blöschl, Transformation of point rainfall to areal rainfall: Intensity-duration frequency curves, *Journal of Hydrology 204*(91): 4, 150-167, 1998.

Smith, J.A., and A.A. Bradley, Space time structures of extreme storm rainfall in the southern plains, *Journal of Applied Meteorology 33*: 1402-1417, 1994.

Smith, J.A., and W.F. Krajewski, Statistical modeling of space-time rainfall using radar and rain gauge observations, *Water Resources Research 23*(10): 1893-1900, 1987.

Smith, J.A., and W.F. Krajewski, On the estimation of climatologically Z-R relationships, *Journal of Applied Meteorology 30*: 1436-1445, 1991.

Srikanthan, R., A review of the methods for estimating areal reduction factors for design rainfalls, *Report 95/3,* Cooperative Research Centre for Catchment Hydrology, Mellbourne, Australia, 36, 1995.

Supino, G., *Le Reti Idrauliche* (in Italian), 806, Patron Ed., Bologna, Italy, 1964.

Texas Parks and Wildlife Department,TPWD, Regions of Texas; http://www.tpwd.state.tx.us/expltx/ecomapx.htm, 2004.

University Corporation of Atmospheric Research, Plan Position Indicator Mesoscale Mesoscale and Microscale Meterology, NEXRAD Data Analysis Software. http://box.mmm.ucar.edu/pdas/pdas.html#overview, 2004.

Unysis, SKYVIEW95, Weather Information System, NEXRAD analysis software, http://lwf.ncdc.noaa.gov/oa/radar/radarproductssoftwareunisys.html#PC, 2004a.

Unysis, Weather Processor, WXP, Purdue University. http://weather.unisys.com/wxp/, 2004b.

U.S. Weather Bureau, Rainfall intensity-frequency regime, Part 1-The Ohio Valley, *Technical Paper No. 29*, U.S. Department of Commerce, Washington, D.C., 1957.

U.S. Weather Bureau, Rainfall intensity-frequency regime, Part 2-Southeastern United States, *Technical Paper No. 29,* U.S. Department of Commerce, Washington, D.C, 1958a.

U.S. Weather Bureau, Rainfall intensity-frequency regime, Part 3-The Middle Atlantic Region, *Technical Paper No. 29*, U.S. Department of Commerce, Washington, D.C., 1958b.

Veneziano, D., and A. Langousis, Areal reduction factors for multifractal rainfall*, Geophysical Research Abstracts 6,* 2004.

Vieux, B.E., and P.B. Bedient, Estimation of rainfall for flood prediction from WSR-88D reflevtivity: A case study 17-18 October 1994*, Weather Forecasting 13*: 407-415, 1998.

Vivoni, E.R., and D.D. Sheehan, Using NEXRAD rainfall data in an Arc-View based hydrology model as an educational tool, http://gis.esri.com/library/userconf/proc01/professional/papers/pap374/p374.htm, 2004.

Waymire, E., and V.K. Gupta, The mathematical structure of rainfall representations, 1, A review of the stochastic rainfall models*, Water Resources Research 17*: 1261–1272, 1981a.

Waymire, E., and V.K. Gupta, The mathematical structure of rainfall representations 2, a review of the theory of point processes, *Water Resources Research 17:* 1273–1285, 1981b.

Waymire, E., V.K. Gupta, and I. Rodriguez-Iturbe, A spectral theory of a rainfall intensity field at the meso-β scale, *Water Resources Research 10*(10): 1453-1465, 1984.

Weather Service International (WSI), NEXRAD data analysis software, http://sysu1.wsicorp.com/unidata/intro.html, 2004.

Wilson, J. W., and E. A. Brandes, Radar measurement of rainfall: A summary. *Bull. Amer. Meteorol. Soc.*, *60*, 1048-1058, 1979.

Wildernet, Various Regions of Texas, http://areas.wildernet.com/pages/area.cfm?areaID=TXTR&CU_ID=1, 2004.

World Meteorological Organization, Manual for estimation of probable maximum precipitation, *Operational Hydrologic Rep. (1) Paper.332*, Geneva, Switzerland, 1986.

Zawadzki, I., Statistical properties of precipitation patterns*, Journal of Applied Meteorology 12:* 459-472, 1973.

APPENDIX A

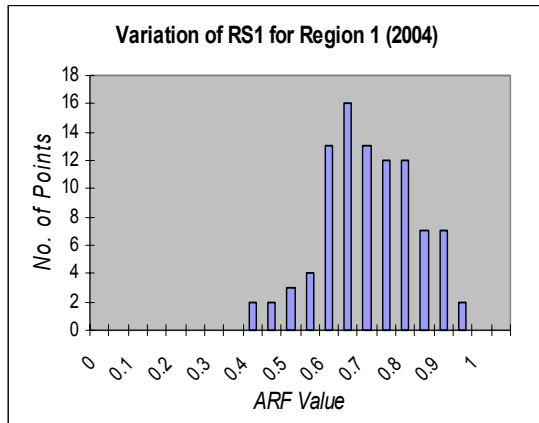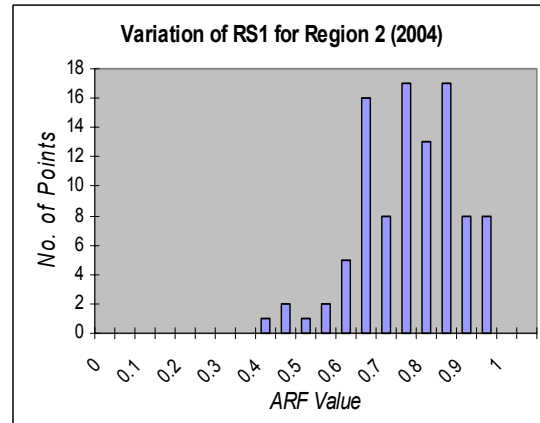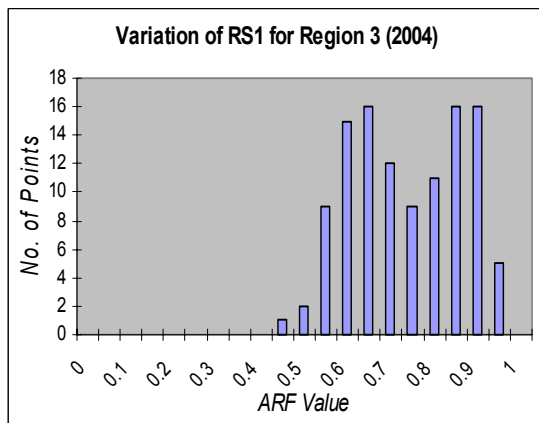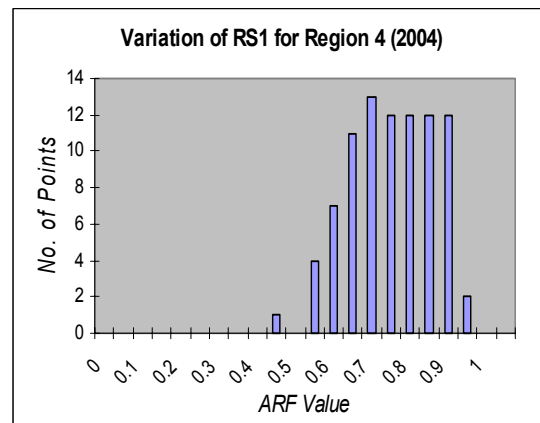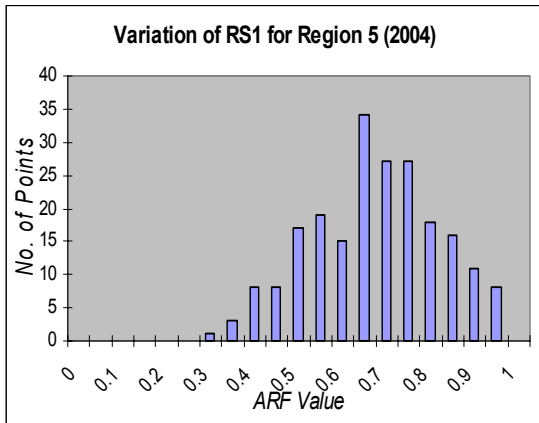Figures showing variation in square ARF ratios for various years.
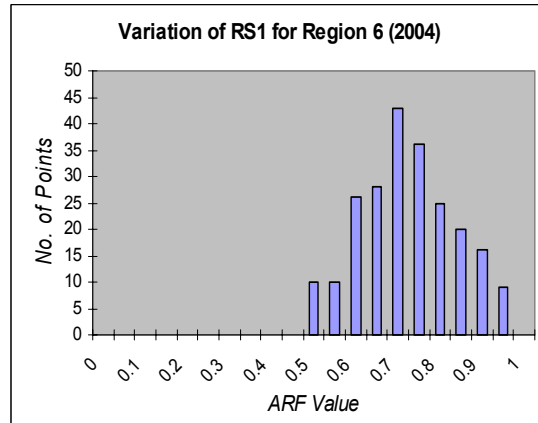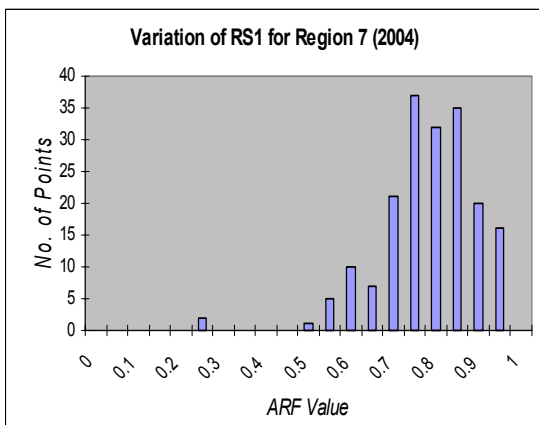

Figure A1

Figure A2
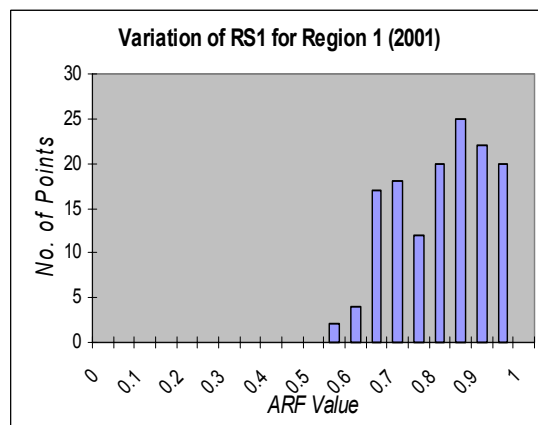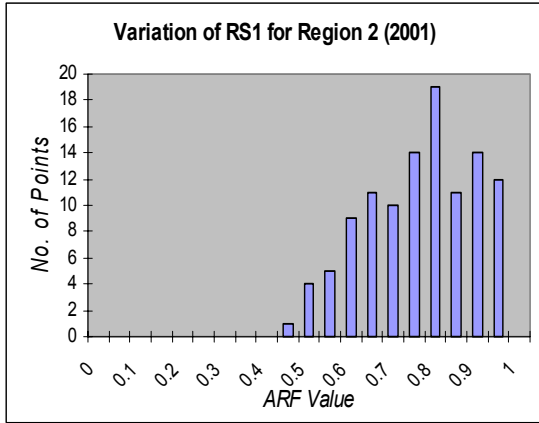

Figure A3

Figure A4

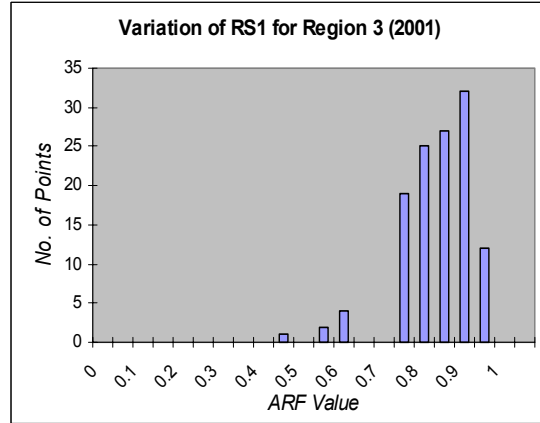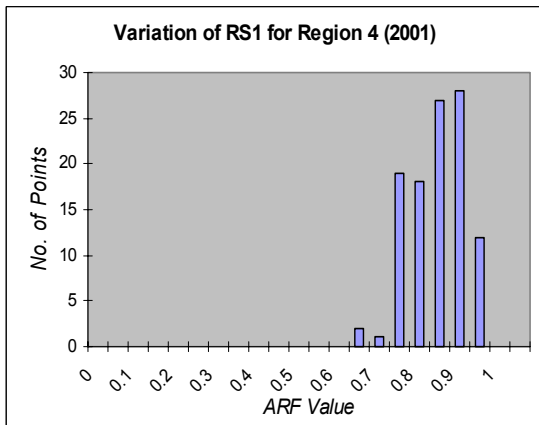Figure A5

Figure A6

Figure A7

Figure A8

Figure A9

Figure A10

Figure A11

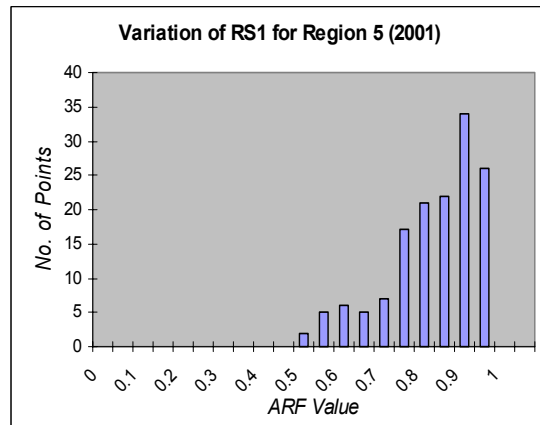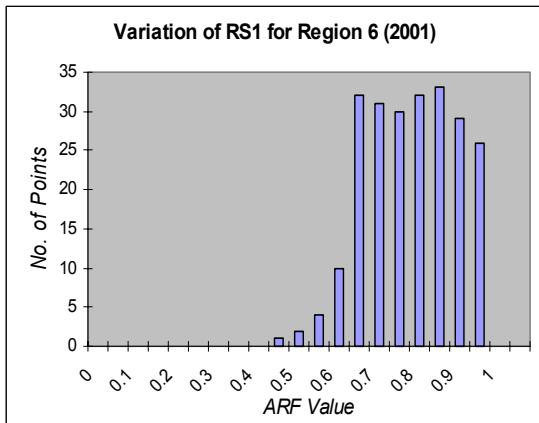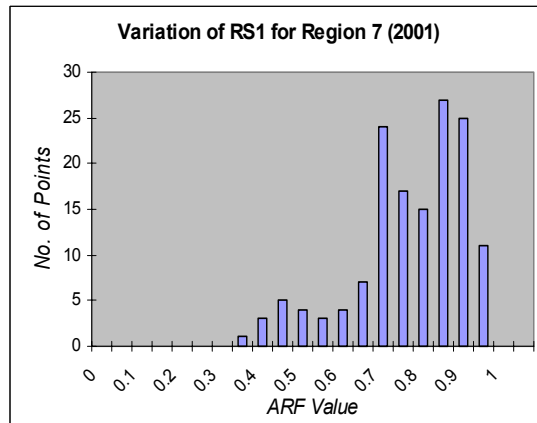Figure A12

Figure A13

Figure A14

VITA

Tarun Deep Gill

ADDRESS

14004 Westward Drive, Fontana, California

(323)788-2786

EDUCATION

- Master of Science in Civil Engineering, May 2005

  Texas A&M University

- Bachelor of Science in Civil Engineering, May 2001

  Thapar Institute of Engineering and Techonology, India

EXPERIENCE

- Texas A&M University, College Station, Texas (August 2003- December 2004)

  Graduate Research Assistant

  Development of a GIS based static storm model

This thesis was typed by the author.